Universität Regensburg
Mathematik

Stable finite element approximations of two-phase flow with soluble surfactant

John W. Barrett, Harald Garcke and Robert Nürnberg

Preprint Nr. 14/2014

Stable Finite Element Approximations of Two-Phase Flow with Soluble Surfactant

John W. Barrett[†] Harald Garcke[‡] Robert Nürnberg[†]

Abstract

A parametric finite element approximation of incompressible two-phase flow with soluble surfactants is presented. The Navier–Stokes equations are coupled to bulk and surfaces PDEs for the surfactant concentrations. At the interface adsorption, desorption and stress balances involving curvature effects and Marangoni forces have to be considered. A parametric finite element approximation for the advection of the interface, which maintains good mesh properties, is coupled to the evolving surface finite element method, which is used to discretize the surface PDE for the interface surfactant concentration. The resulting system is solved together with standard finite element approximations of the Navier–Stokes equations and of the bulk parabolic PDE for the surfactant concentration. Semidiscrete and fully discrete approximations are analyzed with respect to stability, conservation and existence/uniqueness issues. The approach is validated for simple test cases and for complex scenarios, including colliding drops in a shear flow, which are computed in two and three space dimensions.

Key words. incompressible two-phase flow, soluble surfactants, finite elements, front tracking, ALE-ESFEM

1 Introduction

Surface active agents, also called surfactants, are among the most widely used molecules in industry. They may act as detergents, wetting agents, emulsifiers, foaming agents and dispersants. The reason for these many applications is that soluble surfactants can have a pronounced effect on the interface and, hence also, on the evolution in a two-phase flow. In particular, surfactants influence the surface tension at the interface, and local inhomogeneities lead to Marangoni effects. In situations where the surfactant is soluble in one or in both of the two bulk phases, the adsorption and desorption of surfactants at the interface has to be taken into account. This means surfactant molecules can attach

[†]Department of Mathematics, Imperial College London, London, SW7 2AZ, UK
[‡]Fakultät für Mathematik, Universität Regensburg, 93040 Regensburg, Germany

to and detach from the interface, and the corresponding mass balances on the interface and in the bulk have to be taken into account. The fundamental transport mechanisms for surfactants are diffusion in the bulk phases and on the interface, and advection with the underlying fluid velocity.

Adsorption of surfactants to the interface decreases the surface tension, which makes it easier for the interface to deform. It also can be observed, see e.g. the numerical experiments in Section 6, that an interface moves towards regions with a high bulk surfactant concentration. The presence of surfactants typically decreases the rise velocity of bubbles. The reason for this is that Marangoni stresses at the interface imply that the shear free condition at the interface no longer holds, and hence the drag force on the bubble increases. In particular, the rise velocity of a bubble is reduced, and this effect can be used to maximize the contact time between different fluid phases, which can be important to influence the transfer of chemical components. These phenomena demonstrate that the interplay between the fluid velocity and the bulk and surface surfactant concentrations is multifaceted. Due to this versatile interaction it is often difficult to identify the sources for the different phenomena from experiments alone. It is hence important to have reliable numerical methods for this complex problem at hand in order to obtain a better understanding of the interdependence of fluid flow, adsorption, desorption, advection, Marangoni effects and diffusion, see Figure 1 for a schematic description of the different quantities and transport processes.

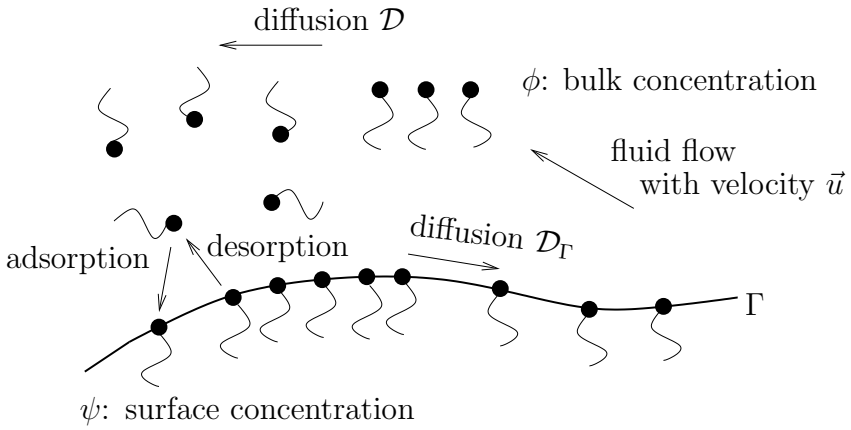

Figure 1: The different quantities and transport phenomena in the bulk and at the interface are schematically illustrated.

In order to mathematically describe the complex physics illustrated in Figure 1, one has to solve the following equations.

- The incompressible Navier–Stokes equations in both phases, see (2.3a–c).
- An advection-diffusion equation for the bulk surfactant concentration in either one or in both phases, see (2.8a).

- A parabolic partial differential equation on the evolving interface describing the conservation of bulk surfactant. Here a source term stemming from desorption and adsorption of surfactants has to be taken into account, see (2.8b) and Figure 1.
- An equilibrium of force equation on the interface, which includes curvature and Marangoni effects, see (2.5a).
- An additional interface equation taking the surface thermodynamics into account. Depending on whether the interface kinetics are slow or fast, this either results in a condition relating the bulk fluxes to differences of chemical potentials, or it leads to the chemical potentials having to be equal, see (2.13) and (2.15). The latter condition contains Henry's law (2.17) as a special case.

In addition,

- the interface has to be advected with a normal velocity which equals the normal part of the fluid velocity, see (2.5b).

Although the overall problem has many applications, not many analytical results exist for this problem. An energy inequality for the insoluble case, which we are also going to use, has been derived by Garcke and Wieland (2006). Bothe and Prüss (2010) used energy methods and semigroup theory to study the stability of equilibria in the soluble case. Garcke *et al.* (2014) introduced a diffuse interface model to describe two-phase flow with soluble surfactants for which an energy inequality can be shown. Moreover, by using matched asymptotic expansions they could show that a novel sharp interface model can be recovered, which also satisfies an energy law. We refer to Section 2 for the precise details of this sharp interface model, which has already been outlined above.

In contrast, over the years many papers presenting numerical methods and computations for interfacial flows with soluble surfactants have appeared. Let us briefly mention the methods that have been used by different groups. Renardy *et al.* (2002) and Alke and Bothe (2007) used the volume of fluid (VOF) method, which approximates the characteristic function of one of the phases. The level set method, which describes the interface as the level set of a function, was considered in the work of Xu *et al.* (2013). Numerical computations based on diffuse interface models have been presented by Liu and Zhang (2010), Teigen *et al.* (2011), Engblom *et al.* (2013) and Garcke *et al.* (2014). The immersed boundary method has been used by Lai *et al.* (2008) and Chen and Lai (2014). A front tracking method for soluble surfactants has been introduced by Muradoglu and Tryggvason (2008) and Tasoglu *et al.* (2008). In addition we mention the arbitrary Lagrangian–Eulerian approach of Ganesan and Tobiska (2012), the segment projection method of Khatri and Tornberg (2014) and the hybrid method studied in Booty and Siegel (2010) and Xu *et al.* (2013). For more references and an introduction to numerical methods for two-phase flow we refer to the book by Groß and Reusken (2011).

In this paper we adapt the approach of Barrett *et al.* (2014, 2013b) to numerically solve the governing equations for soluble surfactants at fluid interfaces. In particular, we

consider the system with the novel free boundary condition in Garcke *et al.* (2014) that allows for a stability estimate. For a particular instance of this model, where the bulk surfactant concentration is assumed to be continuous across the interface, we are able to prove a stability estimate for our semidiscrete finite element approximation. To our knowledge, this is the first stability result for a numerical approximation of two-phase flow with soluble surfactant in the literature. In addition, the numerical method introduced by the present authors ensures *good mesh properties*, i.e. *equidistribution of interface mesh points* in 2d, see Barrett *et al.* (2007), and *conformal polyhedral surfaces* in 3d, see Barrett *et al.* (2008). In addition, a simple XFEM strategy ensures *discrete volume conservation* and often *mass conservation* and *stability estimates* can be shown. The mesh properties also make a reliable computation of the PDE on the evolving interface possible. To solve this PDE we use the evolving surface finite element method (ESFEM) of Dziuk and Elliott (2007), see also the ALE-ESFEM approach of Elliott and Styles (2012).

The remainder of the paper is organized as follows. In Section 2 we state the governing equations. Two alternative weak formulations for different models of two-phase flow with soluble surfactant are introduced in Section 4. Here we consider a two-sided model (i) with the relaxation condition (2.13), as well as a global model (ii), where the soluble surfactant concentration is assumed to be continuous across the interface. The natural semidiscrete continuous-in-time finite element approximations based on these formulations are presented in Section 4, together with stability proofs for the approximations of model (ii). Fully discrete analogues are discussed in Section 5, with numerical results shown in Section 6. Here we show numerical simulations for colliding drops in shear flow and for rising bubbles, and we also present computations for radially symmetric solutions for a simple test problem involving adsorption and desorption, which underline the accuracy of our numerical method. The details for the employed radially symmetric solutions are discussed in the Appendix.

2 Governing equations

We will now introduce the sharp interface model for two-phase flow with surfactants which we plan to numerically approximate.

Let $\Omega \subset \mathbb{R}^d$ be a given domain, where $d = 2$ or $d = 3$. We now seek a time dependent interface $(\Gamma(t))_{t\in[0,T]}$, $\Gamma(t) \subset \Omega$, which for all $t \in [0,T]$ separates Ω into a domain $\Omega_+(t)$, occupied by one phase, and a domain $\Omega_-(t) := \Omega \setminus \overline{\Omega}_+(t)$, which is occupied by the other phase. Here the phases could represent two different liquids, or a liquid and a gas. Common examples are oil/water or water/air interfaces. See Figure 2 for an illustration. For later use, we assume that $(\Gamma(t))_{t\in[0,T]}$ is a sufficiently smooth evolving hypersurface without boundary that is parameterized by $\vec{x}(\cdot,t) : \Upsilon \to \mathbb{R}^d$, where $\Upsilon \subset \mathbb{R}^d$ is a given reference manifold, i.e. $\Gamma(t) = \vec{x}(\Upsilon,t)$. Then

$$\vec{\mathcal{V}}(\vec{z},t) := \vec{x}_t(\vec{q},t) \qquad \forall\ \vec{z} = \vec{x}(\vec{q},t) \in \Gamma(t) \tag{2.1}$$

defines the velocity of $\Gamma(t)$, and $\vec{\mathcal{V}}\,.\,\vec{\nu}$ is the normal velocity of the evolving hypersurface

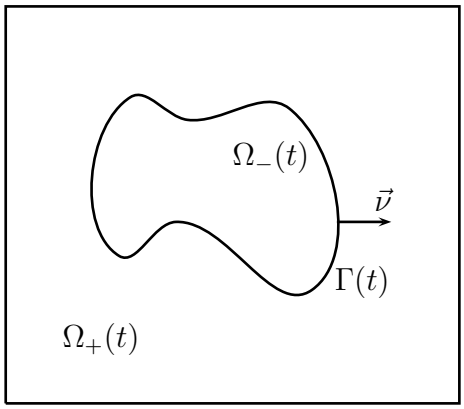

Figure 2: The domain Ω in the case $d = 2$.

$\Gamma(t)$, where $\vec{\nu}(t)$ is the unit normal on $\Gamma(t)$ pointing into $\Omega_+(t)$. Moreover, we define the space-time surface

$$\mathcal{G}_T := \bigcup_{t\in[0,T]} \Gamma(t) \times \{t\}\,. \tag{2.2}$$

Let $\rho(t) = \rho_+\,\mathcal{X}_{\Omega_+(t)} + \rho_-\,\mathcal{X}_{\Omega_-(t)}$, with $\rho_\pm \in \mathbb{R}_{>0}$, denote the fluid densities, where here and throughout $\mathcal{X}_{\mathcal{A}}$ defines the characteristic function for a set $\mathcal{A}$. Denoting by $\vec{u} : \Omega \times [0,T] \to \mathbb{R}^d$ the fluid velocity, by $\underline{\underline{\sigma}} : \Omega \times [0,T] \to \mathbb{R}^{d\times d}$ the stress tensor, and by $\vec{f} : \Omega \times [0,T] \to \mathbb{R}^d$ a possible forcing, the incompressible Navier–Stokes equations in the two phases are given by

$$\rho\,(\vec{u}_t + (\vec{u}\,.\,\nabla)\,\vec{u}) - \nabla\,.\,\underline{\underline{\sigma}} = \vec{f} := \rho\,\vec{f}_1 + \vec{f}_2 \qquad \text{in } \Omega_\pm(t)\,, \tag{2.3a}$$

$$\nabla\,.\,\vec{u} = 0 \qquad \text{in } \Omega_\pm(t)\,, \tag{2.3b}$$

$$[\vec{u}]^+_- = \vec{0} \qquad \text{on } \Gamma(t)\,, \tag{2.3c}$$

$$\vec{u} = \vec{0} \qquad \text{on } \partial_1\Omega\,, \tag{2.3d}$$

$$\vec{u}\,.\,\vec{\mathrm{n}} = 0\,, \quad \underline{\underline{\sigma}}\,\vec{\mathrm{n}}\,.\,\vec{\mathrm{t}} = 0 \quad \forall\ \vec{\mathrm{t}} \in \{\vec{\mathrm{n}}\}^\perp \qquad \text{on } \partial_2\Omega\,, \tag{2.3e}$$

where $\partial\Omega = \partial_1\Omega \cup \partial_2\Omega$, with $\partial_1\Omega \cap \partial_2\Omega = \emptyset$, denotes the boundary of Ω with outer unit normal $\vec{\mathrm{n}}$ and $\{\vec{\mathrm{n}}\}^\perp := \{\vec{\mathrm{t}} \in \mathbb{R}^d : \vec{\mathrm{t}}\,.\,\vec{\mathrm{n}} = 0\}$. Hence (2.3d) prescribes a no-slip condition on $\partial_1\Omega$, while (2.3e) prescribes a free-slip condition on $\partial_2\Omega$. In addition, the stress tensor in (2.3a) is defined by

$$\underline{\underline{\sigma}} = \mu\,(\nabla\,\vec{u} + (\nabla\,\vec{u})^T) - p\,\underline{\underline{Id}} = 2\,\mu\,\underline{\underline{D}}(\vec{u}) - p\,\underline{\underline{Id}}\,, \tag{2.4}$$

where $\underline{\underline{Id}} \in \mathbb{R}^{d\times d}$ denotes the identity matrix, $\underline{\underline{D}}(\vec{u}) := \frac{1}{2}\,(\nabla\vec{u} + (\nabla\vec{u})^T)$ is the rate-of-deformation tensor, $p : \Omega \times [0,T] \to \mathbb{R}$ is the pressure and $\mu(t) = \mu_+\,\mathcal{X}_{\Omega_+(t)} + \mu_-\,\mathcal{X}_{\Omega_-(t)}$, with $\mu_\pm \in \mathbb{R}_{>0}$, denotes the dynamic viscosities in the two phases. On the free surface $\Gamma(t)$, the following conditions need to hold:

$$[\underline{\underline{\sigma}}\,\vec{\nu}]^+_- = -\gamma(\psi)\,\varkappa\,\vec{\nu} - \nabla_s\,\gamma(\psi) \qquad \text{on } \Gamma(t)\,, \tag{2.5a}$$

$$\vec{\mathcal{V}}\,.\,\vec{\nu} = \vec{u}\,.\,\vec{\nu} \qquad \text{on } \Gamma(t)\,, \tag{2.5b}$$

where $\gamma \in C^1([0,\psi_\infty))$, with $\psi_\infty > 0$ and

$$\gamma'(r) < 0 \qquad \forall\, r \in [0,\psi_\infty)\,, \tag{2.6}$$

denotes the surface tension which depends on the interfacial surfactant density $\psi : \mathcal{G}_T \to (0,\psi_\infty)$, recall (2.2), and ∇_s denotes the surface gradient on $\Gamma(t)$. In addition, $\varkappa$ denotes the mean curvature of $\Gamma(t)$, i.e. the sum of the principal curvatures of $\Gamma(t)$, where we have adopted the sign convention that $\varkappa$ is negative where $\Omega_-(t)$ is locally convex. In particular, on letting $\vec{\mathrm{id}}$ denote the identity function in $\mathbb{R}^d$, it holds that

$$\Delta_s\, \vec{\mathrm{id}} = \varkappa\, \vec{\nu} =: \vec{\varkappa} \qquad \text{on } \Gamma(t)\,, \tag{2.7}$$

where $\Delta_s = \nabla_s\,.\,\nabla_s$ is the Laplace–Beltrami operator on $\Gamma(t)$, with $\nabla_s\,.$ denoting surface divergence on $\Gamma(t)$. Moreover, as usual, $[\vec{u}]^+_- := \vec{u}_+ - \vec{u}_-$ and $[\underline{\underline{\sigma}}\,\vec{\nu}]^+_- := \underline{\underline{\sigma}}_+\,\vec{\nu} - \underline{\underline{\sigma}}_-\,\vec{\nu}$ denote the jumps in velocity and normal stress across the interface $\Gamma(t)$. Here and throughout, we employ the shorthand notation $\vec{v}_\pm := \vec{v}\,|_{\Omega_\pm(t)}$ for a function $\vec{v} : \Omega \times [0,T] \to \mathbb{R}^d$; and similarly for scalar and matrix-valued functions. In this paper we consider surfactant that is soluble in the bulk phases. We denote the surfactant's bulk densities by $\phi_\pm$, and the interfacial surfactant density by ψ, see above. The surfactant is transported by the surrounding fluid and, taking also diffusion into account, this can be modelled by

$$\partial_t\, \phi_\pm + \vec{u}\,.\,\nabla\, \phi_\pm - \nabla\,.\,(\mathcal{D}_\pm\, \nabla\, \phi_\pm) = 0 \qquad \text{in } \Omega_\pm(t)\,, \tag{2.8a}$$

$$\partial_t^\bullet\, \psi + \psi\, \nabla_s\,.\vec{u} - \nabla_s\,.\,(\mathcal{D}_\Gamma\, \nabla_s\, \psi) = [\mathcal{D}\, \nabla\, \phi\,.\,\vec{\nu}]^+_- \qquad \text{on } \Gamma(t)\,, \tag{2.8b}$$

$$\nabla\, \phi_+\,.\,\vec{\mathrm{n}} + \lambda_+\,(\phi_+ - g_+) = 0 \qquad \text{on } \partial\Omega\,, \tag{2.8c}$$

where $\mathcal{D}_\pm \in \mathbb{R}_{\geq 0}$ and $\mathcal{D}_\Gamma \in \mathbb{R}_{\geq 0}$ are diffusion coefficients, and where $[\mathcal{D}\, \nabla\, \phi\,.\,\vec{\nu}]^+_- := \mathcal{D}_+\, \nabla\, \phi_+\,.\,\vec{\nu} - \mathcal{D}_-\, \nabla\, \phi_-\,.\,\vec{\nu}$. In addition, $\lambda_+ \geq 0$ and $g_+ > 0$ in the Robin boundary conditions (2.8c) are space-dependent parameters, and for notational convenience we also define $\lambda_- = g_- = 0$. Moreover,

$$\partial_t^\bullet\, \zeta = \zeta_t + \vec{u}\,.\,\nabla\, \zeta \qquad \forall\, \zeta \in H^1(\mathcal{G}_T) \tag{2.9}$$

denotes the material time derivative of ζ on $\Gamma(t)$. Here we stress that for $\zeta \in H^1(\mathcal{G}_T)$ the derivative in (2.9) can be computed by extending ζ to a neighbourhood of $\mathcal{G}_T$. The quantity $\partial_t^\bullet\, \zeta$ is well-defined, and depends only on the values of ζ on $\mathcal{G}_T$, even though ζ_t and $\nabla\, \zeta$ do not make sense for a function on $\mathcal{G}_T$; see e.g. Dziuk and Elliott (2013, p. 324).

In order to formulate the necessary matching conditions that ψ and $\phi_\pm$ need to satisfy on $\Gamma(t)$, we introduce the surface energy function F, which satisfies

$$\gamma(r) = F(r) - r\, F'(r) \qquad \forall\, r \in (0,\psi_\infty)\,, \tag{2.10a}$$

and

$$\lim_{r \to 0} r\, F'(r) = F(0) - \gamma(0) = 0\,. \tag{2.10b}$$

This means in particular that

$$\gamma'(r) = -r\, F''(r) \qquad \forall\, r \in (0,\psi_\infty)\,. \tag{2.11}$$

It immediately follows from (2.11) and (2.6) that $F \in C([0,\psi_\infty)) \cap C^2(0,\psi_\infty)$ is convex. Typical examples for γ and F are given by

$$\gamma(r) = \gamma_0\,(1-\beta\,r)\,, \quad F(r) = \gamma_0\,[1+\beta\,r\,(\ln r - 1)]\,,\ \psi_\infty = \infty\,, \tag{2.12a}$$

which represents a linear equation of state, and by

$$\gamma(r) = \gamma_0\left[1+\beta\,\psi_\infty\,\ln\left(1-\tfrac{r}{\psi_\infty}\right)\right], \quad F(r) = \gamma_0\left[1+\beta\left(r\,\ln\tfrac{r}{\psi_\infty - r} + \psi_\infty\,\ln\tfrac{\psi_\infty - r}{\psi_\infty}\right)\right], \tag{2.12b}$$

the so-called Langmuir equation of state, where $\gamma_0,\ \beta \in \mathbb{R}_{>0}$ are further given parameters, see e.g. Ravera *et al.* (2000).

Defining the relaxation parameters $\alpha_\pm \in \mathbb{R}_{>0}$, the missing interface condition is

$$\pm\,\alpha_\pm\,\mathcal{D}_\pm\,\nabla\,\phi_\pm\,.\,\vec{\nu} = -[F'(\psi) - G'_\pm(\phi_\pm)] \qquad \text{on } \Gamma(t)\,, \tag{2.13}$$

which couples ψ and $\phi_\pm$. This equation relates the bulk fluxes to differences of the chemical potentials $F'(\psi), G'(\phi_+), G'(\phi_-)$, see Garcke *et al.* (2014). Here $G_\pm \in C(\mathbb{R}_{\geq 0}) \cap C^2(\mathbb{R}_{>0})$ are bulk free energy densities that satisfy

$$G''_\pm(s) \geq 0 \qquad \forall\ s \in \mathbb{R}_{>0}\,. \tag{2.14}$$

We observe that $\alpha_\pm \in \mathbb{R}_{>0}$ relax the so-called instantaneous conditions (2.13) with $\alpha_\pm = 0$, which yield an algebraic relationship between ψ and $\phi_\pm$ on $\Gamma(t)$, namely

$$F'(\psi) = G'_-(\phi_-) = G'_+(\phi_+) \qquad \text{on } \Gamma(t)\,. \tag{2.15}$$

A typical example for $G_\pm$ is

$$G_\pm(r) = \gamma_0\,\beta\,r\,[\ln(\theta_\pm\,r) - 1]\,, \tag{2.16}$$

where $\theta_\pm \in \mathbb{R}_{>0}$. In this case the identity $G'_-(\phi_-) = G'_+(\phi_+)$ in (2.15) leads to *Henry's law*

$$\phi_+ = K_H\,\phi_-\,, \tag{2.17}$$

with the Henry constant $K_H = \theta_-/\theta_+$. In order to make (2.13) well-defined, we assume from now on, and throughout this paper, that

$$\psi(\cdot,t) \in (0,\psi_\infty) \quad \text{and} \quad \phi_\pm(\cdot,t) > 0 \qquad \text{on } \Gamma(t)\,. \tag{2.18}$$

We remark that on combining (2.12b) with (2.16), the interface condition (2.13) for the outer phase, say, reduces to

$$\begin{aligned}
\alpha_+\,\mathcal{D}_+\,\nabla\,\phi_+\,.\,\vec{\nu} &= -[F'(\psi) - G'_+(\phi_+)] \\
&= \gamma_0\,\beta\,\ln\frac{\theta_+\,\phi_+\,(\psi_\infty - \psi)}{\psi} \\
&\approx \gamma_0\,\beta\left[\frac{\theta_+\,\phi_+\,(\psi_\infty - \psi)}{\psi} - 1\right] = \frac{\gamma_0\,\beta}{\psi}\,[\theta_+\,\phi_+\,(\psi_\infty - \psi) - \psi]\,,
\end{aligned} \tag{2.19}$$

where we have used the approximation $\ln(1+r) \approx r$ for $|r| \ll 1$. Clearly the condition (2.19) is closely related to conditions proposed by other authors. See e.g. the conditions in Muradoglu and Tryggvason (2008), Alke and Bothe (2009), Teigen *et al.* (2011), Ganesan and Tobiska (2012, (5)), Xu *et al.* (2013), and the kinetic condition in Diamant and Andelman (1996, (2.14)); see also Diamant and Andelman (1996, (23)).

Generalizing the work of Diamant and Andelman (1996) the model (2.3a-e), (2.4), (2.5a,b), (2.8a-c) was supplemented with (2.13) in a paper by Garcke *et al.* (2014). We will see in Subsection 6.1.1 that close to the equilibrium this model is related to the classical equilibrium condition (2.19) studied by the above authors. The important feature of (2.13) is that it allows for an energy inequality, see Garcke *et al.* (2014) and (3.17).

The system (2.3a–e), (2.4), (2.5a,b), (2.8a–c), (2.13) is closed with the initial conditions

$$\begin{aligned} &\Gamma(0) = \Gamma_0\,, \qquad \psi(\cdot,0) = \psi_0 \qquad \text{on } \Gamma_0\,, \qquad \phi_\pm(\cdot,0) = \phi_{\pm,0} \qquad \text{in } \Omega_\pm(0)\,, \\ &\vec{u}(\cdot,0) = \vec{u}_0 \qquad \text{in } \Omega\,, \end{aligned} \tag{2.20}$$

where $\Gamma_0 \subset \Omega$, $\vec{u}_0 : \Omega \to \mathbb{R}^d$, with $\nabla \,.\, \vec{u}_0 = 0$, $\phi_{\pm,0} : \Omega_\pm(0) \to \mathbb{R}_{\geq 0}$, and $\psi_0 : \Gamma_0 \to (0, \psi_\infty)$ are given initial data.

3 Weak formulations

Before introducing our finite element approximations, we will state an appropriate weak formulation. With this in mind, we introduce the function spaces

$$\begin{aligned} &\mathbb{U} := \{\vec{\varphi} \in [H^1(\Omega)]^d : \vec{\varphi} = \vec{0} \text{ on } \partial_1\Omega\,,\ \vec{\varphi}\,.\,\vec{\mathrm{n}} = 0 \text{ a.e. on } \partial_2\Omega\}\,, \quad \mathbb{P} := L^2(\Omega)\,, \\ &\widehat{\mathbb{P}} := \{\eta \in \mathbb{P} : \int_\Omega \eta \,\mathrm{d}\mathcal{L}^d = 0\}\,, \quad \mathbb{V} := L^2(0,T;\mathbb{U}) \cap H^1(0,T;[L^2(\Omega)]^d)\,, \quad \mathbb{S} := H^1(\mathcal{G}_T)\,, \\ &\mathbb{T} := L^2(0,T;H^1(\Omega)) \cap H^1(0,T;H^{-1}(\Omega))\,, \quad \mathbb{T}_\pm := H^1(\mathcal{Q}_{T,\pm})\,, \end{aligned}$$

where, similarly to (2.2), we define

$$\mathcal{Q}_{T,\pm} := \bigcup_{t\in[0,T]} \Omega_\pm(t) \times \{t\}\,.$$

Let $(\cdot,\cdot)$, $(\cdot,\cdot)_{\Omega_\pm(t)}$ and $\langle\cdot,\cdot\rangle_{\Gamma(t)}$ denote the L^2–inner products on Ω, $\Omega_\pm(t)$ and $\Gamma(t)$, respectively.

We recall from Barrett *et al.* (2014) that it follows from (2.3b–e) and (2.5b) that

$$(\rho\,(\vec{u}\,.\,\nabla)\,\vec{u}, \vec{\xi}) = \tfrac{1}{2}\left[(\rho\,(\vec{u}\,.\,\nabla)\,\vec{u}, \vec{\xi}) - (\rho\,(\vec{u}\,.\,\nabla)\,\vec{\xi}, \vec{u}) - \left\langle [\rho]^+_- \,\vec{u}\,.\,\vec{\nu}, \vec{u}\,.\,\vec{\xi}\right\rangle_{\Gamma(t)}\right] \qquad \forall\ \vec{\xi} \in [H^1(\Omega)]^d \tag{3.1}$$

and

$$\frac{\mathrm{d}}{\mathrm{d}t}(\rho\,\vec{u},\vec{\xi}) = (\rho\,\vec{u}_t,\vec{\xi}) + (\rho\,\vec{u},\vec{\xi}_t) - \left\langle [\rho]^+_-\,\vec{u}\,.\,\vec{\nu},\vec{u}\,.\,\vec{\xi}\right\rangle_{\Gamma(t)} \qquad \forall\ \vec{\xi}\in\mathbb{V}\,,$$

respectively. Therefore, it holds that

$$(\rho\,\vec{u}_t,\vec{\xi}) = \tfrac{1}{2}\left[\frac{\mathrm{d}}{\mathrm{d}t}(\rho\,\vec{u},\vec{\xi}) + (\rho\,\vec{u}_t,\vec{\xi}) - (\rho\,\vec{u},\vec{\xi}_t) + \left\langle [\rho]^+_-\,\vec{u}\,.\,\vec{\nu},\vec{u}\,.\,\vec{\xi}\right\rangle_{\Gamma(t)}\right] \qquad \forall\ \vec{\xi}\in\mathbb{V}\,,$$

which on combining with (3.1) yields that

$$\begin{aligned}&(\rho\,[\vec{u}_t + (\vec{u}\,.\,\nabla)\,\vec{u}],\vec{\xi})\\ &\quad = \tfrac{1}{2}\left[\frac{\mathrm{d}}{\mathrm{d}t}(\rho\,\vec{u},\vec{\xi}) + (\rho\,\vec{u}_t,\vec{\xi}) - (\rho\,\vec{u},\vec{\xi}_t) + (\rho,[(\vec{u}\,.\,\nabla)\,\vec{u}]\,.\,\vec{\xi} - [(\vec{u}\,.\,\nabla)\,\vec{\xi}]\,.\,\vec{u})\right] \quad \forall\ \vec{\xi}\in\mathbb{V}\,.\end{aligned} \tag{3.2}$$

Moreover, it holds on noting (2.3e) and (2.5a) that for all $\vec{\xi}\in\mathbb{U}$

$$\int_{\Omega_+(t)\cup\Omega_-(t)} (\nabla\,.\,\underline{\underline{\sigma}})\,.\,\vec{\xi}\,\mathrm{d}\mathcal{L}^d = -2\,(\mu\,\underline{\underline{D}}(\vec{u}),\underline{\underline{D}}(\vec{\xi})) + (p,\nabla\,.\,\vec{\xi}) + \left\langle \gamma(\psi)\,\varkappa\,\vec{\nu} + \nabla_s\,\gamma(\psi),\vec{\xi}\right\rangle_{\Gamma(t)}\,. \tag{3.3}$$

Similarly to (2.9) we define the following time derivative that follows the parameterization $\vec{x}(\cdot,t)$ of $\Gamma(t)$, rather than $\vec{u}$. In particular, we let

$$\partial_t^\circ\,\zeta = \zeta_t + \vec{\mathcal{V}}\,.\,\nabla\,\zeta \qquad \forall\ \zeta\in\mathbb{S}\,, \tag{3.4}$$

recall (2.1). Here we stress once again that this definition is well-defined, even though ζ_t and $\nabla\,\zeta$ do not make sense separately for a function $\zeta\in\mathbb{S}$. On recalling (2.9) we obtain that

$$\partial_t^\circ = \partial_t^\bullet \qquad \text{if} \qquad \vec{\mathcal{V}} = \vec{u} \quad \text{on } \Gamma(t)\,. \tag{3.5}$$

We note that the definition (3.4) differs from the definition of ∂° in Dziuk and Elliott (2013, p. 327), where $\partial^\circ\,\zeta = \zeta_t + (\vec{\mathcal{V}}\,.\,\vec{\nu})\,\vec{\nu}\,.\,\nabla\,\zeta$ for the "normal time derivative". It holds that

$$\frac{\mathrm{d}}{\mathrm{d}t}\,\langle\chi,\zeta\rangle_{\Gamma(t)} = \langle\partial_t^\circ\,\chi,\zeta\rangle_{\Gamma(t)} + \langle\chi,\partial_t^\circ\,\zeta\rangle_{\Gamma(t)} + \left\langle\chi\,\zeta,\nabla_s\,.\,\vec{\mathcal{V}}\right\rangle_{\Gamma(t)} \qquad \forall\ \chi,\zeta\in\mathbb{S}\,, \tag{3.6}$$

see Dziuk and Elliott (2013, Lem. 5.2), and that

$$\langle\zeta,\nabla_s\,.\,\vec{\eta}\rangle_{\Gamma(t)} + \langle\nabla_s\,\zeta,\vec{\eta}\rangle_{\Gamma(t)} = -\,\langle\zeta\,\vec{\eta},\vec{\varkappa}\rangle_{\Gamma(t)} \qquad \forall\ \zeta\in H^1(\Gamma(t)),\ \vec{\eta}\in[H^1(\Gamma(t))]^d\,, \tag{3.7}$$

see Dziuk and Elliott (2013, Def. 2.11). In addition, it holds that

$$\frac{\mathrm{d}}{\mathrm{d}t}\,(\xi,1)_{\Omega_\pm(t)} = (\xi_t,1)_{\Omega_\pm(t)} \mp \left\langle\vec{\mathcal{V}},\xi\,\vec{\nu}\right\rangle_{\Gamma(t)} \qquad \forall\ \xi\in\mathbb{T}_\pm\,. \tag{3.8}$$

Moreover, it follows from (3.8), (2.3b,d,e) and (2.5b) that

$$\frac{\mathrm{d}}{\mathrm{d}t}\,(\xi,1)_{\Omega_\pm(t)} = (\xi_t + \vec{u}\,.\,\nabla\,\xi,1)_{\Omega_\pm(t)} \qquad \forall\ \xi\in\mathbb{T}_\pm\,. \tag{3.9}$$

3.1 Weak formulations with fluidic tangential velocity

In this subsection, we consider weak formulations based on imposing $\vec{\mathcal{V}} = \vec{u}$ on $\Gamma(t)$ as opposed to just $\vec{\mathcal{V}} \,.\, \vec{\nu} = \vec{u} \,.\, \vec{\nu}$ on $\Gamma(t)$, recall (2.5b).

3.1.1 Model (i) — The two-sided relaxed model

The natural weak formulation of the system (2.3a–e), (2.4), (2.5a,b), (2.8a–c) is then given as follows. Find $\Gamma(t) = \vec{x}(\Upsilon, t)$ for $t \in [0,T]$ with $\vec{\mathcal{V}} \in [L^2(\mathcal{G}_T)]^d$, and functions $\vec{u} \in \mathbb{V}$, $p \in L^2(0,T;\widehat{\mathbb{P}})$, $\vec{\varkappa} \in [L^2(\mathcal{G}_T)]^d$, $\phi_\pm \in \mathbb{T}_\pm$ and $\psi \in \mathbb{S}$ such that for almost all $t \in (0,T)$ it holds that

$$\begin{aligned}
&\tfrac{1}{2}\left[\frac{\mathrm{d}}{\mathrm{d}t}(\rho\,\vec{u},\vec{\xi}) + (\rho\,\vec{u}_t,\vec{\xi}) - (\rho\,\vec{u},\vec{\xi}_t) + (\rho,[(\vec{u}\,.\,\nabla)\,\vec{u}]\,.\,\vec{\xi} - [(\vec{u}\,.\,\nabla)\,\vec{\xi}]\,.\,\vec{u})\right] \\
&\qquad + 2\,(\mu\,\underline{\underline{D}}(\vec{u}),\underline{\underline{D}}(\vec{\xi})) - (p,\nabla\,.\,\vec{\xi}) - \left\langle \gamma(\psi)\,\vec{\varkappa} + \nabla_s\,\gamma(\psi),\vec{\xi}\right\rangle_{\Gamma(t)} = (\vec{f},\vec{\xi}) \qquad \forall\ \vec{\xi} \in \mathbb{V}\,,
\end{aligned} \tag{3.10a}$$

$$(\nabla\,.\,\vec{u},\varphi) = 0 \qquad \forall\ \varphi \in \widehat{\mathbb{P}}\,, \tag{3.10b}$$

$$\left\langle \vec{\mathcal{V}} - \vec{u},\vec{\chi}\right\rangle_{\Gamma(t)} = 0 \qquad \forall\ \vec{\chi} \in [L^2(\Gamma(t))]^d\,, \tag{3.10c}$$

$$\langle \vec{\varkappa},\vec{\eta}\rangle_{\Gamma(t)} + \left\langle \nabla_s\,\mathrm{i}\vec{\mathrm{d}},\nabla_s\,\vec{\eta}\right\rangle_{\Gamma(t)} = 0 \qquad \forall\ \vec{\eta} \in [H^1(\Gamma(t))]^d\,, \tag{3.10d}$$

$$\begin{aligned}
&(\partial_t\,\phi_\pm + \vec{u}\,.\,\nabla\,\phi_\pm,\xi)_{\Omega_\pm(t)} + \mathcal{D}_\pm\,(\nabla\,\phi_\pm,\nabla\,\xi)_{\Omega_\pm(t)} + \int_{\partial\Omega} \lambda_\pm\,(\phi_\pm - g_\pm)\,\xi\,\mathrm{d}\mathcal{H}^{d-1} \\
&\qquad = \frac{1}{\alpha_\pm}\left\langle F'(\psi) - G'_\pm(\phi_\pm),\xi\right\rangle_{\Gamma(t)} \qquad \forall\ \xi \in H^1(\Omega_\pm(t))\,,
\end{aligned} \tag{3.10e}$$

$$\begin{aligned}
&\frac{\mathrm{d}}{\mathrm{d}t}\,\langle\psi,\zeta\rangle_{\Gamma(t)} + \mathcal{D}_\Gamma\,\langle\nabla_s\,\psi,\nabla_s\,\zeta\rangle_{\Gamma(t)} = \langle\psi,\partial_t^\circ\,\zeta\rangle_{\Gamma(t)} - \sum_{i\in\{\pm\}} \frac{1}{\alpha_i}\,\langle F'(\psi) - G'_i(\phi_i),\zeta\rangle_{\Gamma(t)} \\
&\qquad\qquad \forall\ \zeta \in \mathbb{S}\,,
\end{aligned} \tag{3.10f}$$

as well as the initial conditions (2.20), where in (3.10c) we have recalled (2.1). Here (3.10a–d) can be derived analogously to the weak formulation presented in Barrett *et al.* (2014), recall (3.2) and (3.3), while (3.10e,f) are a direct consequence of (2.8a–c) and (2.13), recall (3.6) and (3.7). Of course, it follows from (3.10c) and (3.5) that ∂_t° in (3.10f) can be replaced by $\partial_t^\bullet$.

In what follows we would like to derive an energy bound for a solution of (3.10a–f). All of the following considerations are formal, in the sense that we make the appropriate assumptions about the existence, boundedness and regularity of a solution to (3.10a–f). In particular, we assume that (2.18) holds. Choosing $\vec{\xi} = \vec{u}$ in (3.10a) and $\varphi = p(\cdot,t)$ in (3.10b) yields that

$$\tfrac{1}{2}\,\frac{\mathrm{d}}{\mathrm{d}t}\,\|\rho^{\frac{1}{2}}\,\vec{u}\|_0^2 + 2\,\|\mu^{\frac{1}{2}}\,\underline{\underline{D}}(\vec{u})\|_0^2 = (\vec{f},\vec{u}) + \langle\gamma(\psi)\,\vec{\varkappa} + \nabla_s\,\gamma(\psi),\vec{u}\rangle_{\Gamma(t)}\,. \tag{3.11}$$

Choosing $\zeta = F'(\psi)$ in (3.10f), which is well-defined on recalling (2.18), and $\xi = G'_\pm(\phi_\pm)$ in (3.10e) we obtain, on recalling (2.10a), that

$$\begin{aligned}
&\frac{\mathrm{d}}{\mathrm{d}t} \left\langle F(\psi) - \gamma(\psi), 1 \right\rangle_{\Gamma(t)} + \mathcal{D}_\Gamma \left\langle \nabla_s \psi, \nabla_s F'(\psi) \right\rangle_{\Gamma(t)} \\
&\quad + \sum_{i \in \{\pm\}} \left\{ \left(\partial_t \phi_i + \vec{u} \,.\, \nabla \phi_i, G'_i(\phi_i) \right)_{\Omega_i(t)} + \mathcal{D}_i \left(\nabla \phi_i, \nabla G'_i(\phi_i) \right)_{\Omega_i(t)} \right. \\
&\qquad \left. + \frac{1}{\alpha_i} \left\langle |F'(\psi) - G'_i(\phi_i)|^2, 1 \right\rangle_{\Gamma(t)} \right\} \\
&\quad + \int_{\partial\Omega} \lambda_+ \left(\phi_+ - g_+ \right) G'_+(\phi_+) \, \mathrm{d}\mathcal{H}^{d-1} = \left\langle \psi, \partial_t^\circ \, F'(\psi) \right\rangle_{\Gamma(t)} \,. \qquad (3.12)
\end{aligned}$$

Moreover, choosing $\chi = \gamma(\psi)$, $\zeta = 1$ in (3.6), and then choosing $\vec{\eta} = \vec{\mathcal{V}}$, $\zeta = \gamma(\psi)$ in (3.7) gives that

$$\begin{aligned}
\frac{\mathrm{d}}{\mathrm{d}t} \left\langle \gamma(\psi), 1 \right\rangle_{\Gamma(t)} &= \left\langle \partial_t^\circ \, \gamma(\psi), 1 \right\rangle_{\Gamma(t)} + \left\langle \gamma(\psi), \nabla_s \,.\, \vec{\mathcal{V}} \right\rangle_{\Gamma(t)} \\
&= \left\langle \partial_t^\circ \, \gamma(\psi), 1 \right\rangle_{\Gamma(t)} - \left\langle \gamma(\psi) \, \vec{\varkappa} + \nabla_s \, \gamma(\psi), \vec{\mathcal{V}} \right\rangle_{\Gamma(t)} \,. \qquad (3.13)
\end{aligned}$$

In addition, it follows from (2.11) that

$$\partial_t^\circ \, \gamma(\psi) = \gamma'(\psi) \, \partial_t^\circ \, \psi = -\psi \, F''(\psi) \, \partial_t^\circ \, \psi = -\psi \, \partial_t^\circ \, F'(\psi) \,. \qquad (3.14)$$

On choosing $\xi = G_\pm(\phi_\pm)$ in (3.9), it holds that

$$\begin{aligned}
\frac{\mathrm{d}}{\mathrm{d}t} \left(G_\pm(\phi_\pm), 1 \right)_{\Omega_\pm(t)} &= \left(\partial_t \, G_\pm(\phi_\pm) + \vec{u} \,.\, \nabla G_\pm(\phi_\pm), 1 \right)_{\Omega_\pm(t)} \\
&= \left(\partial_t \, \phi_\pm + \vec{u} \,.\, \nabla \, \phi_\pm, G'_\pm(\phi_\pm) \right)_{\Omega_\pm(t)} \,. \qquad (3.15)
\end{aligned}$$

Combining (3.12), (3.13), (3.14) and (3.15) yields that

$$\begin{aligned}
&\frac{\mathrm{d}}{\mathrm{d}t} \left\langle F(\psi), 1 \right\rangle_{\Gamma(t)} + \mathcal{D}_\Gamma \left\langle \nabla_s \, \mathcal{F}(\psi), \nabla_s \, \mathcal{F}(\psi) \right\rangle_{\Gamma(t)} \\
&\quad + \sum_{i \in \{\pm\}} \left\{ \frac{\mathrm{d}}{\mathrm{d}t} \left(G_i(\phi_i), 1 \right)_{\Omega_i(t)} + \mathcal{D}_i \left(\nabla \, \mathcal{B}_i(\phi_i), \nabla \, \mathcal{B}_i(\phi_i) \right)_{\Omega_i(t)} + \frac{1}{\alpha_i} \left\langle |F'(\psi) - G'_i(\phi_i)|^2, 1 \right\rangle_{\Gamma(t)} \right\} \\
&\qquad + \int_{\partial\Omega} \lambda_+ \left(\phi_+ - g_+ \right) G'_+(\phi_+) \, \mathrm{d}\mathcal{H}^{d-1} = - \left\langle \gamma(\psi) \, \vec{\varkappa} + \nabla_s \, \gamma(\psi), \vec{\mathcal{V}} \right\rangle_{\Gamma(t)} \,, \qquad (3.16)
\end{aligned}$$

where, on recalling (2.11), (2.6) and (2.14),

$$\mathcal{F}(r) = \int_0^r [F''(y)]^{\frac{1}{2}} \, \mathrm{d}y \quad \text{and} \quad \mathcal{B}_\pm(r) = \int_0^r [G''_\pm(y)]^{\frac{1}{2}} \, \mathrm{d}y \,.$$

Combining (3.16) with (3.11) implies the a priori energy bound

$$\begin{aligned}
&\frac{\mathrm{d}}{\mathrm{d}t}\left(\tfrac{1}{2}\,\|\rho^{\frac{1}{2}}\,\vec{u}\|_0^2+\sum_{i\in\{\pm\}}(G_i(\phi_i),1)_{\Omega_i(t)}+\langle F(\psi),1\rangle_{\Gamma(t)}\right)+2\,\|\mu^{\frac{1}{2}}\,\underline{\underline{D}}(\vec{u})\|_0^2\\
&\quad+\mathcal{D}_\Gamma\,\langle\nabla_s\,\mathcal{F}(\psi),\nabla_s\,\mathcal{F}(\psi)\rangle_{\Gamma(t)}+\int_{\partial\Omega}\lambda_+\,G_+(\phi_+)\,\mathrm{d}\mathcal{H}^{d-1}\\
&\quad+\sum_{i\in\{\pm\}}\left\{\mathcal{D}_i\,(\nabla\,\mathcal{B}_i(\phi_i),\nabla\,\mathcal{B}_i(\phi_i))_{\Omega_i(t)}+\frac{1}{\alpha_i}\,\big\langle|F'(\psi)-G_i'(\phi_i)|^2,1\big\rangle_{\Gamma(t)}\right\}\\
&\qquad\le(\vec{f},\vec{u})+\int_{\partial\Omega}\lambda_+\,G_+(g_+)\,\mathrm{d}\mathcal{H}^{d-1}\,.
\end{aligned}\tag{3.17}$$

Moreover, the volume of $\Omega_-(t)$ is preserved in time, i.e. the mass of each phase is conserved. To see this, choose $\xi=1$ in (3.8), $\vec{\chi}=\vec{\nu}$ in (3.10c) and $\varphi=\mathcal{X}_{\Omega_-(t)}$ in (3.10b) to obtain

$$\frac{\mathrm{d}}{\mathrm{d}t}\,\mathcal{L}^d(\Omega_-(t))=\left\langle\vec{\mathcal{V}},\vec{\nu}\right\rangle_{\Gamma(t)}=\langle\vec{u},\vec{\nu}\rangle_{\Gamma(t)}=\int_{\Omega_-(t)}\nabla\,.\,\vec{u}\,\mathrm{d}\mathcal{L}^d=0\,.\tag{3.18}$$

In addition, we note that it immediately follows from choosing $\xi=1$ in (3.10e) and $\zeta=1$ in (3.10f), on recalling (3.9) for $\xi=\phi_\pm$, that

$$\frac{\mathrm{d}}{\mathrm{d}t}\left(\sum_{i\in\{\pm\}}(\phi_i,1)_{\Omega_i(t)}+\langle\psi,1\rangle_{\Gamma(t)}\right)=\int_{\partial\Omega}\lambda_+\,(g_+-\phi_+)\,\mathrm{d}\mathcal{H}^{d-1}\,,\tag{3.19}$$

e.g. the total amount of surfactant is preserved if $\lambda_+=0$.

The one-sided relaxed models

The one-sided variants of the model considered so far, e.g. when no soluble surfactant is present in the inner phase $\Omega_-(t)$, is given by (2.3a–e), (2.4), (2.5a,b), (2.20) and (2.8a) with "$\pm$" replaced by "+", (2.8b) with right hand side $\mathcal{D}_+\,\nabla\,\phi_+\,.\,\vec{\nu}$, and (2.8c). In the weak formulation we replace any occurrence of "$\pm$" in (3.10a–f) with "+". Clearly, (3.18) remains valid in this case. The formal energy bound (3.17) also remains valid in the one-sided case, where, as before, the summation in the two sums reduces to "$i=+$". A similar amendment to (3.19) means that its analogue is also valid in the one-sided case.

Of course, the inner one-sided situation, when no surfactant is present in the outer phase $\Omega_+(t)$, can also be considered.

3.1.2 Model (ii) — The global relaxed model

In this subsection we consider the system (2.3a–e), (2.4), (2.5a,b), (2.8a–c), (2.13) with the additional conditions that

$$G_-(r)=G_+(r)=G(r)\qquad\forall\ r\in\mathbb{R}\quad\text{and}\quad[\phi]_-^+=0\qquad\text{on}\ \ \Gamma(t)\,,\tag{3.20}$$

where $[\phi]^+_- = \phi_+ - \phi_-$. Then the weak formulation corresponding to (3.10a–f) is given as follows. Find $\Gamma(t) = \vec{x}(\Upsilon, t)$ for $t \in [0,T]$ with $\vec{\mathcal{V}} \in [L^2(\mathcal{G}_T)]^d$, and functions $\vec{u} \in \mathbb{V}$, $p \in L^2(0,T;\widehat{\mathbb{P}})$, $\vec{\varkappa} \in [L^2(\mathcal{G}_T)]^d$, $\phi \in \mathbb{T}$ and $\psi \in \mathbb{S}$ such that for almost all $t \in (0,T)$ we have that (3.10a–d) and

$$(\phi_t, \xi) - (\vec{u}, \phi \nabla \xi) + (\mathcal{D} \nabla \phi, \nabla \xi) + \int_{\partial\Omega} \lambda_+ (\phi - g_+) \xi \, \mathrm{d}\mathcal{H}^{d-1} = \left(\frac{1}{\alpha_-} + \frac{1}{\alpha_+}\right) \langle F'(\psi) - G'(\phi), \xi \rangle_{\Gamma(t)} \qquad \forall\, \xi \in H^1(\Omega)\,, \quad (3.21a)$$

$$\frac{\mathrm{d}}{\mathrm{d}t} \langle \psi, \zeta \rangle_{\Gamma(t)} + \mathcal{D}_\Gamma \langle \nabla_s \psi, \nabla_s \zeta \rangle_{\Gamma(t)} = \langle \psi, \partial_t^\circ \zeta \rangle_{\Gamma(t)} - \left(\frac{1}{\alpha_-} + \frac{1}{\alpha_+}\right) \langle F'(\psi) - G'(\phi), \zeta \rangle_{\Gamma(t)} \qquad \forall\, \zeta \in \mathbb{S} \quad (3.21b)$$

hold as well as the initial conditions (2.20) without the subscript $\pm$, and where $\mathcal{D}(t) = \mathcal{D}_+ \mathcal{X}_{\Omega_+(t)} + \mathcal{D}_- \mathcal{X}_{\Omega_-(t)}$. Note that in order to motivate later developments, in (3.21a) we have rewritten the convective term as

$$(\vec{u} \,.\, \nabla \phi, \xi) = (\nabla \,.\, (\phi\, \vec{u}), \xi) = -(\vec{u}, \phi \nabla \xi) \qquad \forall\, \xi \in H^1(\Omega)\,,$$

where we have recalled (2.3b,d,e).

The conservation property (3.18) still holds, and (3.19) simplifies to

$$\frac{\mathrm{d}}{\mathrm{d}t} \Big((\phi, 1) + \langle \psi, 1 \rangle_{\Gamma(t)} \Big) = \int_{\partial\Omega} \lambda_+ \, (g_+ - \phi) \, \mathrm{d}\mathcal{H}^{d-1}\,. \quad (3.22)$$

Moreover, the formal energy bound (3.17) now simplifies to

$$\begin{aligned} &\frac{\mathrm{d}}{\mathrm{d}t} \Big(\tfrac{1}{2} \, \|\rho^{\frac{1}{2}} \, \vec{u}\|_0^2 + (G(\phi), 1) + \langle F(\psi), 1 \rangle_{\Gamma(t)} \Big) + 2 \, \|\mu^{\frac{1}{2}} \, \underline{\underline{D}}(\vec{u})\|_0^2 + \mathcal{D}_\Gamma \, \langle \nabla_s \mathcal{F}(\psi), \nabla_s \mathcal{F}(\psi) \rangle_{\Gamma(t)} \\ &\quad + \int_{\partial\Omega} \lambda_+ \, G(\phi) \, \mathrm{d}\mathcal{H}^{d-1} + (\mathcal{D} \nabla \mathcal{B}(\phi), \nabla \mathcal{B}(\phi)) + \left(\frac{1}{\alpha_-} + \frac{1}{\alpha_+}\right) \big\langle |F'(\psi) - G'(\phi)|^2, 1 \big\rangle_{\Gamma(t)} \\ &\quad \leq (\vec{f}, \vec{u}) + \int_{\partial\Omega} \lambda_+ \, G(g_+) \, \mathrm{d}\mathcal{H}^{d-1}\,. \end{aligned} \quad (3.23)$$

To deduce this, we first observe that (3.11) still holds and (3.12) here takes the form

$$\begin{aligned} &\frac{\mathrm{d}}{\mathrm{d}t} \langle F(\psi) - \gamma(\psi), 1 \rangle_{\Gamma(t)} + \mathcal{D}_\Gamma \, \langle \nabla_s \psi, \nabla_s F'(\psi) \rangle_{\Gamma(t)} + (\phi_t, G'(\phi)) - (\vec{u}\, \phi, \nabla G'(\phi)) \\ &\quad + (\mathcal{D} \nabla \phi, \nabla G'(\phi)) + \left(\frac{1}{\alpha_-} + \frac{1}{\alpha_+}\right) \big\langle |F'(\psi) - G'(\phi)|^2, 1 \big\rangle_{\Gamma(t)} \\ &\quad + \int_{\partial\Omega} \lambda_+ \, (\phi - g_+) \, G'(\phi) \, \mathrm{d}\mathcal{H}^{d-1} = \langle \psi, \partial_t^\circ \, F'(\psi) \rangle_{\Gamma(t)}\,. \end{aligned} \quad (3.24)$$

The results (3.13) and (3.14) hold as before, while (3.15) reduces to

$$\frac{\mathrm{d}}{\mathrm{d}t} \, (G(\phi), 1) = (\phi_t, G'(\phi))\,. \quad (3.25)$$

Finally, on recalling (2.14), we introduce $R' = (G')^{-1}$ and then note from (2.3b,d,e) that

$$\begin{aligned} -(\vec{u}, \phi \nabla G'(\phi)) &= -(\vec{u}, R'(G'(\phi)) \nabla G'(\phi)) = -(\vec{u}, \nabla R(G'(\phi))) \\ &= (\nabla . \vec{u}, R(G'(\phi))) = 0 \,. \end{aligned} \tag{3.26}$$

For example, for the choice (2.16) we obtain that $R(r) = \frac{\gamma_0 \beta}{\theta} \exp \frac{r}{\gamma_0 \beta}$. We remark that it does not appear possible to mimic (3.9), which is required in (3.15) to prove the energy bound (3.17) for model (i), for a finite element approximation. However, it is possible to mimic (3.25) and (3.26). Hence in Section 4, we are able to prove a discrete energy bound for our finite element approximations of model (ii) in the case $d = 2$, but not for model (i). The restriction to $d = 2$ is required to mimic (3.13) at a discrete level.

3.2 Weak formulations with free tangential velocity

We note that, in contrast to (3.5), if we relax $\vec{\mathcal{V}} = \vec{u}|_{\Gamma(t)}$ to

$$\vec{\mathcal{V}} . \vec{\nu} = \vec{u} . \vec{\nu} \quad \text{on } \Gamma(t) \,,$$

as in (2.5b), then it holds that

$$\partial_t^\circ \zeta = \partial_t^\bullet \zeta + (\vec{\mathcal{V}} - \vec{u}) . \nabla_s \zeta \qquad \forall \, \zeta \in \mathbb{S} \,. \tag{3.27}$$

3.2.1 Model (i)

Our preferred finite element approximation will be based on the following weak formulation. Find $\Gamma(t) = \vec{x}(\Upsilon, t)$ for $t \in [0, T]$ with $\vec{\mathcal{V}} \in [L^2(\mathcal{G}_T)]^d$, and functions $\vec{u} \in \mathbb{V}$, $p \in L^2(0, T; \widehat{\mathbb{P}})$, $\varkappa \in L^2(\mathcal{G}_T)$, $\phi_\pm \in \mathbb{T}_\pm$ and $\psi \in \mathbb{S}$ such that for almost all $t \in (0, T)$ it

holds that

$$\tfrac{1}{2}\left[\frac{\mathrm{d}}{\mathrm{d}t}(\rho\,\vec{u},\vec{\xi}) + (\rho\,\vec{u}_t,\vec{\xi}) - (\rho\,\vec{u},\vec{\xi}_t) + (\rho,[(\vec{u}\,.\,\nabla)\,\vec{u}]\,.\,\vec{\xi} - [(\vec{u}\,.\,\nabla)\,\vec{\xi}]\,.\,\vec{u})\right]$$
$$+ 2\,(\mu\,\underline{\underline{D}}(\vec{u}),\underline{\underline{D}}(\vec{\xi})) - (p,\nabla\,.\,\vec{\xi}) - \left\langle\gamma(\psi)\,\varkappa\,\vec{\nu} + \nabla_s\,\gamma(\psi),\vec{\xi}\right\rangle_{\Gamma(t)} = (\vec{f},\vec{\xi}) \qquad \forall\ \vec{\xi}\in\mathbb{V}\,, \tag{3.28a}$$

$$(\nabla\,.\,\vec{u},\varphi) = 0 \qquad \forall\ \varphi\in\widehat{\mathbb{P}}\,, \tag{3.28b}$$

$$\left\langle\vec{\mathcal{V}} - \vec{u},\chi\,\vec{\nu}\right\rangle_{\Gamma(t)} = 0 \qquad \forall\ \chi\in L^2(\Gamma(t))\,, \tag{3.28c}$$

$$\langle\varkappa\,\vec{\nu},\vec{\eta}\rangle_{\Gamma(t)} + \left\langle\nabla_s\,\vec{\mathrm{id}},\nabla_s\,\vec{\eta}\right\rangle_{\Gamma(t)} = 0 \qquad \forall\ \vec{\eta}\in[H^1(\Gamma(t))]^d\,, \tag{3.28d}$$

$$(\partial_t\,\phi_\pm + \vec{u}\,.\,\nabla\,\phi_\pm,\xi)_{\Omega_\pm(t)} + \mathcal{D}_\pm\,(\nabla\,\phi_\pm,\nabla\,\xi)_{\Omega_\pm(t)} + \int_{\partial\Omega}\lambda_\pm\,(\phi_\pm - g_\pm)\,\xi\,\mathrm{d}\mathcal{H}^{d-1}$$
$$= \frac{1}{\alpha_\pm}\left\langle F'(\psi) - G'_\pm(\phi_\pm),\xi\right\rangle_{\Gamma(t)} \qquad \forall\ \xi\in H^1(\Omega_\pm(t))\,, \tag{3.28e}$$

$$\frac{\mathrm{d}}{\mathrm{d}t}\,\langle\psi,\zeta\rangle_{\Gamma(t)} + \mathcal{D}_\Gamma\,\langle\nabla_s\,\psi,\nabla_s\,\zeta\rangle_{\Gamma(t)} + \left\langle\psi\,(\vec{\mathcal{V}} - \vec{u}),\nabla_s\,\zeta\right\rangle_{\Gamma(t)}$$
$$= \langle\psi,\partial_t^\circ\,\zeta\rangle_{\Gamma(t)} - \sum_{i\in\{\pm\}}\frac{1}{\alpha_i}\,\langle F'(\psi) - G'_i(\phi_i),\zeta\rangle_{\Gamma(t)} \qquad \forall\ \zeta\in\mathbb{S}\,, \tag{3.28f}$$

as well as the initial conditions (2.20), where in (3.28c,f) we have recalled (2.1). The derivation of (3.28a–d) is analogous to the derivation of (3.10a–d), while for the formulation (3.28f) we note it is clearly consistent with (3.10f) because the latter holds with ∂_t° replaced by $\partial_t^\bullet$, and so the desired result follows immediately from (3.27).

Similarly to (3.11)–(3.17), we can formally show that a solution to (3.28a–f) satisfies the a priori energy bound (3.17). First of all we note that since $\vec{\varkappa} = \varkappa\,\vec{\nu}$, a solution to (3.28a–f) satisfies (3.11). Secondly we observe that the analogue of (3.16) has as right hand side

$$\begin{aligned}
&-\left\langle\gamma(\psi)\,\vec{\varkappa} + \nabla_s\,\gamma(\psi),\vec{\mathcal{V}}\right\rangle_{\Gamma(t)} - \left\langle\psi\,(\vec{\mathcal{V}} - \vec{u}),\nabla_s\,F'(\psi)\right\rangle_{\Gamma(t)}\\
&\quad= -\left\langle\gamma(\psi)\,\varkappa\,\vec{\nu} + \nabla_s\,\gamma(\psi),\vec{\mathcal{V}}\right\rangle_{\Gamma(t)} + \left\langle\nabla_s\,\gamma(\psi),\vec{\mathcal{V}} - \vec{u}\right\rangle_{\Gamma(t)}\\
&\quad= -\,\langle\gamma(\psi)\,\varkappa\,\vec{\nu} + \nabla_s\,\gamma(\psi),\vec{u}\rangle_{\Gamma(t)}\ ,
\end{aligned} \tag{3.29}$$

where we have used (3.28c) with $\chi = \gamma(\psi)\,\varkappa$ and (2.11). Of course, (3.29) now cancels with the last term in (3.11), and so we obtain (3.17). Moreover, the properties (3.18) and (3.19) also hold.

3.2.2 Model (ii)

Here we consider the case that the extra condition (3.20) also holds.

Find $\Gamma(t) = \vec{x}(\Upsilon, t)$ for $t \in [0,T]$ with $\vec{\mathcal{V}} \in [L^2(\mathcal{G}_T)]^d$, and functions $\vec{u} \in \mathbb{V}$, $p \in L^2(0,T;\widehat{\mathbb{P}})$, $\varkappa \in L^2(\mathcal{G}_T)$, $\phi \in \mathbb{T}$ and $\psi \in \mathbb{S}$ such that for almost all $t \in (0,T)$ we have that (3.28a–d), (3.21a) and

$$\frac{\mathrm{d}}{\mathrm{d}t} \langle \psi, \zeta \rangle_{\Gamma(t)} + \mathcal{D}_\Gamma \langle \nabla_s \psi, \nabla_s \zeta \rangle_{\Gamma(t)} + \left\langle \psi\, (\vec{\mathcal{V}} - \vec{u}), \nabla_s \zeta \right\rangle_{\Gamma(t)}$$
$$= \langle \psi, \partial_t^\circ \zeta \rangle_{\Gamma(t)} - \left(\frac{1}{\alpha_-} + \frac{1}{\alpha_+} \right) \langle F'(\psi) - G'(\phi), \zeta \rangle_{\Gamma(t)} \quad \forall\, \zeta \in \mathbb{S} \tag{3.30}$$

hold subject to the initial conditions (2.20) without the subscript $\pm$.

We note that a solution to (3.28a–d), (3.21a) and (3.30) satisfies (3.23), (3.18) and (3.22).

4 Semidiscrete finite element approximation

For simplicity we consider Ω to be a polyhedral domain. Then let $\mathcal{T}^h$ be a regular partitioning of Ω into disjoint open simplices o_j^h, $j = 1, \ldots, J_\Omega^h$. Associated with $\mathcal{T}^h$ are the finite element spaces

$$S_k^h := \{ \chi \in C(\overline{\Omega}) : \chi|_o \in \mathcal{P}_k(o) \quad \forall\, o \in \mathcal{T}^h \} \subset H^1(\Omega)\,, \qquad k \in \mathbb{N}\,,$$

where $\mathcal{P}_k(o)$ denotes the space of polynomials of degree k on o. We also introduce S_0^h, the space of piecewise constant functions on $\mathcal{T}^h$. Let $\{\varphi_{k,j}^h\}_{j=1}^{K_k^h}$ be the standard basis functions for S_k^h, $k \geq 0$. We introduce $I_k^h : C(\overline{\Omega}) \to S_k^h$, $k \geq 1$, the standard interpolation operators, such that $(I_k^h\, \vec{\eta})(\vec{p}_{k,j}^{\,h}) = \eta(\vec{p}_{k,j}^{\,h})$ for $j = 1, \ldots, K_k^h$; where $\{\vec{p}_{k,j}^{\,h}\}_{j=1}^{K_k^h}$ denotes the coordinates of the degrees of freedom of S_k^h, $k \geq 1$. In an analogous fashion we introduce $\vec{I}_k^h : [C(\overline{\Omega})]^d \to [S_k^h]^d$, $k \geq 1$. In addition we define the standard projection operator $I_0^h : L^1(\Omega) \to S_0^h$, such that

$$(I_0^h \eta)|_o = \frac{1}{\mathcal{L}^d(o)} \int_o \eta \, \mathrm{d}\mathcal{L}^d \qquad \forall\, o \in \mathcal{T}^h\,.$$

Our approximation to the velocity and pressure on $\mathcal{T}^h$ will be finite element spaces $\mathbb{U}^h \subset \mathbb{U}$ and $\mathbb{P}^h(t) \subset \mathbb{P}$, where for the latter we also assume that $S_1^h \subset \mathbb{P}^h(t)$. We require also the space $\widehat{\mathbb{P}}^h(t) := \mathbb{P}^h(t) \cap \widehat{\mathbb{P}}$. Based on the authors' earlier work in Barrett *et al.* (2013a, 2014), we will select velocity/pressure finite element spaces that satisfy the LBB inf-sup condition, see e.g. Girault and Raviart (1986, p. 114), and augment the pressure space by a single additional basis function, namely by the characteristic function of the inner phase. For the obtained spaces $(\mathbb{U}^h, \mathbb{P}^h(t))$ we are unable to prove that they satisfy an LBB condition. The extension of the given pressure finite element space, which is an example of an XFEM approach, leads to exact volume conservation of the two phases within the finite element framework. For the non-augmented spaces we may choose, for example, the lowest order Taylor–Hood element P2–P1, or the P2–(P1+P0) element on

setting $\mathbb{U}^h = [S_2^h]^d \cap \mathbb{U}$, and $\mathbb{P}^h = S_1^h$ or $S_1^h + S_0^h$, respectively. We refer to Barrett *et al.* (2013a, 2014) for more details.

The parametric finite element spaces in order to approximate $\vec{x}$ and $\varkappa$ in (3.28a–d) are defined as follows. Similarly to Barrett *et al.* (2008), we introduce the following discrete spaces, based on the work of Dziuk (1991). Let $\Gamma^h(t) \subset \mathbb{R}^d$ be a $(d-1)$-dimensional *polyhedral surface*, i.e. a union of non-degenerate $(d-1)$-simplices with no hanging vertices (see Deckelnick *et al.* (2005, p. 164) for $d = 3$), approximating the closed surface $\Gamma(t)$. In particular, let $\Gamma^h(t) = \bigcup_{j=1}^{J_\Gamma} \overline{\sigma_j^h(t)}$, where $\{\sigma_j^h(t)\}_{j=1}^{J_\Gamma}$ is a family of mutually disjoint open $(d-1)$-simplices with vertices $\{\vec{q}_k^h(t)\}_{k=1}^{K_\Gamma}$. Then let

$$\begin{aligned}\underline{V}(\Gamma^h(t)) &:= \{\vec{\chi} \in [C(\Gamma^h(t))]^d : \vec{\chi}|_{\sigma_j^h} \text{ is linear } \forall\ j = 1, \ldots, J_\Gamma\}\\ &=: [W(\Gamma^h(t))]^d \subset [H^1(\Gamma^h(t))]^d\,,\end{aligned}$$

where $W(\Gamma^h(t)) \subset H^1(\Gamma^h(t))$ is the space of scalar continuous piecewise linear functions on $\Gamma^h(t)$, with $\{\chi_k^h(\cdot,t)\}_{k=1}^{K_\Gamma}$ denoting the standard basis of $W(\Gamma^h(t))$, i.e.

$$\chi_k^h(\vec{q}_l^h(t), t) = \delta_{kl} \qquad \forall\ k, l \in \{1, \ldots, K_\Gamma\}\,, t \in [0,T]\,. \tag{4.1}$$

For later purposes, we also introduce $\pi^h(t) : C(\Gamma^h(t)) \to W(\Gamma^h(t))$, the standard interpolation operator at the nodes $\{\vec{q}_k^h(t)\}_{k=1}^{K_\Gamma}$, and similarly $\vec{\pi}^h(t) : [C(\Gamma^h(t))]^d \to \underline{V}(\Gamma^h(t))$.

For scalar and vector functions η, ζ on $\Gamma^h(t)$ we introduce the L^2–inner product $\langle\cdot,\cdot\rangle_{\Gamma^h(t)}$ over the polyhedral surface $\Gamma^h(t)$ as follows

$$\langle \eta, \zeta \rangle_{\Gamma^h(t)} := \int_{\Gamma^h(t)} \eta\,.\,\zeta \,\mathrm{d}\mathcal{H}^{d-1}\,.$$

If η, ζ are piecewise continuous, with possible jumps across the edges of $\{\sigma_j^h\}_{j=1}^{J_\Gamma}$, we introduce the mass lumped inner product $\langle\cdot,\cdot\rangle^h_{\Gamma^h(t)}$ as

$$\langle \eta, \zeta \rangle^h_{\Gamma^h(t)} := \tfrac{1}{d} \sum_{j=1}^{J_\Gamma} \mathcal{H}^{d-1}(\sigma_j^h) \sum_{k=1}^{d} (\eta\,.\,\zeta)((\vec{q}_{j_k}^h)^-), \tag{4.2}$$

where $\{\vec{q}_{j_k}^h\}_{k=1}^d$ are the vertices of σ_j^h, and where we define $\eta((\vec{q}_{j_k}^h)^-) := \lim_{\sigma_j^h \ni \vec{p} \to \vec{q}_{j_k}^h} \eta(\vec{p})$. Similarly to (4.2) we define $\langle\cdot,\cdot\rangle^h_{\partial\Omega}$, where the mass lumping is now with respect to the edges/faces of elements in $\mathcal{T}^h$ that make up the boundary $\partial\Omega$. In addition, let

$$(\eta, \zeta)^h := \int_\Omega I_1^h\,[\eta\,\zeta]\,\mathrm{d}\mathcal{L}^d \qquad \forall\ \eta, \zeta \in C(\overline{\Omega})\,. \tag{4.3}$$

On choosing an arbitrary fixed $t_0 \in (0,T)$, we can represent each $\vec{z} \in \Gamma^h(t_0)$ as

$$\vec{z} = \sum_{k=1}^{K_\Gamma} \chi_k^h(\vec{z}, t_0)\, \vec{q}_k^h(t_0)\,.$$

Now we can parameterize $\Gamma^h(t)$ by $\vec{X}^h(\cdot,t):\Gamma^h(t_0)\to\mathbb{R}^d$, where $\vec{z}\mapsto\sum_{k=1}^{K_\Gamma}\chi_k^h(\vec{z},t_0)\,\vec{q}_k^h(t)$, i.e. $\Gamma^h(t_0)$ plays the role of a reference manifold for $(\Gamma^h(t))_{t\in[0,T]}$. Then, similarly to (2.1), we define the discrete velocity for $\vec{z}\in\Gamma^h(t_0)$ by

$$\vec{\mathcal{V}}^h(\vec{z},t_0):=\frac{\mathrm{d}}{\mathrm{d}t}\,\vec{X}^h(\vec{z},t_0)=\sum_{k=1}^{K_\Gamma}\chi_k^h(\vec{z},t_0)\,\frac{\mathrm{d}}{\mathrm{d}t}\,\vec{q}_k^h(t_0)\,, \tag{4.4}$$

which corresponds to Dziuk and Elliott (2013, (5.23)). In addition, similarly to (3.4), we define

$$\partial_t^{\circ,h}\,\zeta(\vec{z},t_0)=\frac{\mathrm{d}}{\mathrm{d}t}\,\zeta(\vec{X}^h(\vec{z},t_0),t_0)=\zeta_t(\vec{z},t_0)+\vec{\mathcal{V}}^h(\vec{z},t_0)\,.\,\nabla\,\zeta(\vec{z},t_0)\qquad\forall\,\zeta\in H^1(\mathcal{G}_T^h)\,, \tag{4.5}$$

where, similarly to (2.2), we have defined the discrete space-time surface

$$\mathcal{G}_T^h:=\bigcup_{t\in[0,T]}\Gamma^h(t)\times\{t\}\,.$$

It immediately follows from (4.5) that $\partial_t^{\circ,h}\,\vec{\mathrm{id}}=\vec{\mathcal{V}}^h$ on $\Gamma^h(t)$. For later use, we also introduce the finite element spaces

$$\begin{aligned}W(\mathcal{G}_T^h)&:=\{\chi\in C(\mathcal{G}_T^h):\chi(\cdot,t)\in W(\Gamma^h(t))\quad\forall\,t\in[0,T]\}\,,\\ W_T(\mathcal{G}_T^h)&:=\{\chi\in W(\mathcal{G}_T^h):\partial_t^{\circ,h}\,\chi\in C(\mathcal{G}_T^h)\}\,.\end{aligned}$$

On differentiating (4.1) with respect to t, we obtain that

$$\partial_t^{\circ,h}\,\chi_k^h=0\quad\forall\,k\in\{1,\ldots,K_\Gamma\}\,, \tag{4.6}$$

see also Dziuk and Elliott (2013, Lem. 5.5). It follows directly from (4.6) that

$$\partial_t^{\circ,h}\,\zeta(\cdot,t)=\sum_{k=1}^{K_\Gamma}\chi_k^h(\cdot,t)\,\frac{\mathrm{d}}{\mathrm{d}t}\,\zeta_k(t)\quad\text{on }\Gamma^h(t) \tag{4.7}$$

for $\zeta(\cdot,t)=\sum_{k=1}^{K_\Gamma}\zeta_k(t)\,\chi_k^h(\cdot,t)\in W(\Gamma^h(t))$. Moreover, it holds that

$$\frac{\mathrm{d}}{\mathrm{d}t}\int_{\sigma_j^h(t)}\zeta\,\mathrm{d}\mathcal{H}^{d-1}=\int_{\sigma_j^h(t)}\partial_t^{\circ,h}\,\zeta+\zeta\,\nabla_s\,.\,\vec{\mathcal{V}}^h\,\mathrm{d}\mathcal{H}^{d-1}\quad\forall\,\zeta\in H^1(\sigma_j^h(t))\,,j\in\{1,\ldots,J_\Gamma\}\,, \tag{4.8}$$

see Dziuk and Elliott (2013, Lem. 5.6). It immediately follows from (4.8) that

$$\frac{\mathrm{d}}{\mathrm{d}t}\,\langle\eta,\zeta\rangle_{\Gamma^h(t)}=\left\langle\partial_t^{\circ,h}\,\eta,\zeta\right\rangle_{\Gamma^h(t)}+\left\langle\eta,\partial_t^{\circ,h}\,\zeta\right\rangle_{\Gamma^h(t)}+\left\langle\eta\,\zeta,\nabla_s\,.\,\vec{\mathcal{V}}^h\right\rangle_{\Gamma^h(t)}\qquad\forall\,\eta,\zeta\in W_T(\mathcal{G}_T^h)\,, \tag{4.9}$$

which is a discrete analogue of (3.6). It is not difficult to show that the analogue of (4.9) with numerical integration also holds. We recall this result in the next lemma, together with a discrete variant of (3.7), on recalling (2.7), for the case $d=2$.

LEMMA. 4.1. *It holds that*

$$\frac{\mathrm{d}}{\mathrm{d}t}\,\langle \eta,\zeta\rangle^h_{\Gamma^h(t)} = \left\langle \partial_t^{\circ,h}\,\eta,\zeta\right\rangle^h_{\Gamma^h(t)} + \left\langle \eta,\partial_t^{\circ,h}\,\zeta\right\rangle^h_{\Gamma^h(t)} + \left\langle \eta\,\zeta,\nabla_s\,.\,\vec{\mathcal{V}}^h\right\rangle^h_{\Gamma^h(t)} \quad \forall\ \eta,\zeta\in W_T(\mathcal{G}^h_T)\,. \tag{4.10}$$

In addition, if $d=2$, it holds that

$$\langle \zeta,\nabla_s\,.\,\vec{\eta}\rangle_{\Gamma^h(t)} + \langle \nabla_s\,\zeta,\vec{\eta}\rangle_{\Gamma^h(t)} = \left\langle \nabla_s\,\vec{\mathrm{id}},\nabla_s\,\vec{\pi}^h\,(\zeta\,\vec{\eta})\right\rangle_{\Gamma^h(t)} \quad \forall\ \zeta\in W(\Gamma^h(t))\,,\vec{\eta}\in \underline{V}(\Gamma^h(t))\,. \tag{4.11}$$

Proof. See the proof of Lemma 3.1 in Barrett *et al.* (2013b). □

Given $\Gamma^h(t)$, we let $\Omega^h_+(t)$ denote the exterior of $\Gamma^h(t)$ and let $\Omega^h_-(t)$ denote the interior of $\Gamma^h(t)$, so that $\Gamma^h(t)=\partial\Omega^h_-(t)=\overline{\Omega^h_-(t)}\cap\overline{\Omega^h_+(t)}$. We then partition the elements of the bulk mesh $\mathcal{T}^h$ into interior, exterior and interfacial elements as follows. Let

$$\begin{aligned}
\mathcal{T}^h_{\Omega^h_-}(t) &:= \{o\in\mathcal{T}^h : o\subset\Omega^h_-(t)\}\,,\\
\mathcal{T}^h_{\Omega^h_+}(t) &:= \{o\in\mathcal{T}^h : o\subset\Omega^h_+(t)\}\,,\\
\mathcal{T}^h_{\Gamma^h}(t) &:= \{o\in\mathcal{T}^h : o\cap\Gamma^h(t)\neq\emptyset\}\,.
\end{aligned}$$

Clearly $\mathcal{T}^h(t)=\mathcal{T}^h_{\Omega^h_-}(t)\cup\mathcal{T}^h_{\Omega^h_+}(t)\cup\mathcal{T}^h_{\Gamma}(t)$ is a disjoint partition. In addition, we define the piecewise constant unit normal $\vec{\nu}^h(t)$ to $\Gamma^h(t)$ such that $\vec{\nu}^h(t)$ points into $\Omega^h_+(t)$. Moreover, we introduce the discrete density $\rho^h(t)\in S^h_0$ and the discrete viscosity $\mu^h(t)\in S^h_0$ as

$$\rho^h(t)\,|_o = \begin{cases} \rho_- & o\in\mathcal{T}^h_{\Omega^h_-}(t)\,,\\ \rho_+ & o\in\mathcal{T}^h_{\Omega^h_+}(t)\,,\\ \frac12\,(\rho_-+\rho_+) & o\in\mathcal{T}^h_{\Gamma^h}(t)\,,\end{cases} \quad\text{and}\quad \mu^h(t)\,|_o = \begin{cases} \mu_- & o\in\mathcal{T}^h_{\Omega^h_-}(t)\,,\\ \mu_+ & o\in\mathcal{T}^h_{\Omega^h_+}(t)\,,\\ \frac12\,(\mu_-+\mu_+) & o\in\mathcal{T}^h_{\Gamma^h}(t)\,.\end{cases} \tag{4.12}$$

For later use we note that

$$\frac{\mathrm{d}}{\mathrm{d}t}\,\mathcal{L}^d(\Omega^h_-(t)) = \mp\left\langle \vec{\mathcal{V}}^h,\vec{\nu}^h\right\rangle_{\Gamma^h(t)} = 0\,, \tag{4.13}$$

which is the discrete analogue of (3.8) for $\xi=1$.

In what follows we will introduce two different finite element approximations for the free boundary problem (2.3a–e), (2.4), (2.5a,b), (2.8a–c). Here $\vec{U}^h(\cdot,t)\in\mathbb{U}^h$ will be an approximation to $\vec{u}(\cdot,t)$, while $P^h(\cdot,t)\in\widehat{\mathbb{P}}^h(t)$ approximates $p(\cdot,t)$ and $\Psi^h(\cdot,t)\in W(\Gamma^h(t))$ approximates $\psi(\cdot,t)$. In order to define approximations of $\phi_\pm(\cdot,t)$, we define the spaces

$$S^h_{1,\pm}(t) := \{\chi\in S^h_1 : \chi(\vec{p}^h_{1,j})=0 \ \text{ if } \ \mathrm{supp}(\varphi^h_{1,j})\subset\overline{\Omega^h_\mp(t)}\}\,, \tag{4.14}$$

as well as

$$\mathcal{Q}^h_{T,\pm} := \{\chi\in H^1(0,T;S^h_1) : \chi(\cdot,t)\in S^h_{1,\pm}(t) \text{ for almost all } t\in(0,T)\}\,.$$

We also define

$$(\chi,\varphi)^h_{\Omega^h_\pm(t)} := \sum_{j=1}^{J^h_\Omega} v^h_{\Omega^h_\pm(t)}(o^h_j) \int_{o^h_j} \chi\,\varphi \,\mathrm{d}\mathcal{L}^d \quad \forall\ \chi,\varphi \in L^2(\Omega)\,, \tag{4.15}$$

where

$$v^h_{\Omega^h_\pm(t)}(o) = \begin{cases} 1 & o \in \mathcal{T}^h_{\Omega^h_\pm}(t)\,, \\ 0 & o \in \mathcal{T}^h_{\Omega^h_\mp}(t)\,, \\ \frac{1}{2} & o \in \mathcal{T}^h_{\Gamma^h}(t)\,. \end{cases}$$

Similarly to (4.15), we define

$$(\chi,\varphi)^{h,h}_{\Omega^h_\pm(t)} := \sum_{j=1}^{J^h_\Omega} v^h_{\Omega^h_\pm(t)}(o^h_j) \int_{o^h_j} I^h_1\,[\chi\,\varphi] \,\mathrm{d}\mathcal{L}^d \quad \forall\ \chi,\varphi \in C(\overline{\Omega})\,. \tag{4.16}$$

Following similar ideas in Barrett *et al.* (2003); Barrett and Nürnberg (2004), we introduce regularizations $F_\varepsilon \in C^2(-\infty,\psi_\infty)$ of $F \in C^2(0,\psi_\infty)$, where $\varepsilon > 0$ is a regularization parameter. In particular, we set

$$F_\varepsilon(r) = \begin{cases} F(r) & r \geq \varepsilon\,, \\ F(\varepsilon) + F'(\varepsilon)\,(r-\varepsilon) + \frac{1}{2}\,F''(\varepsilon)\,(r-\varepsilon)^2 & r \leq \varepsilon\,, \end{cases} \tag{4.17a}$$

which in view of (2.10a) leads to

$$\gamma_\varepsilon(r) = \begin{cases} \gamma(r) & r \geq \varepsilon\,, \\ \gamma(\varepsilon) + \frac{1}{2}\,F''(\varepsilon)\,(\varepsilon^2 - r^2) & r \leq \varepsilon\,, \end{cases} \tag{4.17b}$$

so that

$$\gamma_\varepsilon(r) = F_\varepsilon(r) - r\,F'_\varepsilon(r) \quad \text{and} \quad \gamma'_\varepsilon(r) = -r\,F''_\varepsilon(r) \qquad \forall\ r < \psi_\infty\,. \tag{4.18}$$

Similarly to (4.17a), we introduce $G_{\pm,\varepsilon} \in C^2(\mathbb{R})$ defined by

$$G_{\pm,\varepsilon}(r) = \begin{cases} G_\pm(r) & r \geq \varepsilon\,, \\ G_\pm(\varepsilon) + G'_\pm(\varepsilon)\,(r-\varepsilon) + \frac{1}{2}\,G''_\pm(\varepsilon)\,(r-\varepsilon)^2 & r \leq \varepsilon\,. \end{cases} \tag{4.19}$$

Finally we note that from now on we assume that $\vec{f}_i \in L^2(0,T;[C(\overline{\Omega})]^d)$, $i = 1,2$, so that $\vec{I}^h_2\,\vec{f}_i$, $i = 1,2$, is well-defined for almost all $t \in (0,T)$.

4.1 Approximations with fluidic tangential velocity

When designing a parametric finite element approximation for two-phase flow, a careful decision has to be made about the *discrete tangential velocity* of $\Gamma^h(t)$. The most natural choice is to select the velocity of the fluid, i.e. (3.10c) is appropriately discretized. This then gives a natural discretization of the surfactant transport equation (2.8b). Note also that the approximation of curvature, recall (2.7), where now $\vec{\varkappa} = \varkappa\,\vec{\nu}$ is discretized directly, goes back to the seminal paper Dziuk (1991).

4.1.1 Model (i)

Overall, we then obtain the following semidiscrete continuous-in-time finite element approximation, which is the semidiscrete analogue of the weak formulation (3.10a–f). Given $\Gamma^h(0)$, $\vec{U}^h(\cdot,0) \in \mathbb{U}^h$, $\Phi^h_\pm(\cdot,0) \in S^h_{1,\pm}(0)$ and $\Psi^h(\cdot,0) \in W(\Gamma^h(0))$, find $\Gamma^h(t)$ such that $\vec{\mathrm{id}}\,|_{\Gamma^h(t)} \in \underline{V}(\Gamma^h(t))$ for $t \in [0,T]$, and functions $\vec{U}^h \in H^1(0,T;\mathbb{U}^h)$, $P^h \in \mathbb{P}^h_T := \{\varphi \in L^2(0,T;\widehat{\mathbb{P}}) : \varphi(t) \in \widehat{\mathbb{P}}^h(t) \text{ for a.e. } t \in (0,T)\}$, $\vec{\kappa}^h \in [W(\mathcal{G}^h_T)]^d$, $\Phi^h_\pm \in \mathcal{Q}^h_{T,\pm}$ and $\Psi^h \in W_T(\mathcal{G}^h_T)$ such that for almost all $t \in (0,T)$ it holds that

$$\begin{aligned}
&\tfrac{1}{2}\left[\frac{\mathrm{d}}{\mathrm{d}t}\left(\rho^h\,\vec{U}^h,\vec{\xi}\right) + \left(\rho^h\,\vec{U}^h_t,\vec{\xi}\right) - \left(\rho^h\,\vec{U}^h,\vec{\xi}_t\right)\right] \\
&\qquad + 2\left(\mu^h\,\underline{\underline{D}}(\vec{U}^h),\underline{\underline{D}}(\vec{\xi})\right) + \tfrac{1}{2}\left(\rho^h,[(\vec{U}^h\,.\,\nabla)\,\vec{U}^h]\,.\,\vec{\xi} - [(\vec{U}^h\,.\,\nabla)\,\vec{\xi}]\,.\,\vec{U}^h\right) \\
&\qquad - \left(P^h,\nabla\,.\,\vec{\xi}\right) = \left(\rho^h\,\vec{f}^h_1 + \vec{f}^h_2,\vec{\xi}\right) + \left\langle \gamma_\varepsilon(\Psi^h)\,\vec{\kappa}^h + \nabla_s\,\pi^h\,[\gamma_\varepsilon(\Psi^h)],\vec{\xi}\right\rangle^h_{\Gamma^h(t)} \\
&\qquad\qquad \forall\ \vec{\xi} \in H^1(0,T;\mathbb{U}^h)\,, \qquad (4.20a)
\end{aligned}$$

$$\left(\nabla\,.\,\vec{U}^h,\varphi\right) = 0 \qquad \forall\ \varphi \in \widehat{\mathbb{P}}^h(t)\,, \qquad (4.20b)$$

$$\left\langle \vec{\mathcal{V}}^h,\vec{\chi}\right\rangle^h_{\Gamma^h(t)} = \left\langle \vec{U}^h,\vec{\chi}\right\rangle^h_{\Gamma^h(t)} \qquad \forall\ \vec{\chi} \in \underline{V}(\Gamma^h(t))\,, \qquad (4.20c)$$

$$\left\langle \vec{\kappa}^h,\vec{\eta}\right\rangle^h_{\Gamma^h(t)} + \left\langle \nabla_s\,\vec{\mathrm{id}},\nabla_s\,\vec{\eta}\right\rangle_{\Gamma^h(t)} = 0 \qquad \forall\ \vec{\eta} \in \underline{V}(\Gamma^h(t))\,, \qquad (4.20d)$$

$$\begin{aligned}
&\left(\partial_t\,\Phi^h_\pm,\xi\right)^{h,h}_{\Omega^h_\pm(t)} + \left(\vec{U}^h\,.\,\nabla\,\Phi^h_\pm,\xi\right)^h_{\Omega^h_\pm(t)} + \mathcal{D}_\pm\left(\nabla\,\Phi^h_\pm,\nabla\,\xi\right)^h_{\Omega^h_\pm(t)} + \left\langle \lambda_\pm\,(\Phi^h_\pm - g_\pm),\xi\right\rangle^h_{\partial\Omega} \\
&\qquad = \frac{1}{\alpha_\pm}\left\langle F'_\varepsilon(\Psi^h) - G'_{\pm,\varepsilon}(\Phi^h_\pm),\xi\right\rangle^h_{\Gamma^h(t)} \qquad \forall\ \xi \in S^h_{1,\pm}(t)\,, \qquad (4.20e)
\end{aligned}$$

$$\begin{aligned}
&\frac{\mathrm{d}}{\mathrm{d}t}\left\langle \Psi^h,\chi\right\rangle^h_{\Gamma^h(t)} + \mathcal{D}_\Gamma\left\langle \nabla_s\,\Psi^h,\nabla_s\,\chi\right\rangle_{\Gamma^h(t)} \\
&\qquad = \left\langle \Psi^h,\partial_t^{\circ,h}\,\chi\right\rangle^h_{\Gamma^h(t)} - \sum_{i\in\{\pm\}}\frac{1}{\alpha_i}\left\langle F'_\varepsilon(\Psi^h) - G'_{i,\varepsilon}(\Phi^h_i),\chi\right\rangle^h_{\Gamma^h(t)} \qquad \forall\ \chi \in W_T(\mathcal{G}^h_T)\,, \\
&\qquad\qquad (4.20f)
\end{aligned}$$

where we recall (4.4). Here we have defined $\vec{f}^h_i(\cdot,t) := \vec{I}^h_2\,\vec{f}_i(\cdot,t)$, $i = 1,2$. We observe that (4.20c) collapses to $\vec{\mathcal{V}}^h = \vec{\pi}^h\,\vec{U}^h\,|_{\Gamma^h(t)} \in \underline{V}(\Gamma^h(t))$. In the next subsection, on the approximation of model (ii), this will be crucial for the stability analysis. It is for this reason that we use mass lumping in (4.20c), which then leads to mass lumping having to be used in the last term in (4.20a), as well as for the first term in (4.20d).

Note that the scheme (4.20a–d,f), without the last term on the right hand side of (4.20f), is very similar to the scheme ($\mathrm{A_{sd}}$) in Barrett *et al.* (2013b) for the approximation of two-phase flow with insoluble surfactants. The only difference is that the regularized surface tension density γ_ε in (4.20a) is replaced by γ in ($\mathrm{A_{sd}}$) in Barrett *et al.* (2013b). We recall that this poses no difficulties in Barrett *et al.* (2013b), because there a discrete maximum principle can be shown for Ψ^h. In this paper, on the other hand, the extra term

on the right hand side of (4.20f) appears to make it impossible to derive a positivity result for Ψ^h. It is for this reason, that we employ the regularizations γ_ε and F_ε in (4.20a–f).

We recall that as there appears to be no discrete variant of (3.9), it does not seem to be possible to prove a discrete analogue of the conservation property (3.19) for (4.20a–f).

We remark that the formulation (4.20f) for the surfactant transport equation (2.8b) falls into the framework of ESFEM (Evolving surface finite element method) as coined by the authors in Dziuk and Elliott (2007). In this particular instance, the velocity of $\Gamma^h(t)$ is not a priori fixed, rather it arises implicitly through the evolution of $\Gamma^h(t)$ as determined by (4.20a–f). Here we recall the important property (4.6), which means that (4.20f) simplifies if formulated in terms of the basis functions $\{\chi^h_k(\cdot,t)\}_{k=1}^{K_\Gamma}$ of $W(\Gamma^h(t))$.

For later use we observe that (4.20b), on recalling that $\vec{U}^h.\,\vec{n}=0$ on $\partial\Omega$ and the fact that $S^h_1 \subset \mathbb{P}^h(t)$, implies that for all $t\in(0,T)$

$$(\vec{U}^h, \nabla\,\varphi) = 0 \qquad \forall\ \varphi \in S^h_1\,. \tag{4.21}$$

4.1.2 Model (ii)

Similarly to (4.12), we introduce $\mathcal{D}^h(t)\in S^h_0$ defined by

$$\mathcal{D}^h(t)\,|_o = \begin{cases} \mathcal{D}_- & o\in \mathcal{T}^h_{\Omega^h_-}(t)\,,\\ \mathcal{D}_+ & o\in \mathcal{T}^h_{\Omega^h_+}(t)\,,\\ \frac12\,(\mathcal{D}_- + \mathcal{D}_+) & o\in \mathcal{T}^h_{\Gamma^h}(t)\,. \end{cases}$$

We also introduce the matrix function $\Xi^h_\varepsilon : S^h_1 \to [S^h_0]^{d\times d}$ defined such that for all $z^h\in S^h_1$ and almost everywhere in Ω it holds that

$$\Xi^h_\varepsilon(z^h)\,\nabla\, I^h_1\,[G'_\varepsilon(z^h)] = \nabla\, I^h_1\,[R_\varepsilon(G'_\varepsilon(z^h))]\,, \tag{4.22}$$

where $R_\varepsilon\in C^2(\mathbb{R})$ is defined such that

$$R'_\varepsilon(G'_\varepsilon(s)) = s \qquad \forall\ s\in\mathbb{R}\,.$$

This means that

$$R_\varepsilon(r) = \begin{cases} R(r) & r\geq G'(\varepsilon)\,,\\ R(G'(\varepsilon)) + \varepsilon\,(r-G'(\varepsilon)) + \frac12\,[G''(\varepsilon)]^{-1}\,(r-G'(\varepsilon))^2 & r\leq G'(\varepsilon)\,, \end{cases}$$

where $R\in C^2(\mathbb{R})$ is such that $R'(G'(s)) = s$ for all $s\in\mathbb{R}$.

Here we introduce (4.22) in order to be able to mimic (3.26) on the discrete level, where we also apply (4.21) to the function $\varphi = I^h_1\,[R_\varepsilon(G'_\varepsilon(\Phi^h))]$. We note that (4.22) is the natural extension of the approaches in Grün and Rumpf (2000); Barrett and Nürnberg (2004), see also Barrett and Boyaval (2011). The construction for Ξ^h_ε is given as follows.

Let $\widehat{o}$ denote the standard reference simplex in $\mathbb{R}^d$, with vertices $\{\vec{0}, \vec{e}_1, \ldots, \vec{e}_d\}$. For each $o \in \mathcal{T}^h$, with vertices $\{\vec{\mathrm{p}}_i\}_{i=0}^d$ there exists an affine linear map $\mathcal{M}_o : \widehat{o} \to o$ with $\mathcal{M}_o(\vec{z}) = \vec{\mathrm{p}}_0 + M_o\,\vec{z}$ for all $\vec{z} \in \mathbb{R}^d$, where $M_o \in \mathbb{R}^{d\times d}$ is nonsingular, such that $\mathcal{M}_o(\vec{e}_i) = \vec{\mathrm{p}}_i$, $i = 1, \ldots, d$. On noting that $\nabla\,\xi = (M_o^T)^{-1}\,[\nabla\,(\xi \circ \mathcal{M}_o)] \circ (\mathcal{M}_o)^{-1}$ on o, we define

$$\Xi_\varepsilon^h(z^h)\,|_o = (M_o^T)^{-1}\,\widehat{\Xi}_{\varepsilon,o}^h(z^h)\,M_o^T\,, \tag{4.23a}$$

where $\widehat{\Xi}_{\varepsilon,o}^h(z^h) \in \mathbb{R}^{d\times d}$ is the diagonal matrix with entries

$$[\widehat{\Xi}_{\varepsilon,o}^h(z^h)]_{ii} = \begin{cases} \dfrac{R_\varepsilon(G_\varepsilon'(z^h(\vec{\mathrm{p}}_i))) - R_\varepsilon(G_\varepsilon'(z^h(\vec{\mathrm{p}}_0)))}{G_\varepsilon'(z^h(\vec{\mathrm{p}}_i)) - G_\varepsilon'(z^h(\vec{\mathrm{p}}_0))} & z^h(\vec{\mathrm{p}}_i) \neq z^h(\vec{\mathrm{p}}_0)\,, \\ z^h(\vec{\mathrm{p}}_0) & z^h(\vec{\mathrm{p}}_i) = z^h(\vec{\mathrm{p}}_0)\,. \end{cases} \tag{4.23b}$$

We then obtain the following semidiscrete continuous-in-time finite element approximation, which is the analogue of the weak formulation (3.10a–d) and (3.21a,b). Given $\Gamma^h(0)$, $\vec{U}^h(\cdot,0) \in \mathbb{U}^h$, $\Phi^h(\cdot,0) \in S_1^h$ and $\Psi^h(\cdot,0) \in W(\Gamma^h(0))$, find $\Gamma^h(t)$ such that $\vec{\mathrm{id}}\,|_{\Gamma^h(t)} \in \underline{V}(\Gamma^h(t))$ for $t \in [0,T]$, and functions $\vec{U}^h \in H^1(0,T;\mathbb{U}^h)$, $P^h \in \mathbb{P}_T^h$, $\vec{\kappa}^h \in [W(\mathcal{G}_T^h)]^d$, $\Phi^h \in H^1(0,T;S_1^h)$ and $\Psi^h \in W_T(\mathcal{G}_T^h)$ such that for almost all $t \in (0,T)$ we have that (4.20a–d) and

$$\begin{aligned} &\big(\Phi_t^h, \xi\big)^h - \Big(\vec{U}^h, \Xi_\varepsilon^h(\Phi^h)\,\nabla\xi\Big) + \big(\mathcal{D}^h\,\nabla\,\Phi^h, \nabla\,\xi\big) + \big\langle \lambda_+\,(\Phi^h - g_+), \xi\big\rangle_{\partial\Omega}^h \\ &\qquad = \left(\frac{1}{\alpha_-} + \frac{1}{\alpha_+}\right)\big\langle F_\varepsilon'(\Psi^h) - I_1^h\,[G_\varepsilon'(\Phi^h)], \xi\big\rangle_{\Gamma^h(t)}^h \qquad \forall\ \xi \in S_1^h\,, \end{aligned} \tag{4.24a}$$

$$\begin{aligned} &\frac{\mathrm{d}}{\mathrm{d}t}\,\big\langle \Psi^h, \chi\big\rangle_{\Gamma^h(t)}^h + \mathcal{D}_\Gamma\,\big\langle \nabla_s\,\Psi^h, \nabla_s\,\chi\big\rangle_{\Gamma^h(t)} \\ &\qquad = \Big\langle \Psi^h, \partial_t^{\circ,h}\,\chi\Big\rangle_{\Gamma^h(t)}^h - \left(\frac{1}{\alpha_-} + \frac{1}{\alpha_+}\right)\big\langle F_\varepsilon'(\Psi^h) - I_1^h\,[G_\varepsilon'(\Phi^h)], \chi\big\rangle_{\Gamma^h(t)}^h \quad \forall\ \chi \in W_T(\mathcal{G}_T^h) \end{aligned} \tag{4.24b}$$

hold.

In the following lemma we derive a discrete analogue of (3.11).

LEMMA. 4.2. *Let* $\{(\Gamma^h, \vec{U}^h, P^h, \vec{\kappa}^h, \Phi^h, \Psi^h)(t)\}_{t\in[0,T]}$ *be a solution to* (4.20a–d), (4.24a,b). *Then*

$$\begin{aligned} &\tfrac{1}{2}\,\frac{\mathrm{d}}{\mathrm{d}t}\,\|[\rho^h]^{\frac12}\,\vec{U}^h\|_0^2 + 2\,\|[\mu^h]^{\frac12}\,\underline{\underline{D}}(\vec{U}^h)\|_0^2 \\ &\qquad = (\rho^h\,\vec{f}_1^{\,h} + \vec{f}_2^{\,h}, \vec{U}^h) + \Big\langle \gamma_\varepsilon(\Psi^h)\,\vec{\kappa}^h + \nabla_s\,\pi^h\,[\gamma_\varepsilon(\Psi^h)], \vec{U}^h\Big\rangle_{\Gamma^h(t)}^h\,. \end{aligned} \tag{4.25}$$

Proof. The desired result (4.25) follows immediately on choosing $\vec{\xi} = \vec{U}^h$ in (4.20a) and $\varphi = P^h$ in (4.20b). □

The next theorem derives a discrete analogue of the energy law (3.23). Here, similarly to (3.12), it will be crucial to test (4.20f) with an appropriate discrete variant of $F'(\psi)$. It is for this reason that we have to make the following well-posedness assumption.

$$\Psi^h(\cdot,t) < \psi_\infty \quad \text{on } \Gamma^h(t)\,, \quad \forall\ t \in [0,T]\,. \tag{4.26}$$

In addition, as a priori it is not possible to ensure positivity of Ψ^h and Φ^h on $\Gamma^h(t)$, we have introduced the regularizations (4.17a) and (4.19).

The stability proof in the next theorem needs the following mild assumption on the bulk mesh $\mathcal{T}^h$.

($\mathcal{A}_1$) Either $\mathcal{D}_- = \mathcal{D}_+ = 0$, or $d = 2$ and $\mathcal{T}^h$ is weakly acute; that is, for any pair of adjacent triangles the sum of opposite angles relative to the common edge does not exceed π.

THEOREM. 4.3. *Let* $\{(\Gamma^h, \vec{U}^h, P^h, \vec{\kappa}^h, \Phi^h, \Psi^h)(t)\}_{t\in[0,T]}$ *be a solution to* (4.20a–d), (4.24a,b). *Then*

$$\frac{\mathrm{d}}{\mathrm{d}t}\left(\left(\Phi^h,1\right) + \left\langle \Psi^h,1\right\rangle_{\Gamma^h(t)}\right) = \left\langle \lambda_+, g_+ - \Phi^h\right\rangle^h_{\partial\Omega}\,. \tag{4.27}$$

In addition, if $d = 2$ *and* (4.26) *and* ($\mathcal{A}_1$) *hold, then*

$$\begin{aligned}\frac{\mathrm{d}}{\mathrm{d}t}\Big(\tfrac{1}{2}\,\|[\rho^h]^{\frac12}\,\vec{U}^h\|_0^2 + \left(G_\varepsilon(\Phi^h),1\right)^h + \left\langle F_\varepsilon(\Psi^h),1\right\rangle^h_{\Gamma^h(t)}\Big) + 2\,\|[\mu^h]^{\frac12}\,\underline{\underline{D}}(\vec{U}^h)\|_0^2 \\ + \left\langle \lambda_+, G_\varepsilon(\Phi^h)\right\rangle^h_{\partial\Omega} + \left(\frac{1}{\alpha_-}+\frac{1}{\alpha_+}\right)\left\langle |F_\varepsilon'(\Psi^h) - I_1^h\,[G_\varepsilon'(\Phi^h)]|^2,1\right\rangle^h_{\Gamma^h(t)} \\ \leq \left(\rho^h\,\vec{f}_1^{\,h} + \vec{f}_2^{\,h}, \vec{U}^h\right) + \left\langle \lambda_+, G_\varepsilon(g_+)\right\rangle^h_{\partial\Omega}\,.\end{aligned} \tag{4.28}$$

Proof. The conservation property (4.27) follows immediately from choosing $\xi = 1$ in (4.24a) and $\chi = 1$ in (4.24b).

For the proof of (4.28) we note that the assumption (4.26) means that we can choose $\chi = \pi^h\,[F_\varepsilon'(\Psi^h)]$ in (4.24b) to yield, on recalling (4.18), that

$$\begin{aligned}&\frac{\mathrm{d}}{\mathrm{d}t}\left\langle F_\varepsilon(\Psi^h) - \gamma_\varepsilon(\Psi^h),1\right\rangle^h_{\Gamma^h(t)} + \mathcal{D}_\Gamma\left\langle \nabla_s\,\Psi^h, \nabla_s\,\pi^h\,[F_\varepsilon'(\Psi^h)]\right\rangle_{\Gamma^h(t)} \\ &\quad = \left\langle \Psi^h, \partial_t^{\circ,h}\,\pi^h\,[F_\varepsilon'(\Psi^h)]\right\rangle^h_{\Gamma^h(t)} - \left(\frac{1}{\alpha_-}+\frac{1}{\alpha_+}\right)\left\langle F_\varepsilon'(\Psi^h) - I_1^h\,[G_\varepsilon'(\Phi^h)], F_\varepsilon'(\Psi^h)\right\rangle^h_{\Gamma^h(t)}\,.\end{aligned} \tag{4.29}$$

Moreover, choosing $\xi = I_1^h\,[G_\varepsilon'(\Phi^h)]$ in (4.24a) yields, on recalling (4.22) and (4.21) with $\varphi = I_1^h\,[R_\varepsilon(G_\varepsilon'(\Phi^h))]$, that

$$\begin{aligned}&\left(\Phi_t^h, G_\varepsilon'(\Phi^h)\right)^h + \left(\mathcal{D}^h\,\nabla\,\Phi^h, \nabla\,I_1^h\,[G_\varepsilon'(\Phi^h)]\right) + \left\langle \lambda_+\,(\Phi^h - g_+), G_\varepsilon'(\Phi^h)\right\rangle^h_{\partial\Omega} \\ &\qquad = \left(\frac{1}{\alpha_-}+\frac{1}{\alpha_+}\right)\left\langle F_\varepsilon'(\Psi^h) - I_1^h\,[G_\varepsilon'(\Phi^h)], I_1^h\,G_\varepsilon'(\Phi^h)\right\rangle^h_{\Gamma^h(t)}\,.\end{aligned} \tag{4.30}$$

Combining (4.29) and (4.30) yields, similarly to (3.24), that

$$\begin{aligned}
&\frac{\mathrm{d}}{\mathrm{d}t}\left\langle F_\varepsilon(\Psi^h)-\gamma_\varepsilon(\Psi^h),1\right\rangle^h_{\Gamma^h(t)}+\mathcal{D}_\Gamma\left\langle\nabla_s\,\Psi^h,\nabla_s\,\pi^h\left[F'_\varepsilon(\Psi^h)\right]\right\rangle_{\Gamma^h(t)}+\left(\Phi^h_t,G'_\varepsilon(\Phi^h)\right)^h\\
&\quad+\left(\mathcal{D}^h\,\nabla\,\Phi^h,\nabla\,I^h_1\left[G'_\varepsilon(\Phi^h)\right]\right)+\left(\frac{1}{\alpha_-}+\frac{1}{\alpha_+}\right)\left\langle|F'_\varepsilon(\Psi^h)-I^h_1\left[G'_\varepsilon(\Phi^h)\right]|^2,1\right\rangle^h_{\Gamma^h(t)}\\
&\quad+\left\langle\lambda_+\left(\Phi^h-g_+\right),G'_\varepsilon(\Phi^h)\right\rangle^h_{\partial\Omega}=\left\langle\Psi^h,\partial_t^{\circ,h}\,\pi^h\left[F'_\varepsilon(\Psi^h)\right]\right\rangle^h_{\Gamma^h(t)}\,. \qquad (4.31)
\end{aligned}$$

For the remainder of the proof we assume that $d=2$. It follows from (4.18), (4.2) and (4.7) that we have a discrete analogue of (3.14), i.e.

$$\left\langle\Psi^h,\partial_t^{\circ,h}\,\pi^h\left[F'_\varepsilon(\Psi^h)\right]\right\rangle^h_{\Gamma^h(t)}=-\left\langle\partial_t^{\circ,h}\,\pi^h\left[\gamma_\varepsilon(\Psi^h)\right],1\right\rangle^h_{\Gamma^h(t)}\,, \qquad (4.32)$$

which means that (4.31), together with (4.10), (4.11) and (4.20c,d), implies that

$$\begin{aligned}
&\frac{\mathrm{d}}{\mathrm{d}t}\left(\left(G_\varepsilon(\Phi^h),1\right)^h+\left\langle F_\varepsilon(\Psi^h),1\right\rangle^h_{\Gamma^h(t)}\right)+\mathcal{D}_\Gamma\left\langle\nabla_s\,\Psi^h,\nabla_s\,\pi^h\left[F'_\varepsilon(\Psi^h)\right]\right\rangle_{\Gamma^h(t)}\\
&\quad+\left(\mathcal{D}^h\,\nabla\,\Phi^h,\nabla\,I^h_1\left[G'_\varepsilon(\Phi^h)\right]\right)+\left(\frac{1}{\alpha_-}+\frac{1}{\alpha_+}\right)\left\langle|F'_\varepsilon(\Psi^h)-I^h_1\left[G'_\varepsilon(\Phi^h)\right]|^2,1\right\rangle^h_{\Gamma^h(t)}\\
&\quad+\left\langle\lambda_+\left(\Phi^h-g_+\right),G'_\varepsilon(\Phi^h)\right\rangle^h_{\partial\Omega}=\left\langle\pi^h\left[\gamma_\varepsilon(\Psi^h)\right],\nabla_s\,.\,\vec{\mathcal{V}}^h\right\rangle_{\Gamma^h(t)}\\
&\qquad=\left\langle\nabla_s\,\vec{\mathrm{id}},\nabla_s\,\pi^h\left[\gamma_\varepsilon(\Psi^h)\,\vec{\mathcal{V}}^h\right]\right\rangle_{\Gamma^h(t)}-\left\langle\nabla_s\,\pi^h\left[\gamma_\varepsilon(\Psi^h)\right],\vec{\mathcal{V}}^h\right\rangle_{\Gamma^h(t)}\\
&\qquad=-\left\langle\vec{\kappa}^h,\gamma_\varepsilon(\Psi^h)\,\vec{U}^h\right\rangle^h_{\Gamma^h(t)}-\left\langle\nabla_s\,\pi^h\left[\gamma_\varepsilon(\Psi^h)\right],\vec{U}^h\right\rangle^h_{\Gamma^h(t)}\,. \qquad (4.33)
\end{aligned}$$

Next, on noting for $\mathcal{D}_\Gamma>0$ that F'_ε is monotonic, we have that

$$\mathcal{D}_\Gamma\left\langle\nabla_s\,\Psi^h,\nabla_s\,\pi^h\left[F'_\varepsilon(\Psi^h)\right]\right\rangle_{\Gamma^h(t)}\geq 0\,, \qquad (4.34)$$

and similarly, on noting the assumption $(\mathcal{A}_1)$ and that G'_ε is monotonic, it holds that

$$\left(\mathcal{D}\,\nabla\,\Phi^h,\nabla\,I^h_1\left[G'_\varepsilon(\Phi^h)\right]\right)\geq 0\,. \qquad (4.35)$$

It follows from (4.33), (4.34), (4.35) and the convexity of G_ε that

$$\begin{aligned}
&\frac{\mathrm{d}}{\mathrm{d}t}\left(\left(G_\varepsilon(\Phi^h),1\right)^h+\left\langle F_\varepsilon(\Psi^h),1\right\rangle^h_{\Gamma^h(t)}\right)+\left(\frac{1}{\alpha_-}+\frac{1}{\alpha_+}\right)\left\langle|F'_\varepsilon(\Psi^h)-I^h_1\left[G'_\varepsilon(\Phi^h)\right]|^2,1\right\rangle^h_{\Gamma^h(t)}\\
&\quad+\left\langle\lambda_+,G_\varepsilon(\Phi^h)\right\rangle^h_{\partial\Omega}\\
&\qquad\leq-\left\langle\vec{\kappa}^h,\gamma_\varepsilon(\Psi^h)\,\vec{U}^h\right\rangle^h_{\Gamma^h(t)}-\left\langle\nabla_s\,\pi^h\left[\gamma_\varepsilon(\Psi^h)\right],\vec{U}^h\right\rangle^h_{\Gamma^h(t)}+\left\langle\lambda_+,G_\varepsilon(g_+)\right\rangle^h_{\partial\Omega}\,. \qquad (4.36)
\end{aligned}$$

Combining (4.36) with (4.25) yields the desired result (4.28). □

Clearly, (4.27) and (4.28) are natural discrete analogues of (3.22) and (3.23), respectively.

REMARK. 4.4. *The convex nature of F, together with the fact that F' is singular at the origin, allows us to derive upper bounds on the negative part of Ψ^h for the two cases* (2.12a,b). *On recalling* (4.17a) *and* (2.10a), *it holds that*

$$F_\varepsilon(r) = \gamma(\varepsilon) + F'(\varepsilon)\, r + \tfrac{1}{2}\, F''(\varepsilon)\, (r-\varepsilon)^2 \geq \tfrac{1}{2}\, F''(\varepsilon)\, r^2 \geq \tfrac{1}{2}\, \varepsilon^{-1}\, \gamma_0\, \beta\, r^2 \qquad \forall\ r \leq 0\,,$$

provided that ε is sufficiently small. Hence the bound (4.28), *on noting that $g_+ > 0$ and a Korn inequality, yields that*

$$\big\langle [\Psi^h]^2_-, 1 \big\rangle^h_{\Gamma^h(t)} \leq C\, \varepsilon \qquad \forall\ t \in [0,T]$$

for some positive constant C, and for ε sufficiently small. Similarly, for the typical example of G as in (2.16) *without the subscripts $\pm$, it follows that*

$$\big([\Phi^h]^2_-, 1\big)^h \leq C\, \varepsilon \qquad \forall\ t \in [0,T]$$

for some positive constant C, and for ε sufficiently small. Here, on recalling (4.19), *we have observed that $G_\varepsilon(r) \geq -\gamma_0\, \beta\, \varepsilon + \frac{1}{2}\, \varepsilon^{-1}\, \gamma_0\, \beta\, r^2$ for $r \leq 0$, and for ε sufficiently small.*

4.2 Approximations with implicit tangential velocity

In contrast to the semidiscrete schemes introduced in §4.1, we now consider approximations where the *discrete tangential velocity* is not a priori fixed. Note that the resulting approximation of curvature was first proposed by the authors in Barrett *et al.* (2007, 2008).

4.2.1 Model (i)

We propose the following semidiscrete continuous-in-time finite element approximation, which is the semidiscrete analogue of the weak formulation (3.28a–f). Given $\Gamma^h(0)$, $\vec{U}^h(\cdot,0) \in \mathbb{U}^h$, $\Phi^h_\pm(\cdot,0) \in S^h_{1,\pm}(0)$ and $\Psi^h(\cdot,0) \in W(\Gamma^h(0))$, find $\Gamma^h(t)$ such that $\vec{\mathrm{id}}\,|_{\Gamma^h(t)} \in \underline{V}(\Gamma^h(t))$ for $t \in [0,T]$, and functions $\vec{U}^h \in H^1(0,T;\mathbb{U}^h)$, $P^h \in \mathbb{P}^h_T$, $\kappa^h \in W(\mathcal{G}^h_T)$,

$\Phi^h_\pm \in \mathcal{Q}^h_{T,\pm}$ and $\Psi^h \in W_T(\mathcal{G}^h_T)$ such that for almost all $t \in (0,T)$ it holds that

$$\begin{aligned}
&\tfrac12 \left[\frac{\mathrm{d}}{\mathrm{d}t} \left(\rho^h \, \vec{U}^h, \vec{\xi} \right) + \left(\rho^h \, \vec{U}^h_t, \vec{\xi} \right) - \left(\rho^h \, \vec{U}^h, \vec{\xi}_t \right) \right] \\
&\qquad + 2 \left(\mu^h \, \underline{\underline{D}}(\vec{U}^h), \underline{\underline{D}}(\vec{\xi}) \right) + \tfrac12 \left(\rho^h, [(\vec{U}^h \,.\, \nabla) \, \vec{U}^h] \,.\, \vec{\xi} - [(\vec{U}^h \,.\, \nabla) \, \vec{\xi}] \,.\, \vec{U}^h \right) \\
&\qquad - \left(P^h, \nabla \,.\, \vec{\xi} \right) = \left(\rho^h \, \vec{f}^h_1 + \vec{f}^h_2, \vec{\xi} \right) + \left\langle \pi^h \left[\gamma_\varepsilon(\Psi^h) \, \kappa^h \right] \vec{\nu}^h, \vec{\xi} \right\rangle_{\Gamma^h(t)} \\
&\qquad\qquad + \left\langle \nabla_s \, \pi^h \left[\gamma_\varepsilon(\Psi^h) \right], \vec{\xi} \right\rangle^h_{\Gamma^h(t)} \qquad \forall \, \vec{\xi} \in H^1(0,T;\mathbb{U}^h) \,, \qquad (4.37a) \\
&\left(\nabla \,.\, \vec{U}^h, \varphi \right) = 0 \quad \forall \, \varphi \in \widehat{\mathbb{P}}^h(t) \,, \qquad (4.37b) \\
&\left\langle \vec{\mathcal{V}}^h, \chi \, \vec{\nu}^h \right\rangle^h_{\Gamma^h(t)} = \left\langle \vec{U}^h, \chi \, \vec{\nu}^h \right\rangle_{\Gamma^h(t)} \quad \forall \, \chi \in W(\Gamma^h(t)) \,, \qquad (4.37c) \\
&\left\langle \kappa^h \, \vec{\nu}^h, \vec{\eta} \right\rangle^h_{\Gamma^h(t)} + \left\langle \nabla_s \, \mathrm{i}\vec{\mathrm{d}}, \nabla_s \, \vec{\eta} \right\rangle_{\Gamma^h(t)} = 0 \quad \forall \, \vec{\eta} \in \underline{V}(\Gamma^h(t)) \,, \qquad (4.37d) \\
&\left(\partial_t \, \Phi^h_\pm, \xi \right)^{h,h}_{\Omega^h_\pm(t)} + \left(\vec{U}^h \,.\, \nabla \, \Phi^h_\pm, \xi \right)^h_{\Omega^h_\pm(t)} + \mathcal{D}_\pm \left(\nabla \, \Phi^h_\pm, \nabla \, \xi \right)^h_{\Omega^h_\pm(t)} + \left\langle \lambda_\pm \left(\Phi^h_\pm - g_\pm \right), \xi \right\rangle^h_{\partial\Omega} \\
&\qquad\qquad = \frac{1}{\alpha_\pm} \left\langle F'_\varepsilon(\Psi^h) - G'_{\pm,\varepsilon}(\Phi^h_\pm), \xi \right\rangle^h_{\Gamma^h(t)} \qquad \forall \, \xi \in S^h_{1,\pm}(t) \,, \qquad (4.37e) \\
&\frac{\mathrm{d}}{\mathrm{d}t} \left\langle \Psi^h, \chi \right\rangle^h_{\Gamma^h(t)} + \mathcal{D}_\Gamma \left\langle \nabla_s \, \Psi^h, \nabla_s \, \chi \right\rangle_{\Gamma^h(t)} = \left\langle \Psi^h, \partial_t^{\circ,h} \, \chi \right\rangle^h_{\Gamma^h(t)} - \left\langle \Psi^h_{\star,\varepsilon} \left(\vec{\mathcal{V}}^h - \vec{U}^h \right), \nabla_s \, \chi \right\rangle^h_{\Gamma^h(t)} \\
&\qquad\qquad - \sum_{i \in \{\pm\}} \frac{1}{\alpha_i} \left\langle F'_\varepsilon(\Psi^h) - G'_{i,\varepsilon}(\Phi^h_i), \chi \right\rangle^h_{\Gamma^h(t)} \qquad \forall \, \chi \in W_T(\mathcal{G}^h_T) \,, \qquad (4.37f)
\end{aligned}$$

where we recall (4.4). Here $\Psi^h_{\star,\varepsilon} = \Psi^h$ for $d = 3$ and, on recalling (4.18),

$$\Psi^h_{\star,\varepsilon} = \begin{cases} -\frac{\gamma_\varepsilon(\Psi^h_k) - \gamma_\varepsilon(\Psi^h_{k-1})}{F'_\varepsilon(\Psi^h_k) - F'_\varepsilon(\Psi^h_{k-1})} & \Psi^h_{k-1} \neq \Psi^h_k \,, \\ \Psi^h_k & \Psi^h_{k-1} = \Psi^h_k \,, \end{cases} \quad \text{on} \quad [\vec{q}^h_{k-1}, \vec{q}^h_k] \quad \forall \, k \in \{1, \dots, K_\Gamma\} \qquad (4.38)$$

for $d = 2$. Here we have introduced the shorthand notation $\Psi^h_k(t) = \Psi^h(\vec{q}^h_k(t), t)$, for $k = 1, \dots, K_\Gamma$, and for notational convenience we have dropped the dependence on t in (4.38). The definition in (4.38), similarly to (4.23b), is chosen such that for $d = 2$ it holds that

$$\begin{aligned}
\left\langle \Psi^h_{\star,\varepsilon} \, \vec{\eta}, \nabla_s \, \pi^h \left[F'_\varepsilon(\Psi^h) \right] \right\rangle^h_{\Gamma^h(t)} = \left\langle \Psi^h_{\star,\varepsilon} \, \vec{\eta}, \nabla_s \, \pi^h \left[F'_\varepsilon(\Psi^h) \right] \right\rangle_{\Gamma^h(t)} = - \left\langle \vec{\eta}, \nabla_s \, \pi^h \left[\gamma_\varepsilon(\Psi^h) \right] \right\rangle_{\Gamma^h(t)} \\
\forall \, \vec{\eta} \in \underline{V}(\Gamma^h(t)) \,. \qquad (4.39)
\end{aligned}$$

Here we note that (4.39) for $\vec{\eta} = \vec{\mathcal{V}}^h - \vec{\pi}^h \, \vec{U}^h \,|_{\Gamma^h(t)}$ mimics (3.29) on the discrete level.

We recall that as there appears to be no discrete variant of (3.9), it does not seem to be possible to prove a discrete analogue of the conservation property (3.19) for (4.37a–f).

We remark that the formulation (4.37f) for the surfactant transport equation (2.8b) falls into the framework of ALE-ESFEM (Arbitrary Eulerian Lagrangian evolving surface

finite element method) as coined by the authors in Elliott and Styles (2012). In this particular instance, the tangential velocity of $\Gamma^h(t)$ is not a priori fixed, rather it arises implicitly through the evolution of $\Gamma^h(t)$ as determined by (4.37a–f).

4.2.2 Model (ii)

We consider the following semidiscrete continuous-in-time finite element approximation, which is the analogue of the weak formulation (3.28a–d), (3.21a) and (3.30).

Given $\Gamma^h(0)$, $\vec{U}^h(\cdot,0) \in \mathbb{U}^h$, $\Phi^h(\cdot,0) \in S_1^h$ and $\Psi^h(\cdot,0) \in W(\Gamma^h(0))$, find $\Gamma^h(t)$ such that $\vec{\mathrm{id}}|_{\Gamma^h(t)} \in \underline{V}(\Gamma^h(t))$ for $t \in [0,T]$, and functions $\vec{U}^h \in H^1(0,T;\mathbb{U}^h)$, $P^h \in \mathbb{P}_T^h$, $\kappa^h \in W(\mathcal{G}_T^h)$, $\Phi^h \in H^1(0,T;S_1^h)$ and $\Psi^h \in W_T(\mathcal{G}_T^h)$ such that for almost all $t \in (0,T)$ we have that (4.37a–d) and

$$\begin{aligned}
&\left(\Phi_t^h, \xi\right)^h - \left(\vec{U}^h, \Xi_\varepsilon^h(\Phi^h)\,\nabla\xi\right) + \left(\mathcal{D}^h\,\nabla\,\Phi^h, \nabla\,\xi\right) + \left\langle \lambda_+\,(\Phi^h - g_+), \xi\right\rangle_{\partial\Omega}^h \\
&\qquad = \left(\frac{1}{\alpha_-} + \frac{1}{\alpha_+}\right)\left\langle F_\varepsilon'(\Psi^h) - I_1^h\,[G_\varepsilon'(\Phi^h)], \xi\right\rangle_{\Gamma^h(t)}^h \qquad \forall\ \xi \in S_1^h\,, \quad (4.40a)\\
&\frac{\mathrm{d}}{\mathrm{d}t}\left\langle \Psi^h, \chi\right\rangle_{\Gamma^h(t)}^h + \mathcal{D}_\Gamma\left\langle \nabla_s\,\Psi^h, \nabla_s\,\chi\right\rangle_{\Gamma^h(t)} = \left\langle \Psi^h, \partial_t^{\circ,h}\,\chi\right\rangle_{\Gamma^h(t)}^h \\
&\qquad - \left\langle \Psi_{\star,\varepsilon}^h\left(\vec{\mathcal{V}}^h - \vec{U}^h\right), \nabla_s\,\chi\right\rangle_{\Gamma^h(t)}^h - \left(\frac{1}{\alpha_-} + \frac{1}{\alpha_+}\right)\left\langle F_\varepsilon'(\Psi^h) - I_1^h\,[G_\varepsilon'(\Phi^h)], \chi\right\rangle_{\Gamma^h(t)}^h \\
&\qquad\qquad \forall\ \chi \in W_T(\mathcal{G}_T^h) \qquad (4.40b)
\end{aligned}$$

hold.

Similarly to Lemma 4.2, in the following lemma we derive a discrete analogue of (3.11).

LEMMA. 4.5. *Let* $\{(\Gamma^h, \vec{U}^h, P^h, \kappa^h, \Phi^h, \Psi^h)(t)\}_{t\in[0,T]}$ *be a solution to* (4.37a–d), (4.40a,b). *Then*

$$\begin{aligned}
&\tfrac{1}{2}\,\frac{\mathrm{d}}{\mathrm{d}t}\,\|[\rho^h]^{\frac12}\,\vec{U}^h\|_0^2 + 2\,\|[\mu^h]^{\frac12}\,\underline{\underline{D}}(\vec{U}^h)\|_0^2 \\
&\quad = (\rho^h\,\vec{f}_1^{\,h} + \vec{f}_2^{\,h}, \vec{U}^h) + \left\langle \pi^h\,[\gamma_\varepsilon(\Psi^h)\,\kappa^h]\,\vec{\nu}^h, \vec{U}^h\right\rangle_{\Gamma^h(t)} + \left\langle \nabla_s\,\pi^h\,[\gamma_\varepsilon(\Psi^h)], \vec{U}^h\right\rangle_{\Gamma^h(t)}^h . \quad (4.41)
\end{aligned}$$

Proof. The desired result (4.41) follows immediately on choosing $\vec{\xi} = \vec{U}^h$ in (4.37a) and $\varphi = P^h$ in (4.37b). □

The next theorem derives a discrete analogue of the energy law (3.23), similarly to Theorem 4.3, together with an exact volume conservation property.

THEOREM. 4.6. *Let* $\{(\Gamma^h, \vec{U}^h, P^h, \kappa^h, \Phi^h, \Psi^h)(t)\}_{t\in[0,T]}$ *be a solution to* (4.37a–d), (4.40a,b). *Then* (4.27) *holds. Moreover, if* $\mathcal{X}_{\Omega_-^h(t)} \in \mathbb{P}^h(t)$ *then*

$$\frac{\mathrm{d}}{\mathrm{d}t}\,\mathcal{L}^d(\Omega_-^h(t)) = 0\,. \qquad (4.42)$$

In addition, if $d = 2$ *and* (4.26) *and* $(\mathcal{A}_1)$ *hold, then*

$$\frac{\mathrm{d}}{\mathrm{d}t}\left(\tfrac{1}{2}\,\|[\rho^h]^{\frac{1}{2}}\,\vec{U}^h\|_0^2 + \big(G_\varepsilon(\Phi^h),1\big)^h + \big\langle F_\varepsilon(\Psi^h),1\big\rangle^h_{\Gamma^h(t)}\right) + 2\,\|[\mu^h]^{\frac{1}{2}}\,\underline{\underline{D}}(\vec{U}^h)\|_0^2$$
$$+ \big\langle \lambda_+, G_\varepsilon(\Phi^h)\big\rangle^h_{\partial\Omega} + \left(\frac{1}{\alpha_-}+\frac{1}{\alpha_+}\right)\big\langle |F_\varepsilon'(\Psi^h) - I_1^h\,[G_\varepsilon'(\Phi^h)]|^2,1\big\rangle^h_{\Gamma^h(t)}$$
$$\leq \Big(\rho^h\,\vec{f}_1^{\,h} + \vec{f}_2^{\,h}, \vec{U}^h\Big) + \langle \lambda_+, G_\varepsilon(g_+)\rangle^h_{\partial\Omega}\,. \quad (4.43)$$

Proof. The conservation property (4.27) follows immediately from choosing $\xi = 1$ in (4.37e) and $\chi = 1$ in (4.37f). Moreover, choosing $\chi = 1$ in (4.37c) and $\varphi = (\mathcal{X}_{\Omega^h_-(t)} - \frac{\mathcal{L}^d(\Omega^h_-(t))}{\mathcal{L}^d(\Omega)}) \in \widehat{\mathbb{P}}^h(t)$ in (4.37b), we obtain from (4.13) that

$$\frac{\mathrm{d}}{\mathrm{d}t}\mathcal{L}^d(\Omega^h_-(t)) = \Big\langle \vec{\mathcal{V}}^h, \vec{\nu}^h\Big\rangle_{\Gamma^h(t)} = \Big\langle \vec{\mathcal{V}}^h, \vec{\nu}^h\Big\rangle^h_{\Gamma^h(t)} = \Big\langle \vec{U}^h, \vec{\nu}^h\Big\rangle_{\Gamma^h(t)} = \int_{\Omega^h_-(t)} \nabla\,.\,\vec{U}^h\,\mathrm{d}\mathcal{L}^d = 0\,,$$

which proves the desired result (4.42). For the remainder of the proof we assume that $d = 2$.

In order to show that (4.43) holds, we now proceed similarly to the continuous argument, recall (3.29). The assumption (4.26) means that we can choose $\chi = \pi^h\,[F_\varepsilon'(\Psi^h)]$ in (4.37f) to yield, similarly to (4.29)–(4.33), on choosing $\xi = I_1^h\,[G_\varepsilon'(\Phi^h)]$ in (4.40a) and on recalling (4.18), (4.10), (4.11), (4.39) and (4.37c,d), that

$$\begin{aligned}
&\frac{\mathrm{d}}{\mathrm{d}t}\left(\big(G_\varepsilon(\Phi^h),1\big)^h + \big\langle F_\varepsilon(\Psi^h),1\big\rangle^h_{\Gamma^h(t)}\right) + \mathcal{D}_\Gamma\,\big\langle \nabla_s\,\Psi^h, \nabla_s\,\pi^h\,[F_\varepsilon'(\Psi^h)]\big\rangle_{\Gamma^h(t)}\\
&\quad + \big(\mathcal{D}^h\,\nabla\,\Phi^h, \nabla\,I_1^h\,[G_\varepsilon'(\Phi^h)]\big) + \left(\frac{1}{\alpha_-}+\frac{1}{\alpha_+}\right)\big\langle |F_\varepsilon'(\Psi^h) - I_1^h\,[G_\varepsilon'(\Phi^h)]|^2,1\big\rangle^h_{\Gamma^h(t)}\\
&\quad + \big\langle \lambda_+\,(\Phi^h - g_+), G_\varepsilon'(\Phi^h)\big\rangle^h_{\partial\Omega}\\
&= \Big\langle \nabla_s\,\vec{\mathrm{id}}, \nabla_s\,\pi^h\,[\gamma_\varepsilon(\Psi^h)\,\vec{\mathcal{V}}^h]\Big\rangle_{\Gamma^h(t)} - \Big\langle \nabla_s\,\pi^h\,[\gamma_\varepsilon(\Psi^h)], \vec{\mathcal{V}}^h\Big\rangle_{\Gamma^h(t)}\\
&\qquad + \Big\langle \vec{\mathcal{V}}^h - \vec{\pi}^h\,\vec{U}^h, \nabla_s\,\pi^h\,[\gamma_\varepsilon(\Psi^h)]\Big\rangle_{\Gamma^h(t)}\\
&= -\Big\langle \kappa^h\,\vec{\nu}^h, \gamma_\varepsilon(\Psi^h)\,\vec{\mathcal{V}}^h\Big\rangle^h_{\Gamma^h(t)} - \Big\langle \vec{U}^h, \nabla_s\,\pi^h\,[\gamma_\varepsilon(\Psi^h)]\Big\rangle^h_{\Gamma^h(t)}\\
&= -\Big\langle \pi^h\,[\gamma_\varepsilon(\Psi^h)\,\kappa^h]\,\vec{\nu}^h, \vec{U}^h\Big\rangle_{\Gamma^h(t)} - \Big\langle \nabla_s\,\pi^h\,[\gamma_\varepsilon(\Psi^h)], \vec{U}^h\Big\rangle^h_{\Gamma^h(t)}\,. \qquad (4.44)
\end{aligned}$$

Similarly to (4.34) and (4.35), we note that the second and third terms on the left hand side of (4.44) are nonnegative. Hence the desired result (4.43) follows from combining (4.44) with (4.41). □

Clearly, the three results in Theorem 4.6 are natural discrete analogues of (3.22), (3.18) and (3.23), respectively. We remark that the condition $\mathcal{X}_{\Omega^h_-(t)} \in \mathbb{P}^h(t)$ is always satisfied for the XFEM$_\Gamma$ approach as introduced in Barrett *et al.* (2013a, 2014). In addition, the results of Remark 4.4 apply to (4.37a–d) and (4.40a,b).

4.2.3 Properties of the implicit tangential velocity

We remark that it is possible to prove that the vertices of the solutions $\Gamma^h(t)$ to the two semidiscrete schemes in §4.2.1 and §4.2.1 are well distributed. As this follows already from the equation (4.37d), we refer to our earlier work in Barrett *et al.* (2007, 2008) for further details. In particular, we observe that in the case $d = 2$, i.e. for the planar two-phase problem, an equidistribution property for the vertices of $\Gamma^h(t)$ can be shown. These good mesh properties mean that for fully discrete schemes based on these semidiscrete approximations no remeshings are required in practice for either $d = 2$ or $d = 3$.

We remark that for the schemes in §4.1 it is not possible to prove (4.42), even if mass lumping was to be dropped from the right hand side of (4.20c), because $\vec{\chi} = \vec{\nu}^h$ is not a valid test function in (4.20c). As a consequence, the volume of the two phases will in general not be conserved in practice. This is an additional advantage of the formulations in §4.2 over the schemes in §4.1.

5 Fully discrete finite element approximation

In this section we consider fully discrete variants of the schemes from Section 4. Here we will choose the time discretization such that existence and uniqueness of the discrete solutions can be guaranteed, and such that we inherit as much of the structure of the stable schemes in Barrett *et al.* (2013a, 2014) as possible, see below for details.

We consider the partitioning $t_m = m\,\tau$, $m = 0, \ldots, M$, of $[0, T]$ into uniform time steps $\tau = T/M$. The time discrete spatial discretizations then directly follow from the finite element spaces introduced in Section 4, where in order to allow for adaptivity in space we consider bulk finite element spaces that change in time.

For all $m \geq 0$, let $\mathcal{T}^m$ be a regular partitioning of Ω into disjoint open simplices o^m_j, $j = 1, \ldots, J^m_\Omega$. Associated with $\mathcal{T}^m$ are the finite element spaces S^m_k for $k \geq 0$. We introduce also $I^m_k : C(\overline{\Omega}) \to S^m_k$, $k \geq 1$, the standard interpolation operators, and the standard projection operator $I^m_0 : L^1(\Omega) \to S^m_0$; and similarly $\vec{I}^m_k : [C(\overline{\Omega})]^d \to [S^m_k]^d$, $k \geq 1$. For the approximation to the velocity and pressure on $\mathcal{T}^m$ will use the finite element spaces $\mathbb{U}^m \subset \mathbb{U}$ and $\mathbb{P}^m \subset \mathbb{P}$, which are the direct time discrete analogues of $\mathbb{U}^h$ and $\mathbb{P}^h(t_m)$, as well as $\widehat{\mathbb{P}}^m \subset \widehat{\mathbb{P}}$. We recall that $(\mathbb{U}^m, \mathbb{P}^m)$ are said to satisfy the LBB inf-sup condition if

$$\inf_{\varphi \in \widehat{\mathbb{P}}^m} \sup_{\vec{\xi} \in \mathbb{U}^m} \frac{(\varphi, \nabla \cdot \vec{\xi})}{\|\varphi\|_0 \, \|\vec{\xi}\|_1} > 0\,. \tag{5.1}$$

Following the XFEM$_\Gamma$ approach introduced in Barrett *et al.* (2013a, 2014), we will often augment $\mathbb{P}^m$ by the single basis function $\mathcal{X}_{\Omega^m_-}$. For this extended finite element space it does not appear possible to show that (5.1) holds, but she schemes in §5.2 with XFEM$_\Gamma$ show excellent volume conservation properties in practice; recall Theorem 4.6.

Similarly, the parametric finite element spaces are given by

$$\underline{V}(\Gamma^m) := \{\vec{\chi} \in [C(\Gamma^m)]^d : \vec{\chi}|_{\sigma_j^m} \text{ is linear } \forall\ j = 1, \dots, J_\Gamma\} =: [W(\Gamma^m)]^d \subset [H^1(\Gamma^m)]^d\,,$$

for $m = 0, \dots, M-1$. Here $\Gamma^m = \bigcup_{j=1}^{J_\Gamma} \overline{\sigma_j^m}$, where $\{\sigma_j^m\}_{j=1}^{J_\Gamma}$ is a family of mutually disjoint open $(d-1)$-simplices with vertices $\{\vec{q}_k^m\}_{k=1}^{K_\Gamma}$. We denote the standard basis of $W(\Gamma^m)$ by $\{\chi_k^m(\cdot,t)\}_{k=1}^{K_\Gamma}$. We also introduce $\pi^m : C(\Gamma^m) \to W(\Gamma^m)$, the standard interpolation operator at the nodes $\{\vec{q}_k^m\}_{k=1}^{K_\Gamma}$, and similarly $\vec{\pi}^m : [C(\Gamma^m)]^d \to \underline{V}(\Gamma^m)$. Throughout this paper, we will parameterize the new closed surface Γ^{m+1} over Γ^m, with the help of a parameterization $\vec{X}^{m+1} \in \underline{V}(\Gamma^m)$, i.e. $\Gamma^{m+1} = \vec{X}^{m+1}(\Gamma^m)$. Moreover, for $m \geq 0$, we will use the notation $\vec{X}^m = \vec{\mathrm{id}}\,|_{\Gamma^m} \in \underline{V}(\Gamma^m)$.

We also introduce the L^2–inner product $\langle\cdot,\cdot\rangle_{\Gamma^m}$ over the current polyhedral surface Γ^m, as well as the the mass lumped inner product $\langle\cdot,\cdot\rangle_{\Gamma^m}^h$.

Given Γ^m, we let Ω_+^m denote the exterior of Γ^m and let Ω_-^m denote the interior of Γ^m, so that $\Gamma^m = \partial\Omega_-^m = \overline{\Omega_-^m} \cap \overline{\Omega_+^m}$. We then partition the elements of the bulk mesh $\mathcal{T}^m$ into interior, exterior and interfacial elements as before, and we introduce ρ^m, $\mu^m \in S_0^m$, for $m \geq 0$, as

$$\rho^m\,|_{o^m} = \begin{cases} \rho_- & o^m \in \mathcal{T}^m_{\Omega_-^m}\,, \\ \rho_+ & o^m \in \mathcal{T}^m_{\Omega_+^m}\,, \\ \frac{1}{2}\,(\rho_- + \rho_+) & o^m \in \mathcal{T}^m_{\Gamma^m}\,, \end{cases} \quad \text{and} \quad \mu^m\,|_{o^m} = \begin{cases} \mu_- & o^m \in \mathcal{T}^m_{\Omega_-^m}\,, \\ \mu_+ & o^m \in \mathcal{T}^m_{\Omega_+^m}\,, \\ \frac{1}{2}\,(\mu_- + \mu_+) & o^m \in \mathcal{T}^m_{\Gamma^m}\,. \end{cases} \tag{5.2}$$

We also set $\rho^{-1} := \rho^0$. In addition, we introduce $\mathcal{D}^{m+1} \in S_0^m$ defined by

$$\mathcal{D}^{m+1}\,|_o = \begin{cases} \mathcal{D}_- & o \in \mathcal{T}^m_{\Omega_-^{m+1}}\,, \\ \mathcal{D}_+ & o \in \mathcal{T}^m_{\Omega_+^{m+1}}\,, \\ \frac{1}{2}\,(\mathcal{D}_- + \mathcal{D}_+) & o \in \mathcal{T}^m_{\Gamma^{m+1}}\,. \end{cases}$$

We also introduce the matrix function $\Xi_\varepsilon^m : S_1^m \to [S_0^m]^{d\times d}$ defined such that for all $z^h \in S_1^m$ and almost everywhere in Ω it holds that

$$\Xi_\varepsilon^m(z^h)\,\nabla\, I_1^m\,[G_\varepsilon'(z^h)] = \nabla\, I_1^m\,[R_\varepsilon(G_\varepsilon'(z^h))]\,,$$

which can be constructed in a fashion analogous to (4.23a,b).

Similarly to (4.14) we introduce

$$S_{1,\pm}^m := \{\chi \in S_1^m : \chi(\vec{p}_{1,j}^m) = 0 \ \text{ if } \ \mathrm{supp}(\varphi_{1,j}^m) \subset \overline{\Omega_\mp^{m+1}}\}\,. \tag{5.3}$$

We also define

$$(\eta,\zeta)^{m,h} := \int_\Omega I_1^m\,[\eta\,\zeta]\,\mathrm{d}\mathcal{L}^d \qquad \forall\ \eta,\zeta \in C(\overline{\Omega})\,, \tag{5.4}$$

as well as

$$(\chi,\varphi)^m_{\Omega_\pm^\ell} := \sum_{j=1}^{J_\Omega^m} v^m_{\Omega_\pm^\ell}(o_j^m) \int_{o_j^m} \chi\,\varphi\,\mathrm{d}\mathcal{L}^d \quad \forall\ \chi,\varphi \in L^2(\Omega)\,, \tag{5.5}$$

where, for $\ell = m$ and $\ell = m+1$,

$$v^m_{\Omega^\ell_\pm}(o) = \begin{cases} 1 & o \in \mathcal{T}^m_{\Omega^\ell_\pm}\,, \\ 0 & o \in \mathcal{T}^m_{\Omega^\ell_\mp}\,, \\ \frac{1}{2} & o \in \mathcal{T}^m_{\Gamma^\ell}\,. \end{cases}$$

Similarly to (5.5), we define

$$(\chi,\varphi)^{m,h}_{\Omega^\ell_\pm} := \sum_{j=1}^{J^m_\Omega} v^m_{\Omega^\ell_\pm}(o^m_j) \int_{o^m_j} I^m_1\,[\chi\,\varphi]\,\mathrm{d}\mathcal{L}^d \quad \forall\ \chi,\varphi \in C(\overline{\Omega})\,. \tag{5.6}$$

Of course, (5.4), (5.5) and (5.6) are the natural fully discrete analogues of (4.3), (4.15) and (4.16), respectively.

We introduce the following pushforward operators for the discrete interfaces Γ^m and Γ^{m-1}. Let $\Pi^m_{m-1} : C(\Gamma^{m-1}) \to W(\Gamma^m)$ be such that

$$(\Pi^m_{m-1}\,z)(\vec{q}^{\,m}_k) = z(\vec{q}^{\,m-1}_k)\,, \qquad k = 1,\dots,K_\Gamma\,, \qquad \forall\ z \in C(\Gamma^{m-1})\,, \tag{5.7}$$

for $m = 1,\dots,M$, and set $\Pi^0_{-1} := \pi^0$. Analogously to (5.7) we also introduce $\vec{\Pi}^m_{m-1} : [C(\Gamma^{m-1})]^d \to \underline{V}(\Gamma^m)$.

5.1 Approximations with fluidic tangential velocity

5.1.1 Model (i)

Our proposed fully discrete equivalent of (4.20a–f) is given as follows. Let Γ^0, an approximation to $\Gamma(0)$, and $\vec{U}^0 \in \mathbb{U}^0$, as well as $\Phi^0_\pm \in S^0_{1,\pm}$, $\Psi^0 \in W(\Gamma^0)$ and $\vec{\kappa}^0 \in \underline{V}(\Gamma^0)$ be given. For $m = 0,\dots,M-1$, find $\vec{U}^{m+1} \in \mathbb{U}^m$, $P^{m+1} \in \widehat{\mathbb{P}}^m$, $\vec{X}^{m+1} \in \underline{V}(\Gamma^m)$ and $\vec{\kappa}^{m+1} \in \underline{V}(\Gamma^m)$ such that

$$\begin{aligned}
&\tfrac{1}{2}\left(\frac{\rho^m\,\vec{U}^{m+1} - (I^m_0\,\rho^{m-1})\,\vec{I}^m_2\,\vec{U}^m}{\tau} + (I^m_0\,\rho^{m-1})\,\frac{\vec{U}^{m+1} - \vec{I}^m_2\,\vec{U}^m}{\tau}, \vec{\xi}\right) \\
&\quad + 2\left(\mu^m\,\underline{\underline{D}}(\vec{U}^{m+1}), \underline{\underline{D}}(\vec{\xi})\right) + \tfrac{1}{2}\left(\rho^m, [(\vec{I}^m_2\,\vec{U}^m\,.\,\nabla)\,\vec{U}^{m+1}]\,.\,\vec{\xi} - [(\vec{I}^m_2\,\vec{U}^m\,.\,\nabla)\,\vec{\xi}]\,.\,\vec{U}^{m+1}\right) \\
&\quad - \left(P^{m+1}, \nabla\,.\,\vec{\xi}\right) = \left(\rho^m\,\vec{f}^{m+1}_1 + \vec{f}^{m+1}_2, \vec{\xi}\right) + \left\langle \gamma_\varepsilon(\Psi^m)\,\vec{\Pi}^m_{m-1}\,\vec{\kappa}^m + \nabla_s\,\pi^m\,[\gamma_\varepsilon(\Psi^m)], \vec{\xi}\right\rangle^h_{\Gamma^m} \\
&\qquad\qquad \forall\ \vec{\xi} \in \mathbb{U}^m\,,
\end{aligned} \tag{5.8a}$$

$$\left(\nabla\,.\,\vec{U}^{m+1}, \varphi\right) = 0 \qquad \forall\ \varphi \in \widehat{\mathbb{P}}^m\,, \tag{5.8b}$$

$$\left\langle \frac{\vec{X}^{m+1} - \vec{X}^m}{\tau}, \vec{\chi}\right\rangle^h_{\Gamma^m} = \left\langle \vec{U}^{m+1}, \vec{\chi}\right\rangle^h_{\Gamma^m} \qquad \forall\ \vec{\chi} \in \underline{V}(\Gamma^m)\,, \tag{5.8c}$$

$$\left\langle \vec{\kappa}^{m+1}, \vec{\eta}\right\rangle^h_{\Gamma^m} + \left\langle \nabla_s\,\vec{X}^{m+1}, \nabla_s\,\vec{\eta}\right\rangle_{\Gamma^m} = 0 \qquad \forall\ \vec{\eta} \in \underline{V}(\Gamma^m) \tag{5.8d}$$

and set $\Gamma^{m+1} = \vec{X}^{m+1}(\Gamma^m)$. Then find $\Phi_\pm^{m+1} \in S_{1,\pm}^m$ and $\Psi^{m+1} \in W(\Gamma^{m+1})$ such that

$$\frac{1}{\tau}\left[\left(\Phi_\pm^{m+1},\xi\right)_{\Omega_\pm^{m+1}}^{m,h} - \left(\widehat{\Phi}_\pm^m,\xi\right)_{\Omega_\pm^{m+1}}^{m,h}\right] + \mathcal{D}_\pm\left(\nabla\,\Phi_\pm^{m+1},\nabla\,\xi\right)_{\Omega_\pm^{m+1}}^m + \left\langle\lambda_\pm\,(\Phi_\pm^{m+1}-g_\pm),\xi\right\rangle_{\partial\Omega}^h$$
$$= \frac{1}{\alpha_\pm}\left\langle F_\varepsilon'(\Pi_m^{m+1}\,\Psi^m) - G_{\pm,\varepsilon}'(\Pi_m^{m+1}\,[(I_1^m\,\Phi_\pm^m)\,|_{\Gamma^m}]),\xi\right\rangle_{\Gamma^{m+1}}^h \qquad \forall\ \xi \in S_{1,\pm}^m\,, \tag{5.8e}$$

$$\frac{1}{\tau}\left\langle\Psi^{m+1},\chi_k^{m+1}\right\rangle_{\Gamma^{m+1}}^h + \mathcal{D}_\Gamma\left\langle\nabla_s\,\Psi^{m+1},\nabla_s\,\chi_k^{m+1}\right\rangle_{\Gamma^{m+1}}$$
$$= \frac{1}{\tau}\left\langle\Psi^m,\chi_k^m\right\rangle_{\Gamma^m}^h - \sum_{i\in\{\pm\}}\frac{1}{\alpha_i}\left\langle F_\varepsilon'(\Pi_m^{m+1}\,\Psi^m) - G_{i,\varepsilon}'(\Pi_m^{m+1}\,[(I_1^m\,\Phi_i^m)\,|_{\Gamma^m}]),\chi_k^{m+1}\right\rangle_{\Gamma^{m+1}}^h$$
$$\forall\ k \in \{1,\dots,K_\Gamma\}\,. \tag{5.8f}$$

Here we have defined $\vec{f}_i^{m+1} := \vec{I}_2^m\,\vec{f}_i(\cdot,t_{m+1})$, $i=1,2$. Note that here ∇_s denotes the surface gradient on Γ^m, and so it depends on m. We observe that (5.8a–f) is a linear scheme in that it leads to a linear system of equations for the unknowns $(\vec{U}^{m+1}, P^{m+1}, \vec{X}^{m+1}, \vec{\kappa}^{m+1}, \Phi_\pm^{m+1}, \Psi^{m+1})$ at each time level. In particular, the system (5.8a–f) clearly decouples into (5.8a,b) for $(\vec{U}^{m+1}, P^{m+1})$, then (5.8c,d) for $(\vec{X}^{m+1}, \vec{\kappa}^{m+1})$ and finally (5.8e,f) for $(\Phi_\pm^{m+1}, \Psi^{m+1})$, where the latter subsystem itself decouples. Our approximation (5.8e) is based on the Lagrange–Galerkin method, see e.g. Douglas and Russell (1982); Pironneau (1982). Here for any $\vec{z} \in \overline{\Omega}$, on letting $\vec{z}_0 = \vec{z} - \tau\,\vec{U}^{m+1}$, we have defined

$$\widehat{\Phi}_\pm^m(\vec{z}) = \begin{cases} \Phi_\pm^m(\vec{z}_0) & \vec{z}_0 \in \widehat{\Omega}_\pm^m\,,\\ \Phi_\pm^m(\vec{z}_0 + s\,(\vec{z}_0 - \vec{z})) & \vec{z}_0 \notin \widehat{\Omega}_\pm^m\,, \end{cases}$$

where $\widehat{\Omega}_\pm^m := \cup_{o\in\mathcal{T}_{\Omega_\pm^m}^m\cup\mathcal{T}_{\Gamma^m}^m}\overline{o}$ and $s \in \arg\min_{\vec{z}_0+s\,(\vec{z}_0-\vec{z})\in\widehat{\Omega}_\pm^m}|s|$.

At first sight, the most natural right hand side for (5.8e) appears to be

$$\frac{1}{\alpha_\pm}\left\langle F_\varepsilon'(\Psi^m) - G_{\pm,\varepsilon}'(I_1^m\,\Phi_\pm^m),\xi\right\rangle_{\Gamma^m}^h\,,$$

but as $\xi \in S_{1,\pm}^m$, recall (5.3), this may not be meaningful. Hence we evaluate this term on Γ^{m+1} in (5.8e). In order to keep the equation linear in the unknown, we push forward the values of Ψ^m and $\Phi_\pm^m$ on Γ^m to Γ^{m+1}.

5.1.2 Model (ii)

Our proposed fully discrete equivalent of (4.20a–d), (4.24a,b) is given as follows. Let Γ^0, an approximation to $\Gamma(0)$, and $\vec{U}^0 \in \mathbb{U}^0$, as well as $\Phi^0 \in S_1^0$, $\Psi^0 \in W(\Gamma^0)$ and $\vec{\kappa}^0 \in \underline{V}(\Gamma^0)$ be given. For $m = 0,\dots,M-1$, find $\vec{U}^{m+1} \in \mathbb{U}^m$, $P^{m+1} \in \widehat{\mathbb{P}}^m$, $\vec{X}^{m+1} \in \underline{V}(\Gamma^m)$ and $\vec{\kappa}^{m+1} \in \underline{V}(\Gamma^m)$ such that (5.8a–d) hold. Then find $\Phi^{m+1} \in S_1^m$ and $\Psi^{m+1} \in W(\Gamma^{m+1})$

such that

$$\left(\frac{\Phi^{m+1}-\Phi^m}{\tau},\xi\right)^{m,h} - \left(\vec{U}^{m+1},\Xi_\varepsilon^m(I_1^m\,\Phi^m)\,\nabla\,\xi\right) + \left(\mathcal{D}^{m+1}\,\nabla\,\Phi^{m+1},\nabla\,\xi\right)$$
$$+\left\langle\lambda_+\,(\Phi^{m+1}-g_+),\xi\right\rangle_{\partial\Omega}^h = \left(\frac{1}{\alpha_-}+\frac{1}{\alpha_+}\right)\langle F_\varepsilon'(\Psi^m) - I_1^m\,[G_\varepsilon'(\Phi^m)],\xi\rangle_{\Gamma^m}^h \quad \forall\,\xi\in S_1^m\,, \tag{5.9a}$$

$$\frac{1}{\tau}\left\langle\Psi^{m+1},\chi_k^{m+1}\right\rangle_{\Gamma^{m+1}}^h + \mathcal{D}_\Gamma\left\langle\nabla_s\,\Psi^{m+1},\nabla_s\,\chi_k^{m+1}\right\rangle_{\Gamma^{m+1}}$$
$$= \frac{1}{\tau}\left\langle\Psi^m,\chi_k^m\right\rangle_{\Gamma^m}^h - \left(\frac{1}{\alpha_-}+\frac{1}{\alpha_+}\right)\langle F_\varepsilon'(\Psi^m) - I_1^m\,[G_\varepsilon'(\Phi^m)],\chi_k^m\rangle_{\Gamma^m}^h \quad \forall\,k\in\{1,\dots,K_\Gamma\}\,. \tag{5.9b}$$

5.2 Approximations with implicit tangential velocity

5.2.1 Model (i)

Our proposed fully discrete equivalent of (4.37a–f), is given as follows. Let Γ^0, an approximation to $\Gamma(0)$, and $\vec{U}^0\in\mathbb{U}^0$, as well as $\Phi_\pm^0\in S_{1,\pm}^0$, $\Psi^0\in W(\Gamma^0)$ and $\kappa^0\in W(\Gamma^0)$ be given. For $m=0,\dots,M-1$, find $\vec{U}^{m+1}\in\mathbb{U}^m$, $P^{m+1}\in\widehat{\mathbb{P}}^m$, $\vec{X}^{m+1}\in\underline{V}(\Gamma^m)$ and $\kappa^{m+1}\in W(\Gamma^m)$ such that

$$\tfrac{1}{2}\left(\frac{\rho^m\,\vec{U}^{m+1}-(I_0^m\,\rho^{m-1})\,\vec{I}_2^m\,\vec{U}^m}{\tau}+(I_0^m\,\rho^{m-1})\,\frac{\vec{U}^{m+1}-\vec{I}_2^m\,\vec{U}^m}{\tau},\vec{\xi}\right)$$
$$+2\left(\mu^m\,\underline{\underline{D}}(\vec{U}^{m+1}),\underline{\underline{D}}(\vec{\xi})\right)+\tfrac{1}{2}\left(\rho^m,[(\vec{I}_2^m\,\vec{U}^m\,.\,\nabla)\,\vec{U}^{m+1}]\,.\,\vec{\xi}-[(\vec{I}_2^m\,\vec{U}^m\,.\,\nabla)\,\vec{\xi}]\,.\,\vec{U}^{m+1}\right)$$
$$-\left(P^{m+1},\nabla\,.\,\vec{\xi}\right)=\left(\rho^m\,\vec{f}_1^{m+1}+\vec{f}_2^{m+1},\vec{\xi}\right)+\left\langle\pi^m\,[\gamma_\varepsilon(\Psi^m)\,\Pi_{m-1}^m\,\kappa^m]\,\vec{\nu}^m,\vec{\xi}\right\rangle_{\Gamma^m}$$
$$+\left\langle\nabla_s\,\pi^m\,[\gamma_\varepsilon(\Psi^m)],\vec{\xi}\right\rangle_{\Gamma^m}^h \qquad \forall\,\vec{\xi}\in\mathbb{U}^m\,, \tag{5.10a}$$

$$\left(\nabla\,.\,\vec{U}^{m+1},\varphi\right)=0\quad\forall\,\varphi\in\widehat{\mathbb{P}}^m\,, \tag{5.10b}$$

$$\left\langle\frac{\vec{X}^{m+1}-\vec{X}^m}{\tau},\chi\,\vec{\nu}^m\right\rangle_{\Gamma^m}^h=\left\langle\vec{U}^{m+1},\chi\,\vec{\nu}^m\right\rangle_{\Gamma^m}\quad\forall\,\chi\in W(\Gamma^m)\,, \tag{5.10c}$$

$$\left\langle\kappa^{m+1}\,\vec{\nu}^m,\vec{\eta}\right\rangle_{\Gamma^m}^h+\left\langle\nabla_s\,\vec{X}^{m+1},\nabla_s\,\vec{\eta}\right\rangle_{\Gamma^m}=0\quad\forall\,\vec{\eta}\in\underline{V}(\Gamma^m) \tag{5.10d}$$

and set $\Gamma^{m+1} = \vec{X}^{m+1}(\Gamma^m)$. Then find $\Phi_\pm^{m+1} \in S_{1,\pm}^m$ and $\Psi^{m+1} \in W(\Gamma^{m+1})$ such that

$$\Phi_\pm^{m+1} \text{ satisfies (5.8e)}\,, \tag{5.10e}$$

$$\begin{aligned}
&\frac{1}{\tau}\left\langle \Psi^{m+1}, \chi_k^{m+1}\right\rangle_{\Gamma^{m+1}}^h + \mathcal{D}_\Gamma\left\langle \nabla_s\,\Psi^{m+1}, \nabla_s\,\chi_k^{m+1}\right\rangle_{\Gamma^{m+1}} \\
&\quad = \frac{1}{\tau}\left\langle \Psi^m, \chi_k^m\right\rangle_{\Gamma^m}^h - \left\langle \Psi_{\star,\varepsilon}^m\left(\frac{\vec{X}^{m+1}-\vec{X}^m}{\tau} - \vec{U}^{m+1}\right), \nabla_s\,\chi_k^m\right\rangle_{\Gamma^m}^h \\
&\qquad - \sum_{i\in\{\pm\}}\frac{1}{\alpha_i}\left\langle F_\varepsilon'(\Pi_m^{m+1}\,\Psi^m) - G_{i,\varepsilon}'(\Pi_m^{m+1}\,[(I_1^m\,\Phi_i^m)\,|_{\Gamma^m}]), \chi_k^{m+1}\right\rangle_{\Gamma^{m+1}}^h \quad \forall\ k\in\{1,\ldots,K_\Gamma\}\,,
\end{aligned} \tag{5.10f}$$

where $\Psi_{\star,\varepsilon}^m = \Psi^m$ for $d=3$ and, on recalling (2.11),

$$\Psi_{\star,\varepsilon}^m = \begin{cases} -\frac{\gamma_\varepsilon(\Psi_k^m)-\gamma_\varepsilon(\Psi_{k-1}^m)}{F_\varepsilon'(\Psi_k^m)-F_\varepsilon'(\Psi_{k-1}^m)} & F_\varepsilon'(\Psi_{k-1}^m)\neq F_\varepsilon'(\Psi_k^m)\,,\\ \frac{1}{2}\,(\Psi_{k-1}^m+\Psi_k^m) & F_\varepsilon'(\Psi_{k-1}^m)= F_\varepsilon'(\Psi_k^m)\,,\end{cases} \quad \text{on}\quad [\vec{q}_{k-1}^m,\vec{q}_k^m]\quad \forall\ k\in\{1,\ldots,K_\Gamma\}$$

for $d=2$, where $\Psi^m = \sum_{k=1}^{K_\Gamma}\Psi_k^m\,\chi_k^m$. We observe that (5.10a–f) is a linear scheme in that it leads to a linear system of equations for the unknowns $(\vec{U}^{m+1}, P^{m+1}, \vec{X}^{m+1}, \kappa^{m+1}, \Phi_\pm^{m+1}, \Psi^{m+1})$ at each time level. In particular, the system (5.10a–f) clearly decouples into (5.10a,b) for $(\vec{U}^{m+1}, P^{m+1})$, then (5.10c,d) for $(\vec{X}^{m+1}, \kappa^{m+1})$ and finally (5.10e,f) for $(\Phi_\pm^{m+1}, \Psi^{m+1})$.

5.2.2 Model (ii)

Our proposed fully discrete equivalent of (4.37a–d), (4.40a,b) is given as follows. Let Γ^0, an approximation to $\Gamma(0)$, and $\vec{U}^0 \in \mathbb{U}^0$, as well as $\Phi^0 \in S_1^0$, $\Psi^0 \in W(\Gamma^0)$ and $\kappa^0 \in W(\Gamma^0)$ be given. For $m=0,\ldots,M-1$, find $\vec{U}^{m+1}\in\mathbb{U}^m$, $P^{m+1}\in\widehat{\mathbb{P}}^m$, $\vec{X}^{m+1}\in \underline{V}(\Gamma^m)$ and $\kappa^{m+1}\in W(\Gamma^m)$ such that (5.10a–d) hold. Then find $\Phi^{m+1}\in S_1^m$ and $\Psi^{m+1}\in W(\Gamma^{m+1})$ such that

$$\Phi^{m+1} \text{ satisfies (5.9a)}\,, \tag{5.11a}$$

$$\begin{aligned}
&\frac{1}{\tau}\left\langle \Psi^{m+1}, \chi_k^{m+1}\right\rangle_{\Gamma^{m+1}}^h + \mathcal{D}_\Gamma\left\langle \nabla_s\,\Psi^{m+1}, \nabla_s\,\chi_k^{m+1}\right\rangle_{\Gamma^{m+1}} \\
&\quad = \frac{1}{\tau}\left\langle \Psi^m, \chi_k^m\right\rangle_{\Gamma^m}^h - \left\langle \Psi_{\star,\varepsilon}^m\left(\frac{\vec{X}^{m+1}-\vec{X}^m}{\tau} - \vec{U}^{m+1}\right), \nabla_s\,\chi_k^m\right\rangle_{\Gamma^m}^h \\
&\qquad - \left(\frac{1}{\alpha_-}+\frac{1}{\alpha_+}\right)\left\langle F_\varepsilon'(\Psi^m) - I_1^m\,[G_\varepsilon'(\Phi^m)], \chi_k^m\right\rangle_{\Gamma^m}^h \qquad \forall\ k\in\{1,\ldots,K_\Gamma\}\,.
\end{aligned} \tag{5.11b}$$

5.3 Existence and uniqueness of the fully discrete solutions

When the velocity/pressure space pair $(\mathbb{U}^m, \widehat{\mathbb{P}}^m)$ does not satisfy (5.1), we need to consider the reduced versions of the schemes proposed in §5.1 and §5.2, see also Barrett *et al.*

(2014). Here the pressure P^{m+1} is eliminated, in order to prove existence of a solution to the reduced system. Let

$$\mathbb{U}_0^m := \{\vec{U} \in \mathbb{U}^m : (\nabla \,.\, \vec{U}, \varphi) = 0 \ \ \forall\ \varphi \in \widehat{\mathbb{P}}^m\}\,.$$

Then any solution $(\vec{U}^{m+1}, P^{m+1}) \in \mathbb{U}^m \times \widehat{\mathbb{P}}^m$ to (5.8a,b) is such that $\vec{U}^{m+1} \in \mathbb{U}_0^m$ satisfies (5.8a) with $\mathbb{U}^m$ replaced by $\mathbb{U}_0^m$; and similarly for (5.10a,b).

In order to prove the existence of a unique solution to our proposed fully discrete finite element approximations we will make the following very mild well-posedness assumption.

($\mathcal{A}_2$) We assume for $m = 0, \ldots, M-1$ that $\mathcal{H}^{d-1}(\sigma_j^m) > 0$ for all $j = 1, \ldots, J_\Gamma$, and that $\Gamma^m \subset \Omega$.

THEOREM. 5.1. *Let the assumption* ($\mathcal{A}_2$) *hold. If the LBB condition* (5.1) *holds, then there exists a unique solution* $(\vec{U}^{m+1}, P^{m+1}) \in \mathbb{U}^m \times \widehat{\mathbb{P}}^m$ *to* (5.8a,b). *In all other cases there exists a unique solution* $\vec{U}^{m+1} \in \mathbb{U}_0^m$ *to the reduced equation* (5.8a) *with* $\mathbb{U}^m$ *replaced by* $\mathbb{U}_0^m$. *In either case, there exists a unique solution* $(\vec{X}^{m+1}, \vec{\kappa}^{m+1}) \in \underline{V}(\Gamma^m) \times \underline{V}(\Gamma^m)$ *to* (5.8c,d) *and a unique solution* $(\Phi_\pm^{m+1}, \Psi^{m+1}) \in S_{1,\pm}^m \times W(\Gamma^{m+1})$ *to* (5.8e,f). *Finally, there exists a unique solution* $(\Phi^{m+1}, \Psi^{m+1}) \in S_1^m \times W(\Gamma^{m+1})$ *to* (5.9a,b) *that satisfies*

$$\left(\Phi^{m+1}, 1\right) + \left\langle \Psi^{m+1}, 1\right\rangle_{\Gamma^{m+1}} = (I_1^m\, \Phi^m, 1) + \left\langle \Psi^m, 1\right\rangle_{\Gamma^m} + \tau \left\langle \lambda_+, g_+ - \Phi_+^{m+1}\right\rangle_{\partial\Omega}^h . \quad (5.12)$$

Proof. As all the systems are linear, existence follows from uniqueness. In order to establish the latter, we will consider the homogeneous system in each case. We begin with: Find $(\vec{U}, P) \in \mathbb{U}^m \times \widehat{\mathbb{P}}^m$ such that

$$\begin{aligned} &\tfrac{1}{2\tau}\left((\rho^m + I_0^m\, \rho^{m-1})\, \vec{U}, \vec{\xi}\right) + 2\left(\mu^m\, \underline{\underline{D}}(\vec{U}), \underline{\underline{D}}(\vec{\xi})\right) - \left(P, \nabla \,.\, \vec{\xi}\right) \\ &\qquad + \tfrac{1}{2}\left(\rho^m, [(\vec{I}_2^m\, \vec{U}^m \,.\, \nabla)\, \vec{U}] \,.\, \vec{\xi} - [(\vec{I}_2^m\, \vec{U}^m \,.\, \nabla)\, \vec{\xi}] \,.\, \vec{U}\right) = 0 \qquad \forall\ \vec{\xi} \in \mathbb{U}^m\,, \qquad (5.13a) \\ &\left(\nabla \,.\, \vec{U}, \varphi\right) = 0 \qquad \forall\ \varphi \in \widehat{\mathbb{P}}^m\,. \qquad (5.13b) \end{aligned}$$

Choosing $\vec{\xi} = \vec{U}$ in (5.13a) and $\varphi = P$ in (5.13b) yields that

$$\tfrac{1}{2}\left((\rho^m + I_0^m\, \rho^{m-1})\, \vec{U}, \vec{U}\right) + 2\,\tau\left(\mu^m\, \underline{\underline{D}}(\vec{U}), \underline{\underline{D}}(\vec{U})\right) = 0\,. \quad (5.14)$$

It immediately follows from (5.14) and Korn's inequality that $\vec{U} = \vec{0} \in \mathbb{U}^m$. Moreover, (5.13a) with $\vec{U} = \vec{0}$ implies, together with (5.1), that $P = 0 \in \widehat{\mathbb{P}}^m$. This shows existence and uniqueness of $(\vec{U}^{m+1}, P^{m+1}) \in \mathbb{U}^m \times \widehat{\mathbb{P}}^m$. The proof for the reduced equation is very similar. The homogeneous system to consider is (5.13a) with $\mathbb{U}^m$ replaced by $\mathbb{U}_0^m$, where we note that the latter is a linear subspace of $\mathbb{U}^m$. As before, (5.14) together with a Korn's inequality yield that $\vec{U} = \vec{0} \in \mathbb{U}_0^m$, and so the existence of a unique solution $\vec{U}^{m+1} \in \mathbb{U}_0^m$ to the reduced equation.

Next we consider: Find $(\vec{X}, \vec{\kappa}) \in \underline{V}(\Gamma^m) \times \underline{V}(\Gamma^m)$ such that

$$\left\langle \vec{X}, \vec{\chi} \right\rangle^h_{\Gamma^m} = 0 \qquad \forall\ \vec{\chi} \in \underline{V}(\Gamma^m)\,, \tag{5.15a}$$

$$\langle \vec{\kappa}, \vec{\eta} \rangle^h_{\Gamma^m} + \left\langle \nabla_s \vec{X}, \nabla_s \vec{\eta} \right\rangle_{\Gamma^m} = 0 \qquad \forall\ \vec{\eta} \in \underline{V}(\Gamma^m)\,, \tag{5.15b}$$

which immediately implies that $\vec{X} = \vec{0}$ and hence $\vec{\kappa} = \vec{0}$.

Moreover, (5.8e,f) are clearly symmetric, positive definite linear systems in $\Phi^{m+1}_\pm$ and Ψ^{m+1}, respectively, which yields the existence of a unique solution $(\Phi^{m+1}_\pm, \Psi^{m+1}) \in S^m_\pm \times W(\Gamma^{m+1})$. Similarly, (5.9a,b) are symmetric, positive definite linear systems in Φ^{m+1} and Ψ^{m+1}, respectively, which yields the existence of a unique solution $(\Phi^{m+1}, \Psi^{m+1}) \in S^m \times W(\Gamma^{m+1})$. The desired result (5.12) follows on choosing $\xi = 1$ in (5.9a) and on summing (5.9b) for $k = 1, \ldots, K_\Gamma$. □

In order to prove the existence of a unique solution to (5.10c,d) we need to make the following very mild additional assumption.

($\mathcal{A}_3$) For $k = 1, \ldots, K_\Gamma$, let $\Theta^m_k := \{\sigma^m_j : \vec{q}^m_k \in \overline{\sigma^m_j}\}$ and set

$$\Lambda^m_k := \bigcup_{\sigma^m_j \in \Theta^m_k} \overline{\sigma^m_j} \qquad \text{and} \qquad \vec{\omega}^m_k := \frac{1}{\mathcal{H}^{d-1}(\Lambda^m_k)} \sum_{\sigma^m_j \in \Theta^m_k} \mathcal{H}^{d-1}(\sigma^m_j)\ \vec{\nu}^m_j\,.$$

Then we further assume that $\dim \operatorname{span}\{\vec{\omega}^m_k\}_{k=1}^{K_\Gamma} = d$, $m = 0, \ldots, M-1$.

We refer to Barrett *et al.* (2007) and Barrett *et al.* (2008) for more details and for an interpretation of this assumption. Given the above definitions, we introduce the piecewise linear vertex normal function

$$\vec{\omega}^m := \sum_{k=1}^{K_\Gamma} \chi^m_k\ \vec{\omega}^m_k \in \underline{V}(\Gamma^m)\,,$$

and note that

$$\langle \vec{v}, w\, \vec{\nu}^m \rangle^h_{\Gamma^m} = \langle \vec{v}, w\, \vec{\omega}^m \rangle^h_{\Gamma^m} \qquad \forall\ \vec{v} \in \underline{V}(\Gamma^m)\,,\ w \in W(\Gamma^m)\,. \tag{5.16}$$

THEOREM. 5.2. *Let the assumption* ($\mathcal{A}_2$) *hold. If the LBB condition* (5.1) *holds, then there exists a unique solution* $(\vec{U}^{m+1}, P^{m+1}) \in \mathbb{U}^m \times \widehat{\mathbb{P}}^m$ *to* (5.10a,b). *In all other cases there exists a unique solution* $\vec{U}^{m+1} \in \mathbb{U}^m_0$ *to the reduced equation* (5.10a) *with* $\mathbb{U}^m$ *replaced by* $\mathbb{U}^m_0$. *In either case, if the assumption* ($\mathcal{A}_3$) *holds, then there exists a unique solution* $(\vec{X}^{m+1}, \kappa^{m+1}) \in \underline{V}(\Gamma^m) \times W(\Gamma^m)$ *to* (5.10c,d) *and a unique solution* $(\Phi^{m+1}_\pm, \Psi^{m+1}) \in S^m_{1,\pm} \times W(\Gamma^{m+1})$ *to* (5.10e,f). *Finally, there exists a unique solution* $(\Phi^{m+1}, \Psi^{m+1}) \in S^m_1 \times W(\Gamma^{m+1})$ *to* (5.11a,b) *that satisfies* (5.12).

Proof. All the results in the theorem, apart from the existence and uniqueness of $(\vec{X}^{m+1}, \kappa^{m+1})$, can be shown exactly as in the proof of Theorem 5.1. For the remaining result we consider: Find $(\vec{X}, \kappa) \in \underline{V}(\Gamma^m) \times W(\Gamma^m)$ such that

$$\left\langle \vec{X}, \chi\, \vec{\nu}^m \right\rangle^h_{\Gamma^m} = 0 \qquad \forall\ \chi \in W(\Gamma^m)\,, \tag{5.17a}$$

$$\langle \kappa\, \vec{\nu}^m, \vec{\eta} \rangle^h_{\Gamma^m} + \left\langle \nabla_s \vec{X}, \nabla_s \vec{\eta} \right\rangle_{\Gamma^m} = 0 \qquad \forall\ \vec{\eta} \in \underline{V}(\Gamma^m)\,. \tag{5.17b}$$

Choosing $\chi = \kappa$ in (5.17a) and $\vec{\eta} = \vec{X}$ in (5.17b) yields that

$$\left\langle \nabla_s \vec{X}, \nabla_s \vec{X} \right\rangle_{\Gamma^m} = 0\,. \tag{5.18}$$

It immediately follows from (5.18) that $\vec{X} = \vec{X}_c \in \mathbb{R}^d$. Together with (5.17a), (5.16) and the assumption $(\mathcal{A}_3)$ this yields that $\vec{X} = \vec{0}$. Now (5.17b) with $\vec{\eta} = \vec{\pi}^m[\kappa\, \vec{\omega}^m]$, recall (5.16), implies that $\kappa = 0$. □

Remark. 5.3. *We recall from* §3.1.1 *that the two one-sided variants of model (i) can also be considered; and these are given by* (2.3a–e)*,* (2.4)*,* (2.5a,b)*,* (2.20) *and* (2.8a) *with "±" replaced by "+" or "−", respectively,* (2.8b) *with right hand side* $\pm \mathcal{D}_\pm \nabla \phi_\pm \,.\, \vec{\nu}$*, respectively, and* (2.8c) *for the outer problem.*

The two approximations (5.8a–f) *and* (5.10a–f) *can be easily adapted to these one-sided situations. In particular, we replace any occurrence of "±" in* (5.8e,f) *and* (5.10e,f) *with "+" or "−", respectively.*

6 Numerical results

For details on the assembly of the linear system arising at each time step of (5.10a–f), as well as details on the adaptive mesh refinement algorithm and the solution procedure, we refer to Barrett *et al.* (2014, 2013b). We recall from Barrett *et al.* (2014) that for the bulk mesh adaptation we use a strategy that results in a fine mesh size h_f around Γ^m and a coarse mesh size h_c further away from it. Here $h_f = \frac{2\,\min\{H_1,H_2\}}{N_f}$ and $h_c = \frac{2\,\min\{H_1,H_2\}}{N_c}$ are given by two integer numbers $N_f > N_c$, where we assume from now on that Ω is given by $\times_{i=1}^d (-H_i, H_i)$. We remark that we implemented our scheme with the help of the finite element toolbox ALBERTA, see Schmidt and Siebert (2005).

For all the schemes in Section 5 we fix $\varepsilon = 10^{-7}$, and in all our numerical experiments presented in this section the discrete surfactant concentrations Ψ^m, Φ^m and $\Phi^m_\pm$ remained above ε throughout the evolution, so that $\gamma_\varepsilon(\Psi^m) = \gamma(\Psi^m)$, $F_\varepsilon(\Psi^m) = F(\Psi^m)$, $G_\varepsilon(\Phi^m) = G(\Phi^m)$ and $G_{\pm,\varepsilon}(\Phi^m_\pm) = G_\pm(\Phi^m_\pm)$, recall (4.17a,b) and (4.19). Unless otherwise stated we use (2.16) and the linear equation of state (2.12a) for the surface tension. In addition, we employ the lowest order Taylor–Hood element P2–P1, together with the XFEM$_\Gamma$ extension from Barrett *et al.* (2013a, 2014), in all computations and set $\vec{U}^0 = \vec{I}^0_2\, \vec{u}_0$,

where $\vec{u}_0 = \vec{0}$ unless stated otherwise. Note that as a consequence of using the XFEM$_\Gamma$ approach from Barrett *et al.* (2013a, 2014), the volume of the phases is almost exactly conserved in all our numerical computations. For the initial interface we always choose a circle/sphere of radius R_0 and set $\kappa^0 = -\frac{d-1}{R_0}$ for the schemes in §5.2. For the schemes in §5.1 we let $\vec{\kappa}^0 \in \underline{V}(\Gamma^0)$ be the solution of (5.8d) with m and $m+1$ replaced by zero. To summarize the discretization parameters we use the shorthand notation $n\,\mathrm{adapt}_{k,l}$ from Barrett *et al.* (2014). The subscripts refer to the fineness of the spatial discretizations, i.e. for the set $n\,\mathrm{adapt}_{k,l}$ it holds that $N_f = 2^k$ and $N_c = 2^l$. For the case $d = 2$ we have in addition that $K_\Gamma = J_\Gamma = L\,2^k$, where $L \in \{1, 2, 3\}$ denotes the number of components for the interface, while for the case $d = 3$ we will state the values of K_Γ and J_Γ for each experiment separately. Finally, the uniform time step size for the set $n\,\mathrm{adapt}_{k,l}$ is given by $\tau = 10^{-3}/n$, and if $n = 1$ we write $\mathrm{adapt}_{k,l}$. Unless otherwise stated, we employ the discretization parameters $2\,\mathrm{adapt}_{9,4}$ in all our computations for $d = 2$.

6.1 Comparison with radially symmetric solutions in 2d

Here we compare numerical solutions for our finite element approximations with radially symmetric solutions for a simple absorption problem for a stationary interface. See the appendix for details on how to compute the radially symmetric solutions.

In the following, we set all the physical parameters to unity, i.e. $\mathcal{D}_\pm = \alpha_\pm = \mathcal{D}_\Gamma = 1$. In addition, we set $\gamma_0 = 1$, $\beta = 0.5$ and $\theta_\pm = 1$ in (2.12a) and (2.16), respectively. We consider the domain $\Omega = B_2(0) = \{\vec{z} \in \mathbb{R}^d : |\vec{z}| < 2\}$, and fix $\Gamma(t) = \Gamma(0) = \partial B_1(0)$, i.e. the unit circle.

As initial data we choose $\phi_{\pm,0} = 1$ and $\psi_0 = 0.01$. Where the boundary conditions on $\partial\Omega$ play a role, we prescribe Dirichlet conditions $\phi_+ = 1$ on $\partial\Omega$.

In all our computations in this subsection we take a nearly uniform triangulation of a polygonal approximation Ω^h of Ω with 2048 elements, see Figure 3. In addition, $\Gamma^m = \Gamma^0$ is given by an equidistributed approximation of the unit circle with 256 elements. Unless otherwise stated, we use the uniform time step size $\tau = 10^{-3}$.

The results of numerical computations for the scheme (5.10a–f), in the case of the two-sided model (i), the one-sided models (i), and the global model (ii), are shown in Figures 4–7. In each case we observe an excellent agreement between numerics and true solution. The evolutions in Figures 4, 6 and 7 eventually settle on the steady state solutions $\psi = \phi_\pm = 1$, $\psi = \phi_+ = 1$ and $\psi = \phi = 1$, respectively. The evolution in Figure 5, on the other hand, quickly finds the steady state solution $\psi = \phi_- = (\phi_{-,0} + d\,\psi_0)/(d+1) = 1.02/3 = 0.34$.

Next we include a simulation where we demonstrate that our model, for small $\alpha_\pm > 0$, approximates (2.15), and in particular Henry's law (2.17). To this end, we fix $\alpha_- = \alpha_+ = 0.01$ and let $\theta_- = \frac{1}{5}$, $\theta_+ = \frac{1}{2}$ for the choice (2.16). In order to satisfy (2.15) at time $t = 0$, we choose $\phi_{-,0} = 1$ as before, let $\psi_0 = \theta_-$ and choose a radially symmetric profile for $\phi_{+,0}$

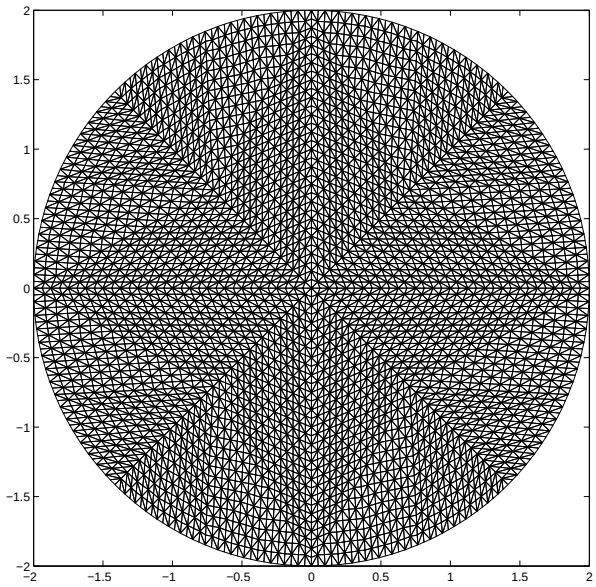

Figure 3: Triangulation of Ω^h with 2048 elements.

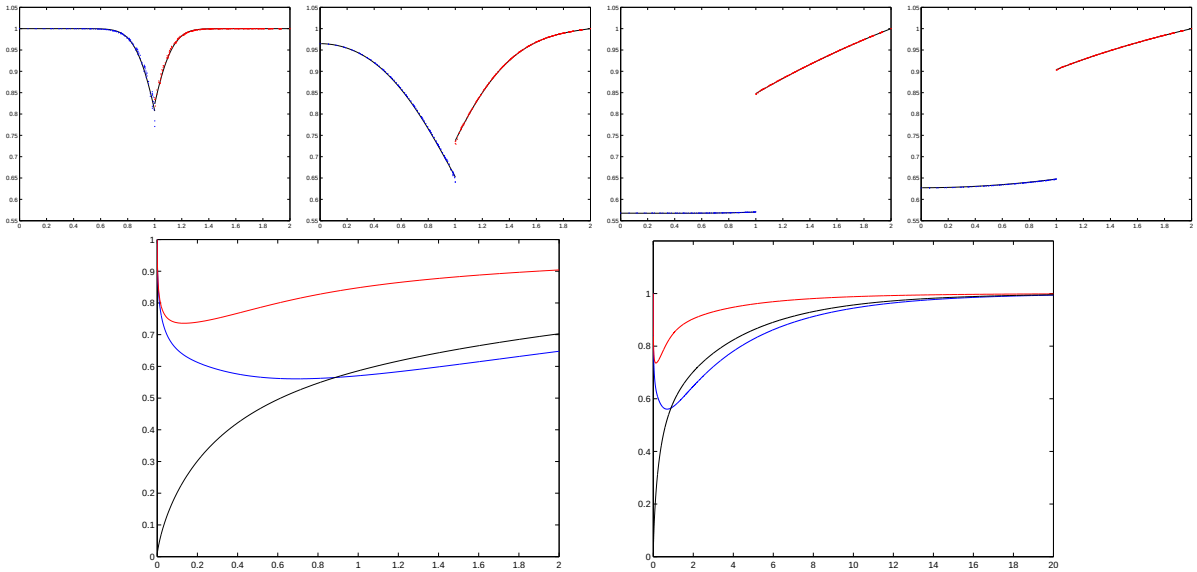

Figure 4: ($d = 2$) Comparison between the radially symmetric solutions $\phi_\pm$ (black lines) and the numerical solution (blue and red dots) at times $t = 0.01$, 0.1, 1, 2 for model (i). Below a plot of $\phi_\pm|_{r=1}$ (blue and red) and ψ (black) over the time interval $[0, 2]$ (left) and over $[0, 20]$ (right).

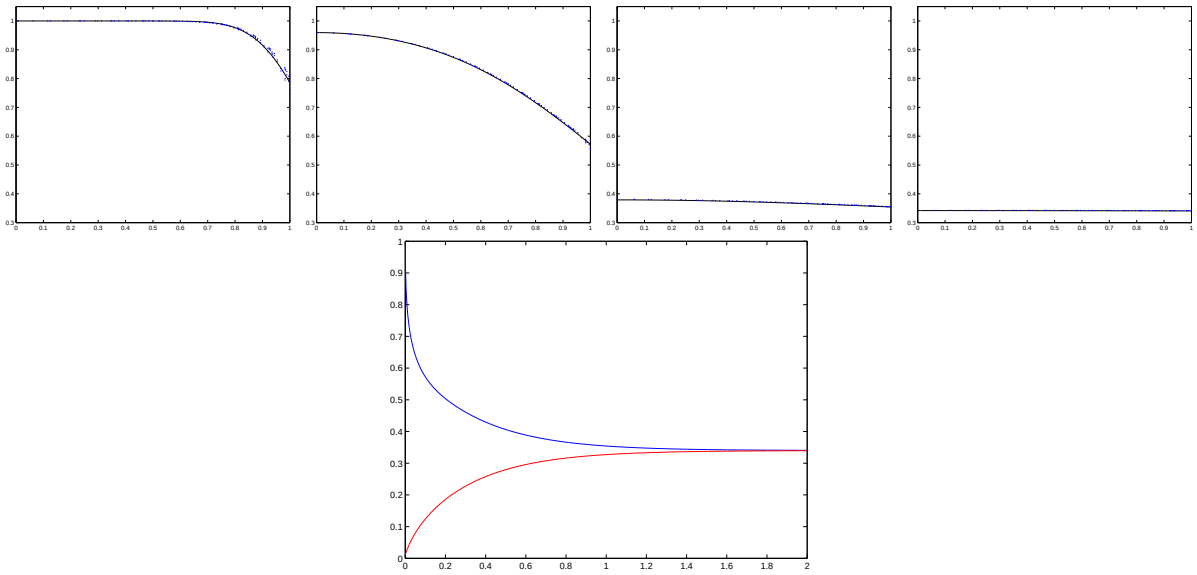

Figure 5: ($d = 2$) Comparison between the radially symmetric solution ϕ_- (black line) and the numerical solution (blue dots) at times $t = 0.01,\ 0.1,\ 1,\ 2$ for the one-sided inner model (i). Below a plot of $\phi_-\,|_{r=1}$ (blue) and ψ (red) over the time interval $[0, 2]$.

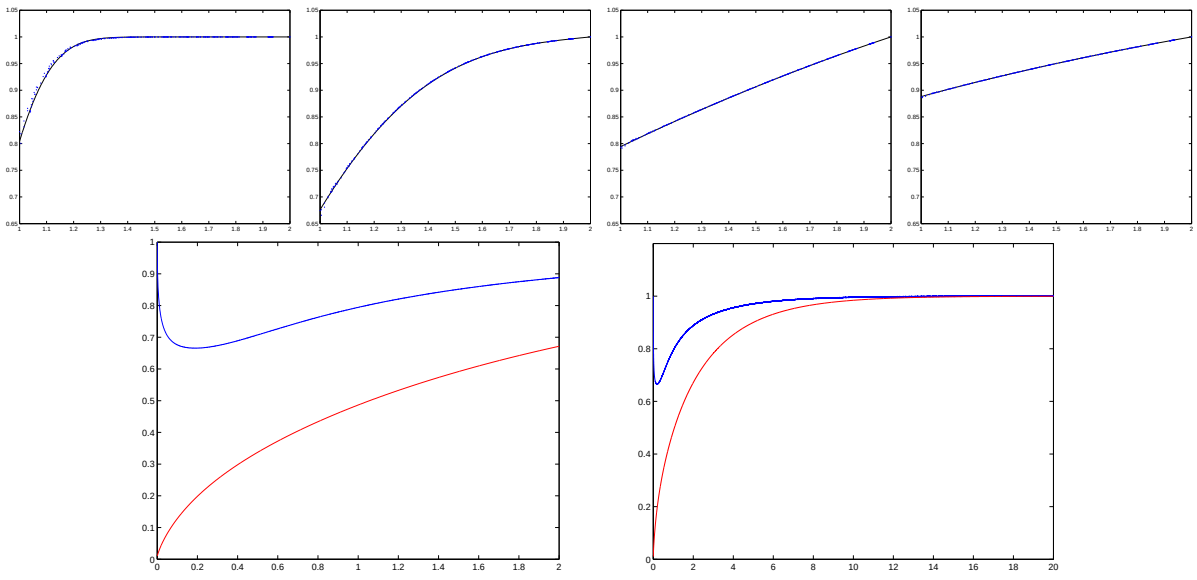

Figure 6: ($d = 2$) Comparison between the radially symmetric solution ϕ_+ (black line) and the numerical solution (blue dots) at times $t = 0.01,\ 0.1,\ 1,\ 2$ for the one-sided outer model (i). Below a plot of $\phi_+\,|_{r=1}$ (blue) and ψ (red) over the time interval $[0, 2]$ (left) and over $[0, 20]$ (right).

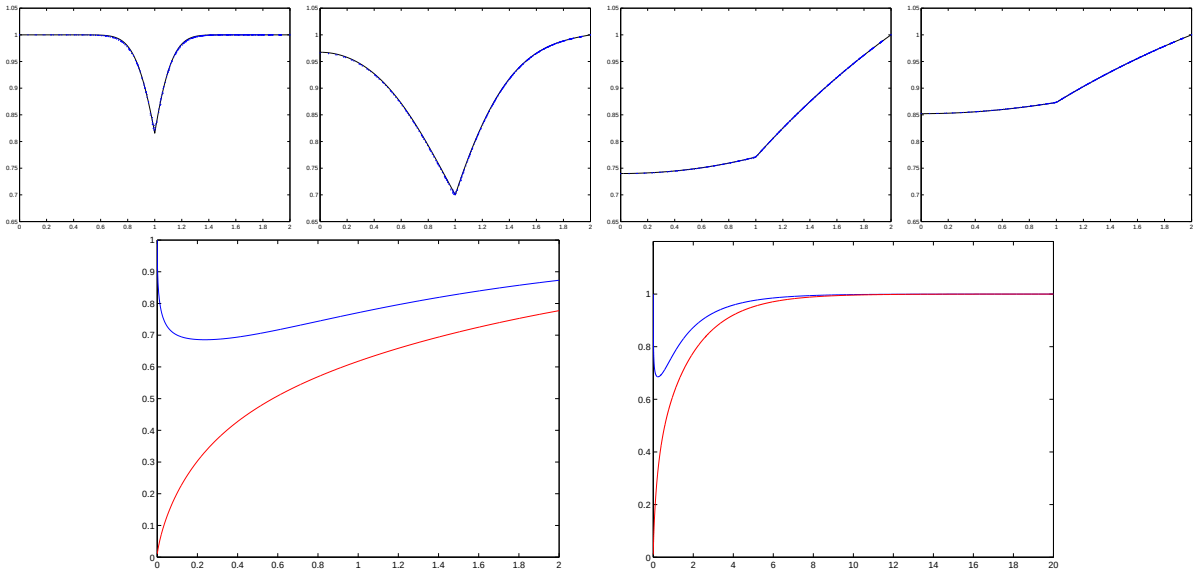

Figure 7: ($d = 2$) Comparison between the radially symmetric solution ϕ (black line) and the numerical solution (blue dots) at times $t = 0.01$, 0.1, 1, 2 for model (ii). Below a plot of $\phi|_{r=1}$ (blue) and ψ (red) over the time interval $[0, 2]$ (left) and over $[0, 20]$ (right).

that is linear in r and such that $\theta_+ \, \phi_{+,0} \, |_{r=1} = \theta_-$ and $\phi_{+,0} \, |_{r=2} = 1$. The time step size is chosen as $\tau = 2 \times 10^{-4}$ for this experiment. All the remaining parameters are as in Figure 4. As can be seen from the plots in Figure 8, there is again an excellent agreement between our numerical solutions and the true radially symmetric solution. Moreover, we see that (2.15), and in particular Henry's law (2.17), is well approximated at all times.

6.1.1 Comparison with other relaxation conditions

Here we relate our relaxation condition (2.19) to alternatives proposed in the literature. Assume we fix $\phi_+ = g_+$ on $\partial\Omega$. Then in steady state, $F'(\psi) = G'_+(\phi_+)$, we have that $\psi = \frac{\theta_+ \, g_+ \, \psi_\infty}{\theta_+ \, g_+ + 1}$. Hence we can approximately replace the last term on the right hand side of (2.19) by

$$\gamma_0 \, \beta \, \frac{\theta_+ \, g_+ + 1}{\theta_+ \, g_+ \, \psi_\infty} \left[\theta_+ \, \phi_+ \, (\psi_\infty - \psi) - \psi \right],$$

which now can be matched to

$$\alpha_+ \left(K_a \, \phi_+ \, (\psi_\infty - \psi) - K_d \, \psi \right) \tag{6.1}$$

in e.g. Ganesan and Tobiska (2012, (5)).

We compare the solutions for the one-sided outer problem with $g_+ = \alpha_+ = 1$, $\theta_+ = \frac{1}{5}$ and (2.12b) with $\gamma_0 = \beta = \psi_\infty = 1$ for a model with (6.1), where we choose $K_a = 1.2$ and $K_d = 6$. In Figure 9 we show a comparison between the corresponding radially symmetric solutions. We see that while the evolution early on disagrees, the eventual steady states are the same, i.e. in both cases the solutions settle on $\theta_+ \, \phi_+ = \frac{1}{5}$ and $\psi = \frac{1}{6}$.

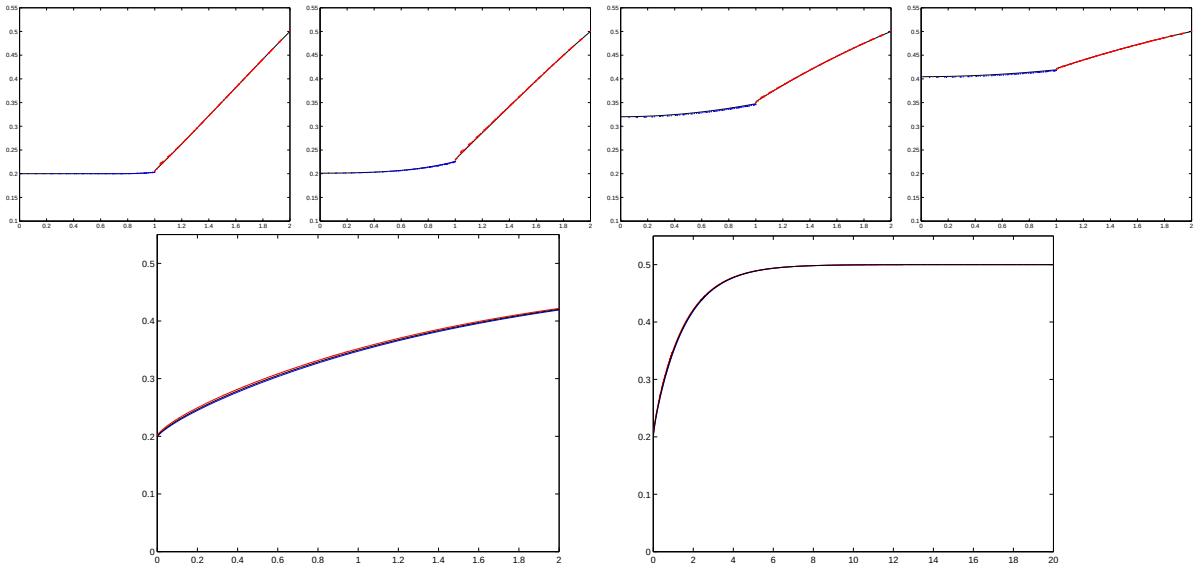

Figure 8: ($d = 2$) Comparison between the radially symmetric solutions $\theta_\pm\, \phi_\pm$ (black lines) and the numerical solution (blue and red dots) at times $t = 0.01,\ 0.1,\ 1,\ 2$ for model (i). Below a plot of $\theta_\pm\, \phi_\pm\,|_{r=1}$ (blue and red) and ψ (black) over the time interval $[0, 2]$ (left) and over $[0, 20]$ (right). The results show that Henry's law (2.17) is well approximated.

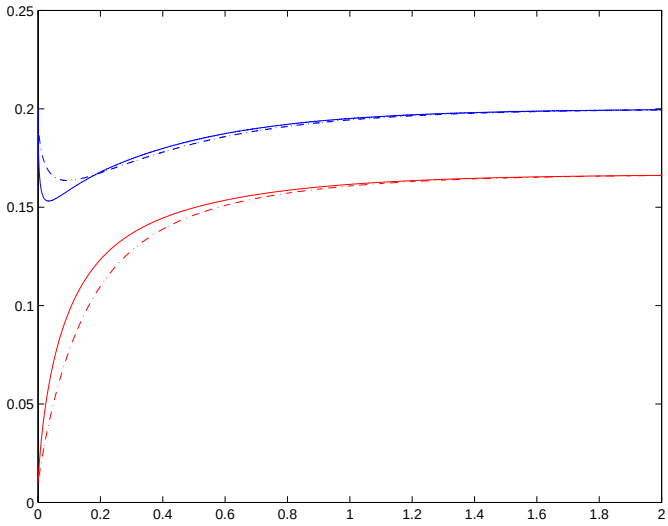

Figure 9: ($d = 2$) Comparison between $\theta_+\, \phi_+\,|_{r=1}$ (blue) and ψ (red) over the time interval $[0, 2]$. Solid lines are for (2.13) with (2.12b), dashed lines are for (6.1).

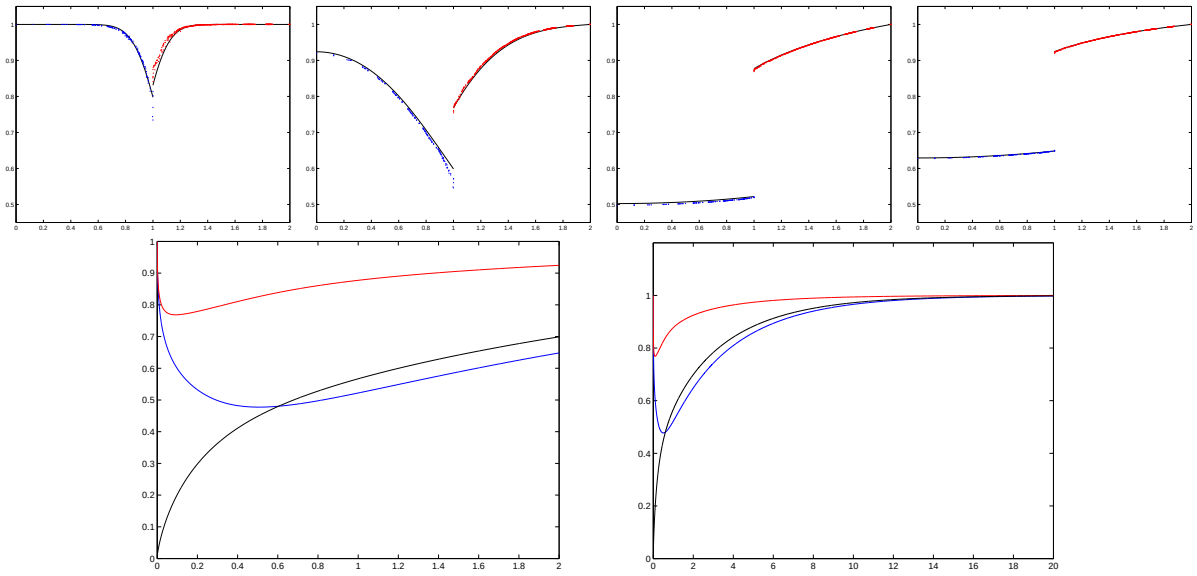

Figure 10: ($d = 3$) Comparison between the radially symmetric solutions $\phi_\pm$ (black lines) and the numerical solution (blue and red dots) at times $t = 0.01$, 0.1, 1, 2 for model (i). Below a plot of $\phi_\pm|_{r=1}$ (blue and red) and ψ (black) over the time interval $[0, 2]$ (left) and over $[0, 20]$ (right).

6.2 Comparison with radially symmetric solutions in 3d

Here we repeat the computations from §6.1, but now for the case $d = 3$. To this end, we use a nearly uniform triangulation of a polyhedral approximation Ω^h of Ω with 24576 elements. In addition, $\Gamma^m = \Gamma^0$ is given by a nearly uniform polyhedral approximation of the unit sphere with $J_\Gamma = 6144$ elements and $K_\Gamma = 3074$ vertices. In all the computations in this section we use the uniform time step size $\tau = 10^{-3}$.

The results of numerical computations for the scheme (5.10a–f), in the case of the two-sided model (i), the one-sided models (i), and the global model (ii), are shown in Figures 10–13. Similarly to the situation in §6.1, the evolutions in Figures 10, 12 and 13 eventually settle on the steady state solutions $\psi = \phi_\pm = 1$, $\psi = \phi_+ = 1$ and $\psi = \phi = 1$, respectively. The evolution in Figure 11, on the other hand, quickly finds the steady state solution $\psi = \phi_- = (\phi_{-,0} + d\,\psi_0)/(d+1) = 1.03/4 \approx 0.26$.

6.3 Numerical simulations

6.3.1 Shear experiment in 2d

In the literature on numerical methods for two-phase flow with surfactant it is often common to consider shear flow experiments for an initially circular bubble in order to study the effect of surfactants and of different equations of state. In this subsection, we will perform such simulations for the schemes (5.8a–d), (5.9a,b) and (5.10a–d), (5.11a,b) for

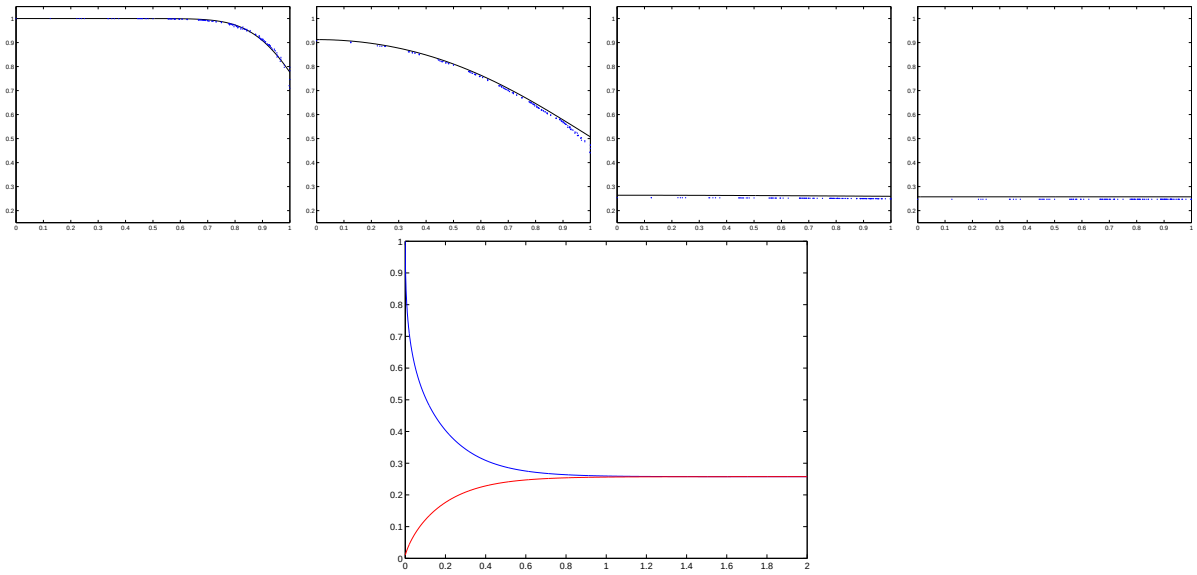

Figure 11: ($d = 3$) Comparison between the radially symmetric solution ϕ_- (black line) and the numerical solution (blue dots) at times $t = 0.01,\ 0.1,\ 1,\ 2$ for the one-sided inner model (i). Below a plot of $\phi_-|_{r=1}$ (blue) and ψ (red) over time.

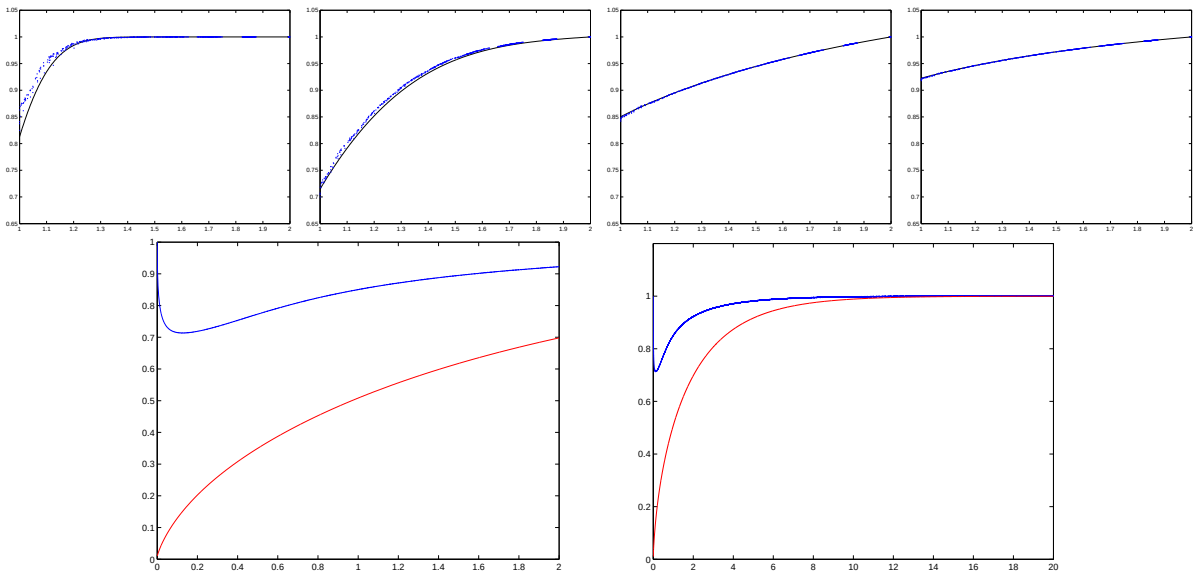

Figure 12: ($d = 3$) Comparison between the radially symmetric solution ϕ_+ (black line) and the numerical solution (blue dots) at times $t = 0.01,\ 0.1,\ 1,\ 2$ for the one-sided outer model (i). Below a plot of $\phi_+|_{r=1}$ (blue) and ψ (red) over the time interval $[0, 2]$ (left) and over $[0, 20]$ (right).

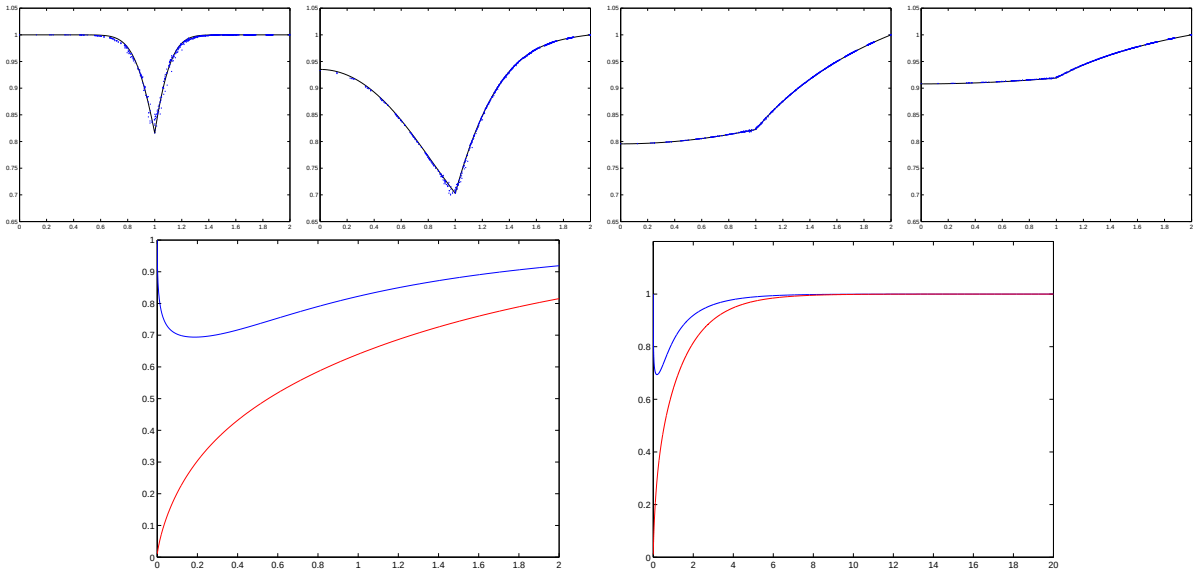

Figure 13: ($d = 3$) Comparison between the radially symmetric solution ϕ (black line) and the numerical solution (blue dots) at times $t = 0.01$, 0.1, 1, 2 for model (ii). Below a plot of $\phi|_{r=1}$ (blue) and ψ (red) over the time interval $[0, 2]$ (left) and over $[0, 20]$ (right).

the model (ii). Here we consider the setup from Lai *et al.* (2008, Fig. 1). In particular, we let $\Omega = (-5, 5) \times (-2, 2)$ and prescribe the inhomogeneous Dirichlet boundary condition $\vec{g}(\vec{z}) = (\frac{1}{2} z_2, 0)^T$ on $\partial\Omega = \partial_1\Omega$. Moreover, $\Gamma_0 = \{\vec{z} \in \mathbb{R}^2 : |\vec{z}| = 1\}$. The physical parameters are given by

$$\rho = 1\,, \quad \mu = 0.1\,, \quad \gamma_0 = 0.2\,, \quad \mathcal{D}_\Gamma = 0.1\,, \quad \mathcal{D}_\pm = \alpha_\pm = 1\,, \quad \vec{f} = \vec{0}\,, \quad \vec{u}_0 = \vec{g}\,.$$

For the surfactant we choose (2.12a) with $\beta = 0.5$, (2.16) with $\theta_\pm = 1$ and let $\psi_0 = \phi_{0,\pm} = 0.1$. Moreover, $\lambda_+ = \frac{1}{4} g_+ = \mathcal{X}_{\partial_+\Omega}$, where $\partial_+\Omega = \{2\} \times [-5, 5]$ denotes the right edge of the boundary of Ω. A computation for the scheme (5.10a–d), (5.11a,b) can be seen in Figure 14. We note that the influx of surfactant from the right boundary leads to the drop deforming more towards the right.

For completeness we also repeat the same simulation for the alternative scheme (5.8a–d), (5.9a,b) from §5.1. As the vertices of the interface approximation are moved with the fluid flow, the distribution of vertices becomes very nonuniform and eventually coalescence of mesh points occurs. This means that the linear systems that need to be solved at each time level become so ill-conditioned that they can no longer be solved in practice. For this experiment that happens shortly after time $t = 7.5$. In Figure 15 we show the distribution of mesh points at time $t = 7.5$ for the discretization parameters $\text{adapt}_{5,2}$ and $\text{adapt}_{7,3}$. The observed coalescence of vertices is in line with numerical results reported in Barrett *et al.* (2013a,b) for the corresponding schemes. As a comparison we show the meshes obtained with the scheme (5.10a–d), (5.11a,b) from §5.2, which we have used for the results in Figure 14, in Figure 16. As can be seen, the vertices are close to being equidistributed. It is for this reason that from now on we will only present numerical simulations for our preferred schemes from §5.2.

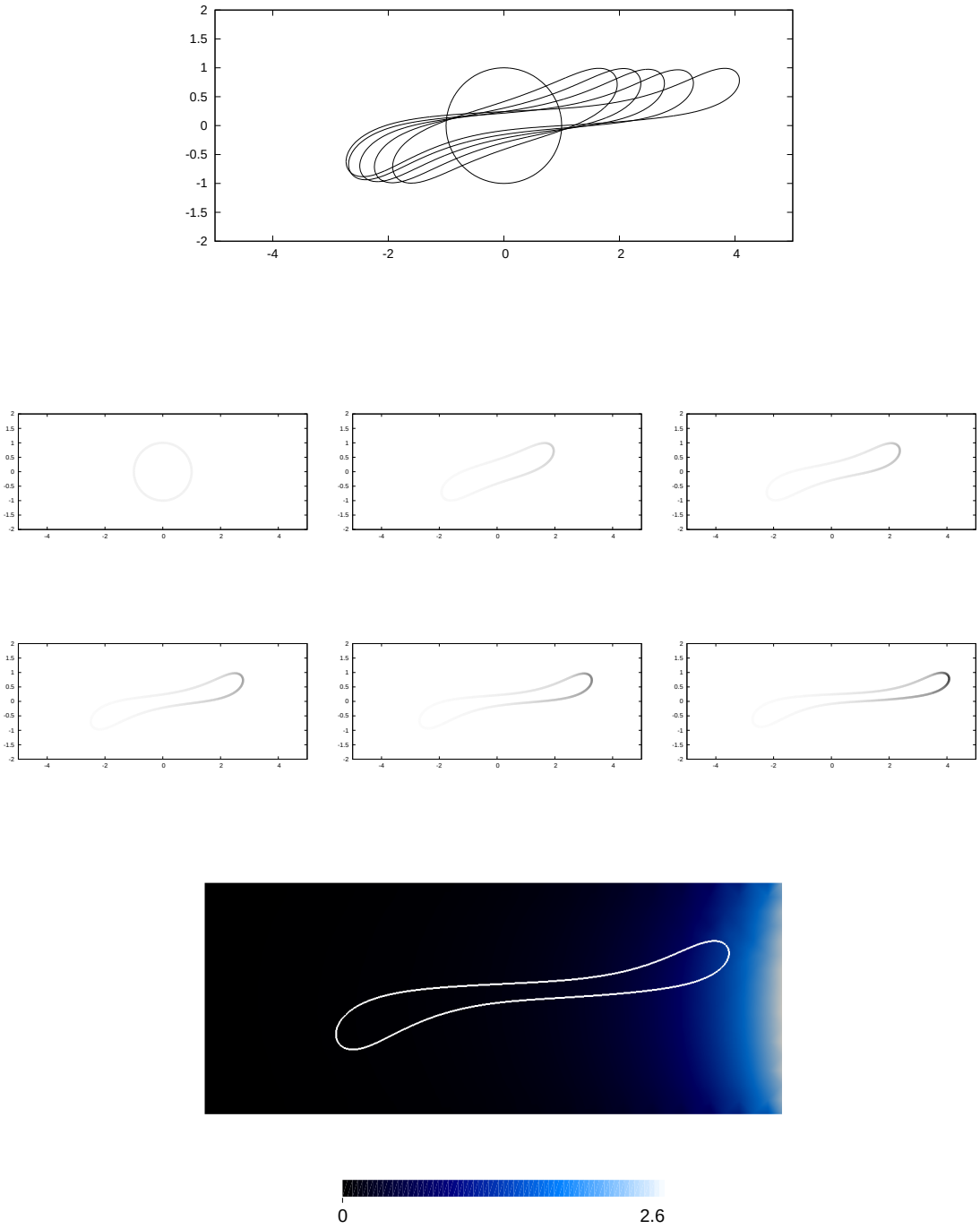

Figure 14: ($d = 2$) The time evolution of a drop in shear flow. Plots are at times $t = 0,\ 10,\ 20, \ldots, 50$. Below the evolution of the surfactant concentration Ψ^m on Γ^m. The grey scales linearly with the surfactant concentration ranging from 0 (white) to 1 (black). The bottom shows the bulk surfactant concentration Φ^M at the final time $T = 50$.

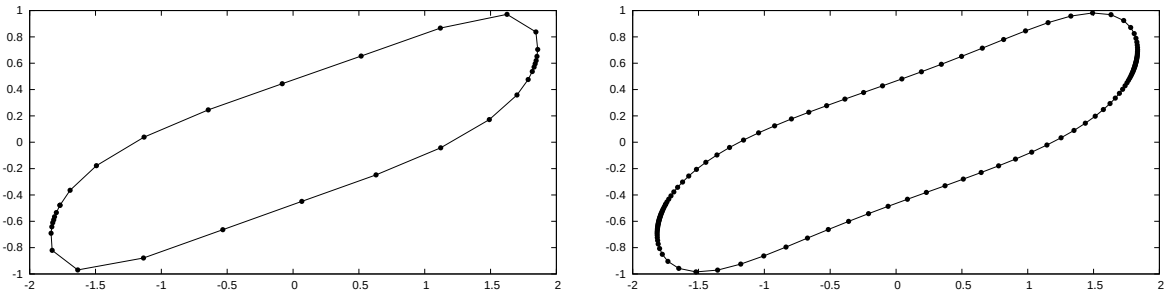

Figure 15: ($d = 2$) The distribution of vertices on Γ^m at time $t = 7.5$ for the scheme (5.8a–d), (5.9a,b) for the discretization parameters $\text{adapt}_{5,2}$ (left) and $\text{adapt}_{7,3}$ (right).

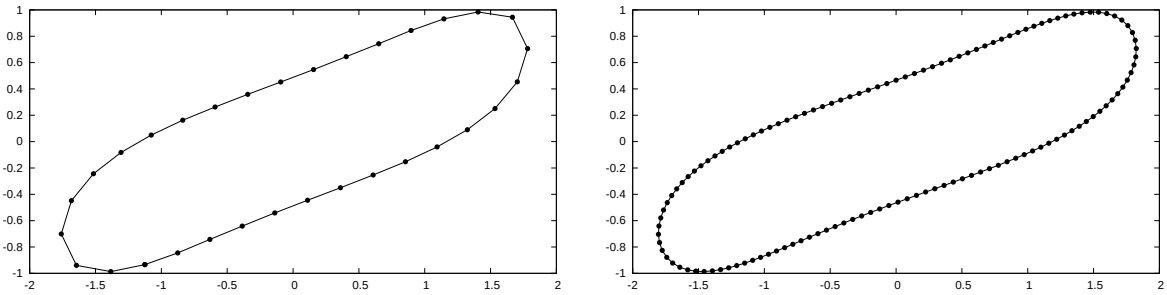

Figure 16: ($d = 2$) The distribution of vertices on Γ^m at time $t = 7.5$ for our preferred scheme (5.10a–d), (5.11a,b) for the discretization parameters $\text{adapt}_{5,2}$ (left) and $\text{adapt}_{7,3}$ (right).

6.3.2 Multiple drops in 2d

The next numerical simulation provides an example where the presence of soluble surfactant induces a flow. The initial configuration is given by three circular drops with constant surfactant concentrations. Clearly, in the absence of soluble surfactant this would be a steady state. However, e.g. for the one-sided outer model (i), the absorption and desorption of surfactant into the outer bulk phase leads to a flow, as can be seen in Figure 17. Here we employ the discretization parameters $2\,\text{adapt}_{7,3}$ for the scheme (5.10a–f). It should be noted that for this experiment, as there are three disconnected components for the inner phase, the XFEM_Γ approach introduced in Barrett *et al.* (2013a, 2014) needs to be naturally extended. In particular, rather than adding only a single additional basis function to $\mathbb{P}^m$, three new basis functions need to be added. The physical parameters are given by

$$\rho = 1\,, \quad \mu = 0.1\,, \quad \gamma_0 = 5\,, \quad \mathcal{D}_\Gamma = 0.1\,, \quad \mathcal{D}_+ = \alpha_+ = 1\,, \quad \vec{f} = \vec{0}\,, \quad \vec{u}_0 = \vec{0}\,.$$

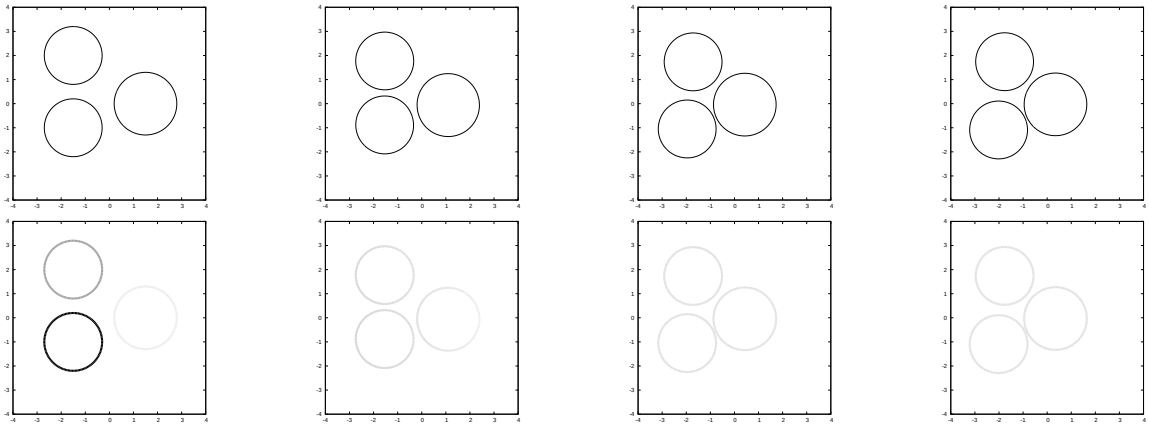

Figure 17: ($d = 2$) The time evolution of three drops. Plots are at times $t = 0$, 5, 20, 100. Below the evolution of the surfactant concentration Ψ^m on Γ^m. The grey scales linearly with the surfactant concentration ranging from 0 (white) to 1 (black).

For the surfactant we choose (2.12a) with $\beta = 0.5$, (2.16) with $\theta_+ = 1$ and let $\phi_{0,+} = 10^{-3}$. Moreover, $\lambda_+ = g_+ = 0$. The initial circles have radii 1.3, 1.2 and 1.2 with centres $(1.5, 0)^T$, $(-1.5, 2)^T$ and $(-1.5, -1)^T$ within the domain $\Omega = (-4, 4)^2$. The initial surfactant concentrations on the circles are given by 0.1, 0.5 and 1, respectively. We note that the final plots in Figure 17 are for a numerically steady state. In this state two of the circular drops nearly touch. Moreover, the surfactant concentrations on the interfaces and in the (outer) bulk phase have each reached the same constant value of about 0.167. The total surfactant amount has been conserved almost exactly in this experiment, with the relative overall loss in surfactant mass less than 0.01%. In Figure 18 we show a plot of the discrete energy

$$\mathcal{E}_+^m = \tfrac{1}{2} \left\| [\rho^{m-1}]^{\frac{1}{2}} \vec{U}^m \right\|_0^2 + \left(G_{+,\varepsilon}(\Phi_+^m), 1 \right)_{\Omega_+^m}^{m,h} + \langle F_\varepsilon(\Psi^m), 1 \rangle_{\Gamma^m}^h$$

over time. Note that although we are only able to prove stability for our semidiscrete approximations of model (ii), recall (4.28) and (4.43), in practice also the fully discrete approximations for the two models (i) and (ii) appear to be stable. In Figure 18 this can be seen by the fact that the discrete energy $\mathcal{E}_+^m$ decreases monotonically over time.

6.3.3 Two colliding drops in 2d shear flow

Here we consider a setup similar to Liu and Zhang (2010, Fig. 11). In particular, we let $\Omega = (-\frac{3}{2}, \frac{3}{2}) \times (-1, 1)$ and prescribe the inhomogeneous Dirichlet boundary condition $\vec{g}(\vec{z}) = (z_2, 0)^T$ on $\partial\Omega = \partial_1\Omega$. Moreover, Γ_0 is given by two circles with radius $\frac{1}{3}$ and centres $(-\frac{2}{3}, \frac{1}{6})^T$ and $(\frac{2}{3}, -\frac{1}{6})^T$. The remaining parameters are given by

$$\rho = 1\,, \quad \mu = 0.1\,, \quad \gamma_0 = 0.2\,, \quad \mathcal{D}_\Gamma = 0.1\,, \quad \mathcal{D}_+ = \alpha_+ = 1\,, \quad \vec{f} = \vec{0}\,, \quad \vec{u}_0 = \vec{g}\,,$$

where we once again choose the one-sided outer model (i) for the soluble surfactant. In addition, we choose (2.12a) with $\beta = 0.5$, (2.16) with $\theta_+ = 1$ and let $\psi_0 = 0.1$ and

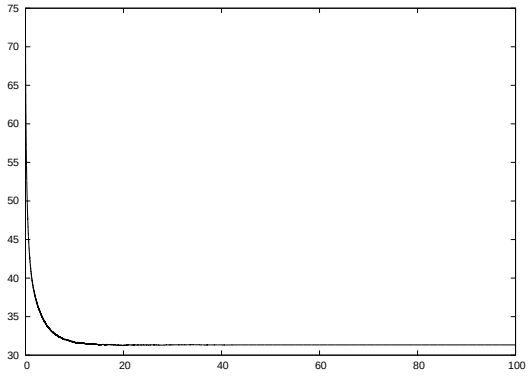

Figure 18: $(d = 2)$ Plot of the discrete energy $\mathcal{E}_+^m$ over time.

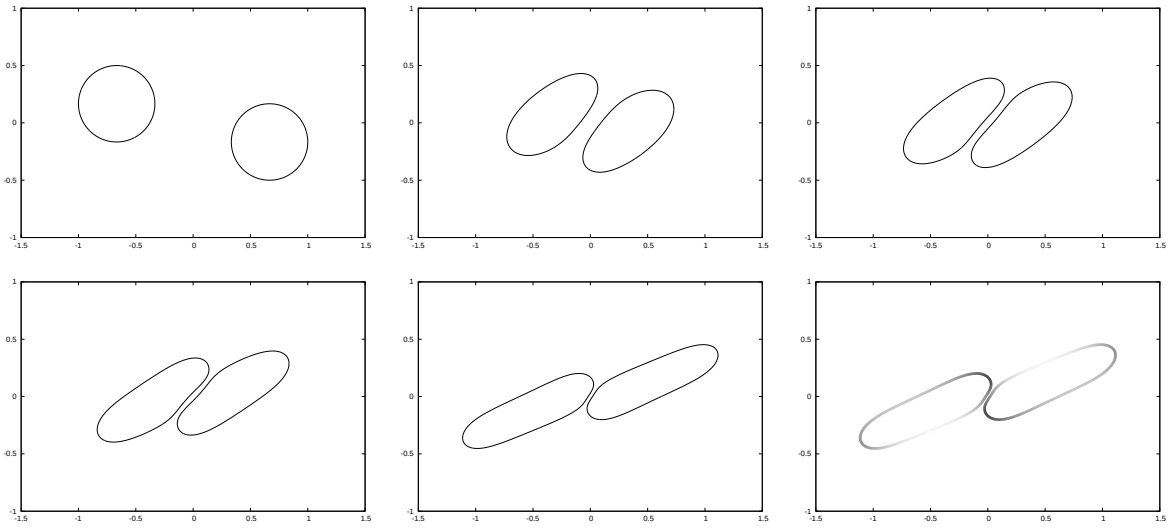

Figure 19: $(d = 2)$ The time evolution of the two drops in the presence of surfactant. Plots are at times $t = 0$, 3, 6, 9, 12. The last plot shows the final surfactant concentration Ψ^M on Γ^M, where the grey scales linearly with the surfactant concentration ranging from 0.7 (white) to 1.1 (black).

$\phi_{0,+} = 2$. Moreover, $\lambda_+ = g_+ = 0$. The evolution for the two colliding drops can be seen in Figure 19, with the final bulk surfactant concentration displayed in Figure 20. Note that the total surfactant amount has been nearly conserved in this experiment, with a small gain in the overall surfactant mass of about 0.5%. As a comparison, we show the evolution of two clean drops, in the absence of surfactant, in Figure 21. In each case, the two drops collide in the middle, and then move away from each other again, with the bubble that starts in the upper left part of the domain always staying to the left of the other bubble. As is to be expected, the two drops deform more in the presence of surfactants.

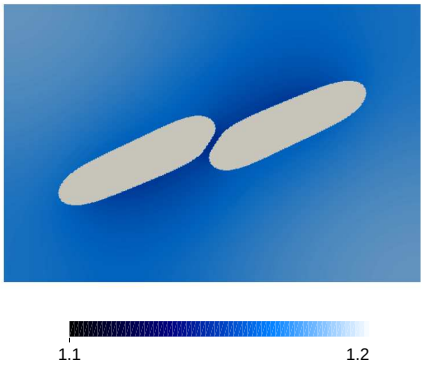

Figure 20: ($d = 2$) The final bulk surfactant concentration Φ_+^M.

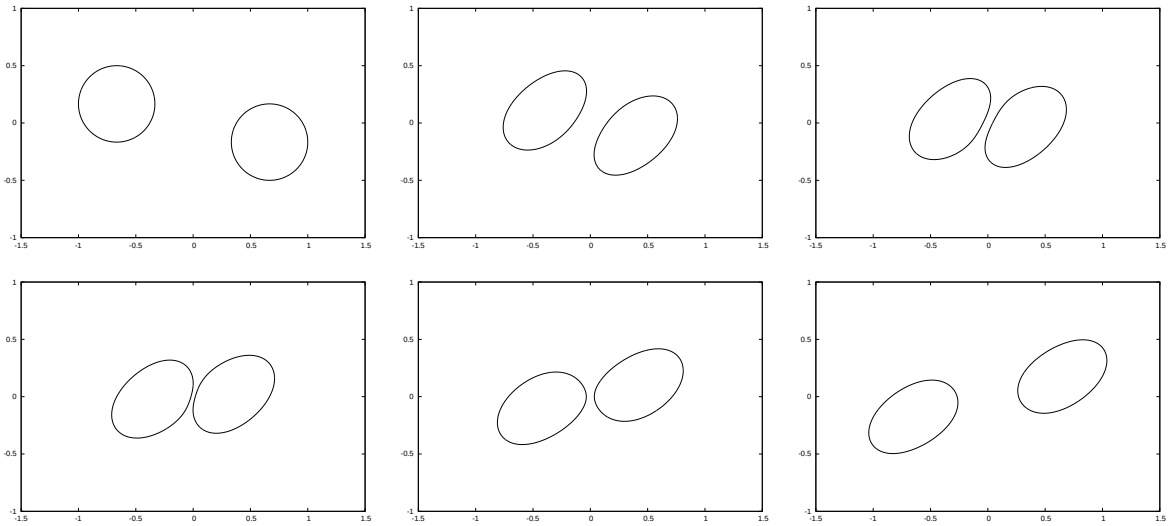

Figure 21: ($d = 2$) The time evolution of the two clean drops in the absence of surfactant. Plots are at times $t = 0$, 2, 4, 6, 8, 10.

6.3.4 Rising bubble experiment in 2d

We use the setup described in Hysing *et al.* (2009), see Figure 2 there; i.e. $\Omega = (0,1)\times(0,2)$ with $\partial_1\Omega = [0,1] \times \{0,2\}$ and $\partial_2\Omega = \{0,1\} \times (0,2)$. Moreover, $\Gamma_0 = \{\vec{z} \in \mathbb{R}^2 : |\vec{z} - (\frac{1}{2},\frac{1}{2})^T| = \frac{1}{4}\}$. The physical parameters, which we choose as in Muradoglu and Tryggvason (2008, Fig. 16), are given by

$$\rho_+ = 1\,, \quad \rho_- = 0.1\,, \quad \mu_+ = \tfrac{1}{2}\,, \quad \mu_- = \tfrac{1}{80}\,, \quad \gamma_0 = 1\,, \quad \vec{f}_1 = -\vec{e}_d\,, \quad \vec{f}_2 = \vec{0}\,,$$

with the time interval defined by $[0,T]$ with $T = 30$. For the surfactant problem we choose the parameters $\psi_0 = \mathcal{D}_\Gamma = 0.01$ and (2.12a) with $\beta = 0.5$. For the soluble surfactant we choose the one-sided outer model (i) with (2.16) and $\theta_+ = 1$, and let $\phi_{0,+} = 1$. Moreover, $\mathcal{D}_+ = 0.1$, $\alpha_+ = 1$ and $\lambda_+ = g_+ = 0$. Overall this experiment is very similar to the simulation presented in Muradoglu and Tryggvason (2008, Fig. 16). To demonstrate the

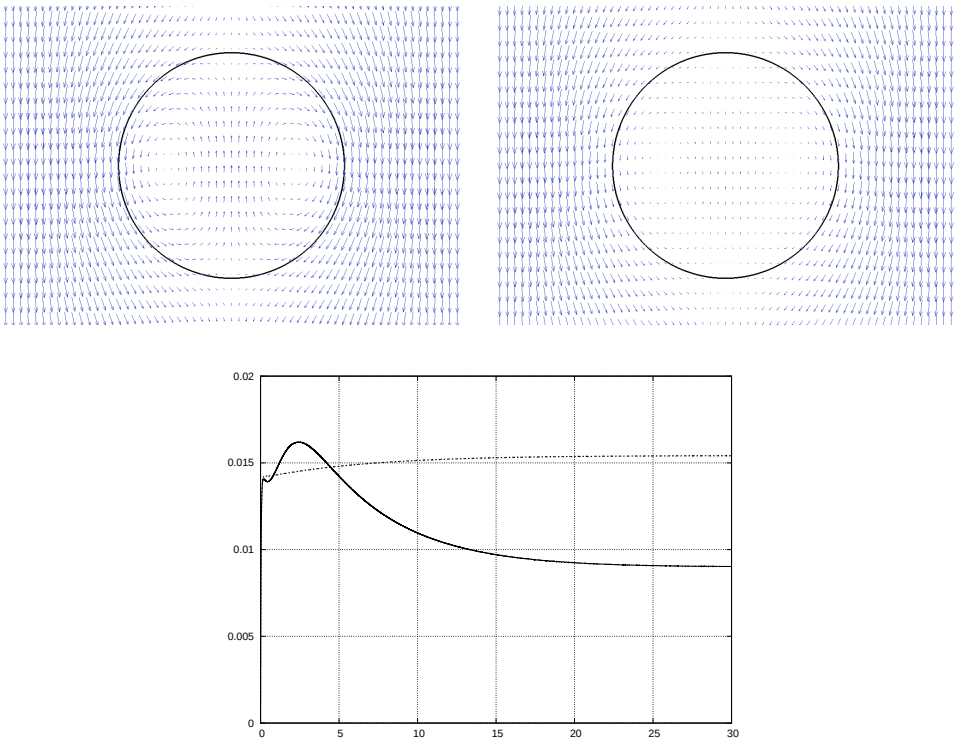

Figure 22: ($d = 2$) Relative velocity vectors $\vec{U}^M - \vec{v}^M$ for the final bubble without surfactant (left) and with surfactant (right) at time $T = 30$. Below a comparison of the rise velocities for the two bubbles, where the dashed line is for the clean bubble.

effect that adding surfactant has on the velocity profile inside the bubble, in Figure 22 we plot the relative velocity $\vec{U}^M - \vec{v}^M$, where $\vec{v}^m = [(\rho^m_-, 1)]^{-1} \int_\Omega \rho^m_- \vec{U}^m \,\mathrm{d}\mathcal{L}^d$, with $\rho^m_- \in S^m_0$ defined similarly to ρ^m in (5.2) but with ρ_+ replaced by zero, for the two cases of clean and contaminated bubble. Clearly, the two vortices inside the clean bubble almost vanish completely when surfactant is added. This reduces the rise velocity significantly, as can be seen at the bottom of Figure 22. Note that in this simulation the total surfactant amount was almost conserved, with the relative overall loss in surfactant mass equal to 0.2%. A plot of the final bulk surfactant concentration Φ^M_+ can be seen in Figure 23.

6.3.5 Two colliding drops in 3d shear flow

Here we consider the natural three dimensional analogue of the simulations in §6.3.3. In particular, we let $\Omega = (-\frac{3}{2}, \frac{3}{2}) \times (-1, 1) \times (-1, 1)$ and prescribe the inhomogeneous Dirichlet boundary condition $\vec{g}(\vec{z}) = (z_3, 0, 0)^T$ on $\partial\Omega = \partial_1\Omega$. Moreover, Γ_0 is given by two spheres with radius $\frac{1}{3}$ and centres $(-\frac{2}{3}, \frac{1}{6}, \frac{1}{6})^T$ and $(\frac{2}{3}, -\frac{1}{6}, -\frac{1}{6})^T$. The remaining parameters are as in §6.3.3. For the discretization parameters we use the same as for $\text{adapt}_{5,2}$ from Barrett *et al.* (2014), but here $(K_\Gamma, J_\Gamma) = (2 \times 1538, 2 \times 3072)$. The evolution for the two colliding drops can be seen in Figure 24, with the discrete surfactant concentrations shown in Figure 25. The total surfactant amount has been conserved almost exactly in this experiment, with the relative overall loss in surfactant mass less than 0.02%. As a

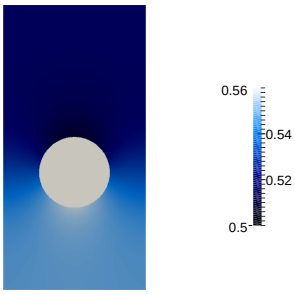

Figure 23: ($d = 2$) The final bulk surfactant concentration Φ_+^M.

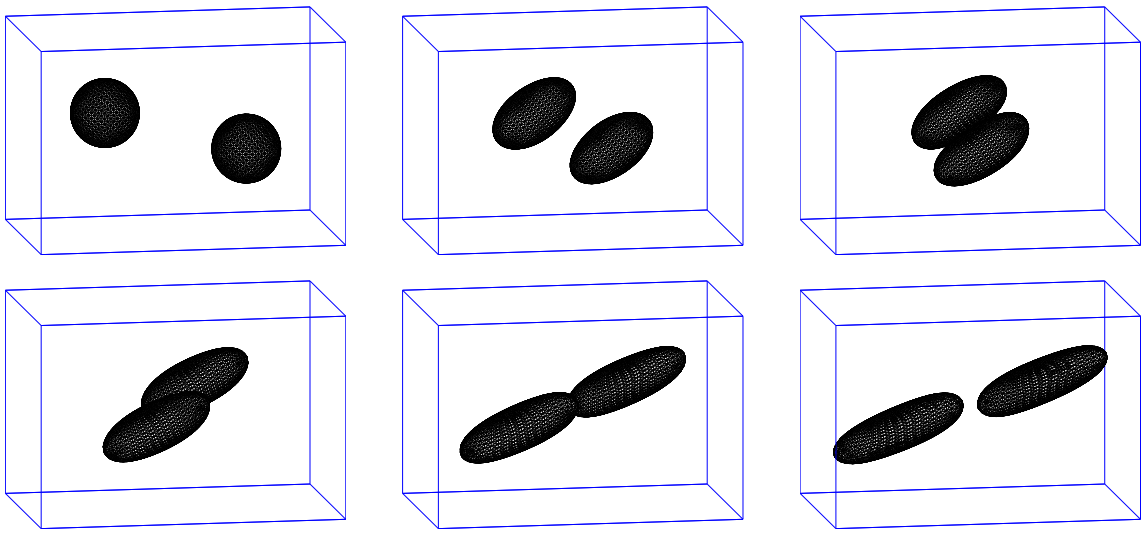

Figure 24: ($d = 3$) The time evolution of the two drops in the presence of surfactant. Plots are at times $t = 0$, 2, 4, 6, 8, 9.

comparison, we show the evolution of two clean drops, in the absence of surfactant, in Figure 26. We can see that, in contrast to the case $d = 2$ in §6.3.3, the two drops do not really bounce off each other in these simulations. As a consequence, the bubble that starts in the upper left of the domains ends up to the right of the other bubble. As in the 2d simulation, the two drops deform significantly more when surfactant is present.

A Radially symmetric solutions for the absorption problem

Here we summarize exact solutions for the absorption problem on a stationary interface Γ that is given by a unit circle. Then a radially symmetric solution for the soluble bulk surfactant concentration needs to satisfy the following systems. For simplicity, we set all the physical parameters to unity, i.e. $\mathcal{D}_\pm = \alpha_\pm = 1$. We refer to Ravera *et al.* (2000), who

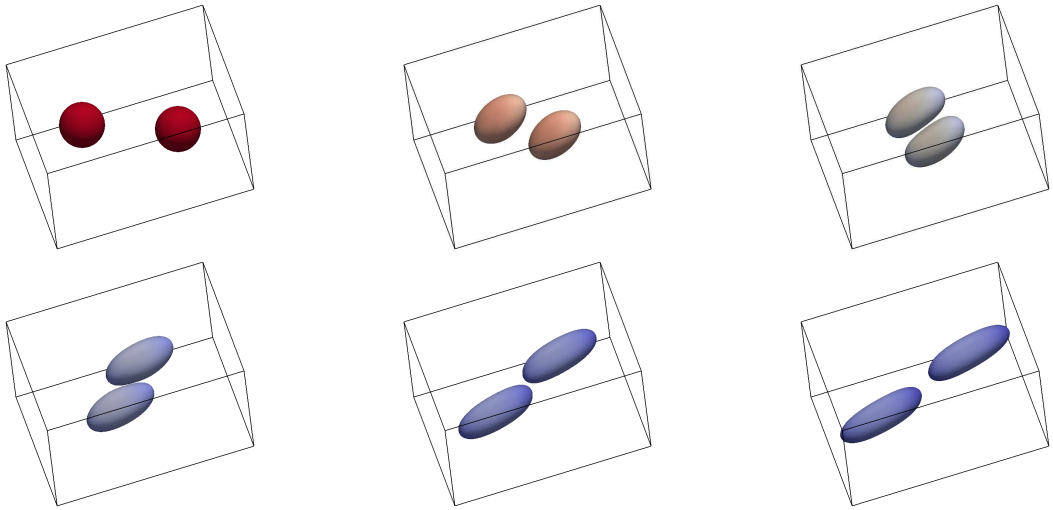

Figure 25: ($d = 3$) The time evolution of the surfactant concentration on the interfaces. Plots are at times $t = 0$, 2, 4, 6, 8, 9. Here the colour ranges from red (0.1) to blue (1.2).

studied a simplified version of this setting.

Model (i)

The two-sided problem for the radially symmetric situation on $B_L(0)$, $L > 1$, with the interface at $\partial B_1(0)$ is given by

$$r^{d-1}\,\partial_t\,\phi_- = \partial_r\,(r^{d-1}\,\partial_r\phi_-) \qquad \text{on } (0,1)\times(0,T) \tag{A.1a}$$

$$r^{d-1}\,\partial_t\,\phi_+ = \partial_r\,(r^{d-1}\,\partial_r\phi_+) \qquad \text{on } (1,L)\times(0,T) \tag{A.1b}$$

$$\frac{\mathrm{d}}{\mathrm{d}t}\,\psi = \partial_r\,\phi_+\,|_{r=1+} - \partial_r\,\phi_-\,|_{r=1-} \qquad \text{on } (0,T) \tag{A.1c}$$

$$\partial_r\,\phi_\pm\,|_{r=1\pm} = -[F'(\psi) - G'_\pm(\phi_\pm\,|_{r=1\pm})] \qquad \text{on } (0,T) \tag{A.1d}$$

$$\partial_r\,\phi_-\,|_{r=0} = 0\,, \quad \phi_+\,|_{r=L} = 1 \qquad \text{on } (0,T) \tag{A.1e}$$

$$\phi_\pm\,|_{t=0} = \phi_{\pm,0} \in \mathbb{R}_{>0}\,, \quad \psi(0) = \psi_0 \in \mathbb{R}_{>0}\,. \tag{A.1f}$$

For the one-sided variants we simply ignore ϕ_-, or ϕ_+, in the above. For example, for the inner phase problem, on partitioning $[0,1]$ into subintervals $[r_{j-1}, r_j]$, $j = 1 \to J$, and on discretizing with continuous piecewise linear finite elements in space, we obtain the system of ODEs

$$A\frac{\mathrm{d}}{\mathrm{d}t}\,\underline{\Phi}^- = \underline{f} - B\,\underline{\Phi}^- \tag{A.2a}$$

$$\frac{\mathrm{d}}{\mathrm{d}t}\,\Psi = -[F'(\Psi) - G'_-(\Phi_J^-)]\,, \tag{A.2b}$$

where $\underline{\Phi}^- = (\Phi_0^-, \ldots, \Phi_J^-)^T \in \mathbb{R}^{J+1}$ and $\underline{f} = (0, \ldots, 0, F'(\Psi) - G'_-(\Phi_J^-))^T \in \mathbb{R}^{J+1}$. Moreover, $A, B \in \mathbb{R}^{(J+1)\times(J+1)}$ are the natural weighted mass- and stiffness matrices for the

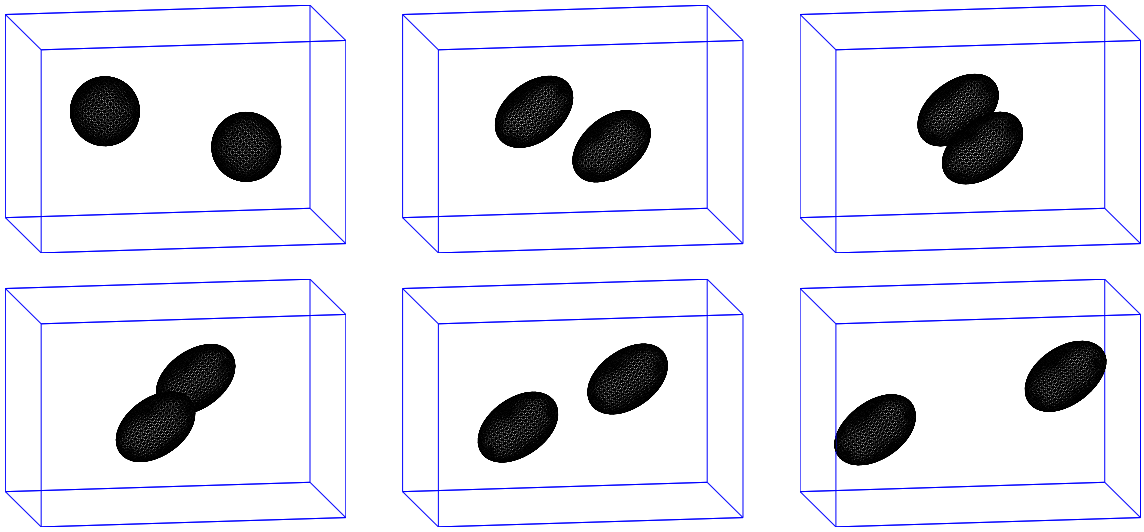

Figure 26: ($d = 3$) The time evolution of the two clean drops in the absence of surfactant. Plots are at times $t = 0$, 2, 4, 6, 8, 10.

introduced partitioning $r_0 < r_1 < \cdots < r_J$, with the weighting factor r^{d-1}. Note that as a consequence, the first condition in (A.1e) is replaced by a weak approximation of $(r^{d-1}\,\partial_r\,\phi_-)\,|_{r=0} = 0$. The system (A.2a,b) can be solved with standard ODE solvers, e.g. with `ode45` in MATLAB. The one-sided outer phase problem, as well as the two-sided problem, can be handled similarly.

Model (ii)

Here we replace $\phi_\pm$ in (A.1a–f) with ϕ, and replace $G_\pm$ with G. As before, on partitioning $[0, L]$ into subintervals and on discretizing with continuous piecewise linear finite elements in space, we obtain a system of ODEs that can be solved with e.g. `ode45` in MATLAB.

References

Alke, A. and Bothe, D. (2007). VOF-simulation of fluid particles influenced by soluble surfactant. In *Proceedings of ICMF2007*.

Alke, A. and Bothe, D. (2009). 3D numerical modeling of soluble surfactant at fluidic interfaces based on the volume-of-fluid method. *FDMP Fluid Dyn. Mater. Process.*, **5**(4), 345–372.

Barrett, J. W. and Boyaval, S. (2011). Existence and approximation of a (regularized) Oldroyd-B model. *Math. Models Methods Appl. Sci.*, **21**(9), 1783–1837.

Barrett, J. W. and Nürnberg, R. (2004). Convergence of a finite-element approximation of surfactant spreading on a thin film in the presence of van der Waals forces. *IMA J. Numer. Anal.*, **24**(2), 323–363.

Barrett, J. W., Garcke, H., and Nürnberg, R. (2003). Finite element approximation of surfactant spreading on a thin film. *SIAM J. Numer. Anal.*, **41**(4), 1427–1464.

Barrett, J. W., Garcke, H., and Nürnberg, R. (2007). A parametric finite element method for fourth order geometric evolution equations. *J. Comput. Phys.*, **222**(1), 441–462.

Barrett, J. W., Garcke, H., and Nürnberg, R. (2008). On the parametric finite element approximation of evolving hypersurfaces in $\mathbb{R}^3$. *J. Comput. Phys.*, **227**(9), 4281–4307.

Barrett, J. W., Garcke, H., and Nürnberg, R. (2013a). Eliminating spurious velocities with a stable approximation of viscous incompressible two-phase Stokes flow. *Comput. Methods Appl. Mech. Engrg.*, **267**, 511–530.

Barrett, J. W., Garcke, H., and Nürnberg, R. (2013b). On the stable numerical approximation of two-phase flow with insoluble surfactant. `http://arxiv.org/abs/1311.4432`.

Barrett, J. W., Garcke, H., and Nürnberg, R. (2014). A stable parametric finite element discretization of two-phase Navier–Stokes flow. *J. Sci. Comp.* (to appear, DOI: 10.1007/s10915-014-9885-2).

Booty, M. and Siegel, M. (2010). A hybrid numerical method for interfacial fluid flow with soluble surfactant. *J. Comput. Phys.*, **229**(10), 3864–3883.

Bothe, D. and Prüss, J. (2010). Stability of equilibria for two-phase flows with soluble surfactant. *Quart. J. Mech. Appl. Math.*, **63**(2), 177–199.

Chen, K.-Y. and Lai, M.-C. (2014). A conservative scheme for solving coupled surface-bulk convection-diffusion equations with an application to interfacial flows with soluble surfactant. *J. Comput. Phys.*, **257**, 1–18.

Deckelnick, K., Dziuk, G., and Elliott, C. M. (2005). Computation of geometric partial differential equations and mean curvature flow. *Acta Numer.*, **14**, 139–232.

Diamant, H. and Andelman, D. (1996). Kinetics of surfactant adsorption at fluid-fluid interfaces. *J. Phys. Chem.*, **100**(32), 13732–13742.

Douglas, Jr., J. and Russell, T. F. (1982). Numerical methods for convection-dominated diffusion problems based on combining the method of characteristics with finite element or finite difference procedures. *SIAM J. Numer. Anal.*, **19**(5), 871–885.

Dziuk, G. (1991). An algorithm for evolutionary surfaces. *Numer. Math.*, **58**(6), 603–611.

Dziuk, G. and Elliott, C. M. (2007). Finite elements on evolving surfaces. *IMA J. Numer. Anal.*, **27**(2), 262–292.

Dziuk, G. and Elliott, C. M. (2013). Finite element methods for surface PDEs. *Acta Numer.*, **22**, 289–396.

Elliott, C. M. and Styles, V. (2012). An ALE ESFEM for solving PDEs on evolving surfaces. *Milan J. Math.*, **80**(2), 469–501.

Engblom, S., Do-Quang, M., Amberg, G., and Tornberg, A.-K. (2013). On diffuse interface modeling and simulation of surfactants in two-phase fluid flow. *Commun. Comput. Phys.*, **14**(4), 879–915.

Ganesan, S. and Tobiska, L. (2012). Arbitrary Lagrangian–Eulerian finite-element method for computation of two-phase flows with soluble surfactants. *J. Comput. Phys.*, **231**(9), 3685–3702.

Garcke, H. and Wieland, S. (2006). Surfactant spreading on thin viscous films: nonnegative solutions of a coupled degenerate system. *SIAM J. Math. Anal.*, **37**(6), 2025–2048.

Garcke, H., Lam, K. F., and Stinner, B. (2014). Diffuse interface modelling of soluble surfactants in two-phase flow. *Comm. Math. Sci.*, **12**(8), 1475–1522.

Girault, V. and Raviart, P.-A. (1986). *Finite Element Methods for Navier–Stokes*. Springer-Verlag, Berlin.

Groß, S. and Reusken, A. (2011). *Numerical methods for two-phase incompressible flows*, volume 40 of *Springer Series in Computational Mathematics*. Springer-Verlag, Berlin.

Grün, G. and Rumpf, M. (2000). Nonnegativity preserving numerical schemes for the thin film equation. *Numer. Math.*, **87**, 113–152.

Hysing, S., Turek, S., Kuzmin, D., Parolini, N., Burman, E., Ganesan, S., and Tobiska, L. (2009). Quantitative benchmark computations of two-dimensional bubble dynamics. *Internat. J. Numer. Methods Fluids*, **60**(11), 1259–1288.

Khatri, S. and Tornberg, A.-K. (2014). An embedded boundary method for soluble surfactants with interface tracking for two-phase flows. *J. Comput. Phys.*, **256**, 768–790.

Lai, M.-C., Tseng, Y.-H., and Huang, H. (2008). An immersed boundary method for interfacial flows with insoluble surfactant. *J. Comput. Phys.*, **227**(15), 7279–7293.

Liu, H. and Zhang, Y. (2010). Phase-field modeling droplet dynamics with soluble surfactants. *J. Comput. Phys.*, **229**(24), 9166–9187.

Muradoglu, M. and Tryggvason, G. (2008). A front-tracking method for computation of interfacial flows with soluble surfactants. *J. Comput. Phys.*, **227**(4), 2238–2262.

Pironneau, O. (1982). On the transport-diffusion algorithm and its applications to the Navier–Stokes equations. *Numer. Math.*, **38**(3), 309–332.

Ravera, F., Ferrari, M., and Liggieri, L. (2000). Adsorption and partitioning of surfactants in liquid-liquid systems. *Adv. Colloid Interface Sci.*, **88**(1-2), 129–177.

Renardy, Y. Y., Renardy, M., and Cristini, V. (2002). A new volume-of-fluid formulation for surfactants and simulations of drop deformation under shear at a low viscosity ratio. *European J. Mech. B Fluids*, **21**(1), 49–59.

Schmidt, A. and Siebert, K. G. (2005). *Design of Adaptive Finite Element Software: The Finite Element Toolbox ALBERTA*, volume 42 of *Lecture Notes in Computational Science and Engineering*. Springer-Verlag, Berlin.

Tasoglu, S., Demirci, U., and Muradoglu, M. (2008). The effect of soluble surfactant on the transient motion of a buoyancy-driven bubble. *Phys. Fluids*, **20**(4), 040805.

Teigen, K. E., Song, P., Lowengrub, J., and Voigt, A. (2011). A diffuse-interface method for two-phase flows with soluble surfactants. *J. Comput. Phys.*, **230**(2), 375–393.

Xu, K., Booty, M. R., and Siegel, M. (2013). Analytical and computational methods for two-phase flow with soluble surfactant. *SIAM J. Appl. Math.*, **73**(1), 523–548.